# THE BATHYMETRY, SEDIMENTOLOGY AND SEISMIC STRATIGRAPHY OF LAKE SIBAYA - NORTHERN KWAZULU-NATAL

by

Warwick Richard Miller

A dissertation submitted to the Faculty of Science, University of Natal (Durban) in fulfilment of the requirements for the degree of Master of Science.

Durban, 1998

# ABSTRACT

The morphology of Lake Sibaya is a product of an ancient fluvial system that drained a coastal landscape dominated by aeolian processes. The sedimentary processes within the lake are driven by wind generated currents. The dominant sedimentary process is one of lake segmentation, whereby prograding bedforms isolate the lake into smaller water bodies. The prograding bedforms include cuspate forelands and sand spits. The size and mobility of these bedforms is a function of sediment availability and current regime.

The bathymetry of Lake Sibaya is discussed, with emphasis on geomorphic features derived from the ancient aeolian landscape as well as features related to modern sedimentary processes. The presence of underwater knickpoints and terraces indicate that lake level fluctuations have been common in Lake Sibaya. It is during lake highstands that large volumes of sand are eroded from aeolian dunes which surround the lake and made available for shoreline progradation. Ancient dune topography is preserved to depths of 20 m below water-level within the lake.

Surface sediment distribution maps were compiled from 515 grab samples and thirteen core samples. Fine grained, well sorted, coarse skewed quartz sand comprises the majority of the surface area of the lake floor. Gyttja is the other dominant sediment type and accumulates in palaeovalleys and depressions on the lake floor. Sediment distribution in Lake Sibaya is discussed in terms of modern lacustrine processes as well as inherited sedimentary characteristics.

The stratigraphy of the sediments underlying Lake Sibaya was investigated using a Uni-Boom seismic profiling system. Seismic profiles were compiled by identifying acoustically reflective surfaces that show regional development. Thirteen seismic overlays were prepared, and are illustrated as west - east and north - south seismic profiles. Five sequences ranging in age from late Cretaceous to Holocene were identified from the seismic profiles, and are described in terms of sequence stratigraphic principles. The seismic sequences were interpreted within a lithostratigraphic framework and are presented as a series of idealised geological sections.

Thirteen sediment cores were collected from the Lake Sibaya area in order to ascertain the accuracy of the stratigraphic interpretation of the seismic records, to investigate reflective horizons identified from seismic records and to collect dateable material. Interpretation of the sediment cores reveals that a proto Lake Sibaya existed on drowned dune topography, during the period ± 43500 BP to ± 25500 BP prior to the Last Glacial Maximum. During the early to mid Holocene the Lake Sibaya site was occupied by a saline lagoon which underwent isolation from the sea ± 5030 BP. Since the mid-Holocene the lake has evolved to totally freshwater conditions and has undergone little sedimentation.

The geological evolution of the Lake Sibaya area is discussed in terms of the geometry of the identified seismic sequences, the sedimentary characteristics of these sequences and the radiocarbon dates provided from the sediment cores. Palaeo-environmental conditions during the accumulation of the sedimentary sequences is discussed where fossil remains permit.

## ACKNOWLEDGEMENTS

The research for this thesis was funded by the Council For Geoscience and completed by the author whilst in the employ of the Council For Geoscience's Marine Geoscience Unit in Durban.

I wish to extend my sincere thanks to my supervisors, Professor Tom Mason (now Armagh Planetarium) and Professor Mike Watkeys of the University of Natal for advice and support throughout the compilation of this dissertation. Thanks to Mr. André du Plessis of the Council For Geoscience for the advice and unlimited patience during the arduous progress of my research. The comradery, support and scientific assistance of my co-workers Dr. Peter Ramsay and Ian Wright both in the field and in the office has been inspirational. My sincerest thanks go to Wade Kidwell and Willem Kupido for logistical support in the field and to Peter Bova for his technical expertise during the problematical geophysical cruises. Many thanks to Kim Lord, Hans Huchstedt and Peter Dillon of the Cape Town branch of the Marine Geoscience Unit for their assistance during the Lake Sibaya coring programme.

Many thanks to the KwaZulu-Natal Nature Conservation Services for allowing me to undertake research in Lake Sibaya and a special thank you to the kitchen staff at Baya camp for providing the numerous wholesome meals to cheer me up when the "Sibaya Triangle" was interfering with the temperamental geophysical instrumentation.

Finally to my better half Manola (see Fig 6.4) many thanks for your encouragement, support and numerous take out lunches during the long hours of solitude whilst I was preparing this thesis.

# TABLE OF CONTENTS

# CHAPTER 1 : INTRODUCTION

## 1.1 LOCALITY

Lake Sibaya is a coastal freshwater lake located on the Makathini Flats of the northern KwaZulu-Natal coastline (Fig.1). The lake occupies a position between 27° 15' S to 27° 25' S and 32° 33' E to 32° 43' E. The lake has an average surface area of ± 65 $km^2$, a maximum depth of 41 m and an average depth of 13 m (Pitman & Hutchinson, 1975). The water level in Lake Sibaya is elevated ± 20 m above mean sea-level and the bottom of the lake is located ± 21 m below mean sea-level. The lake is separated from the sea by the north - south trending coastal dune cordon which ranges in height from 64 m to 172 m above mean sea-level (MSL).

The lake is situated on sediments of Cretaceous to Quaternary age which form a thin covering which blankets most of the Maputaland coastal plain and abuts against the Karoo volcanics of the Lebombo mountain range (Hobday, 1979). Sparse shallow marine and beach deposits of Tertiary age overlie the Cretaceous age siltstones, while Quaternary aged sediments of predominantly aeolian origin, constitute the cover sediments for most of the coastal plain. The Cenozoic sediments are predominantly fine grained sands of aeolian origin.

Lake Sibaya falls into the Coastal Lake Zone (Mountain, 1990) which is characterised by a chain of barrier lakes, lagoons and swamps which occur behind high vegetated coastal dunes. The Coastal Lake Zone is characterised by broad vegetated dune fields with low undulating dune topography. Vegetation is predominantly broad open grasslands interspersed with smaller areas of swamp forest and heavily wooded savannahs (Mountain, 1990).

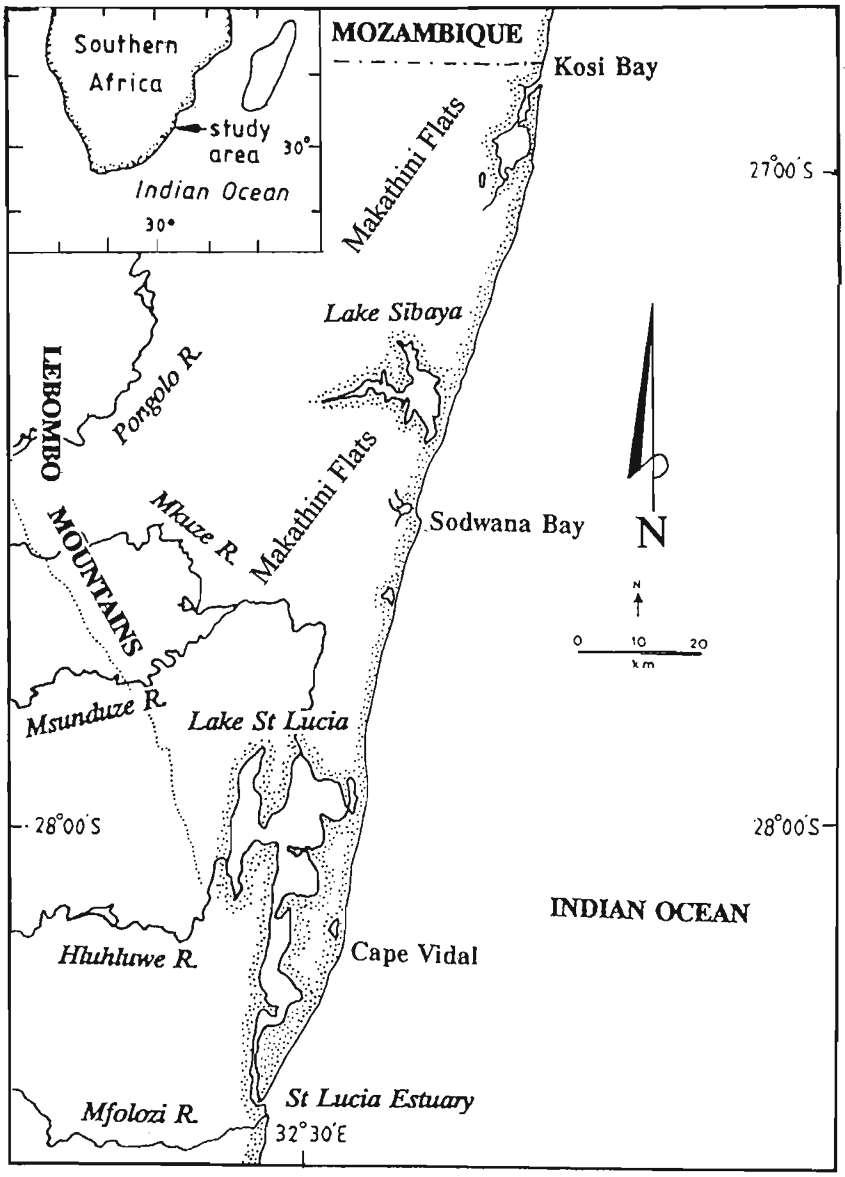


Fig. 1.1 Locality map showing Lake Sibaya and other coastal lakes of the Zululand coastline.

**1.2 AIMS**

The aims of this thesis are fourfold:

- to describe the lake morphology and to produce a bathymetric chart of Lake Sibaya;
- to provide surficial sediment distribution maps of the lake floor and to understand sediment distributions in terms of modern sedimentary processes and inherited sedimentary features;
- to provide seismic profiles across the lake to gain an insight into the lake stratigraphy;
- to core sample "windows" into the sediments below Lake Sibaya, with a view to understanding the stratigraphy below the lake and to obtain dateable material and
- to investigate the geological evolution of Lake Sibaya.

This study commences with the discussion of the regional setting of Lake Sibaya followed by a description of data-collection methods and data analysis. Lake bathymetry is illustrated and lake morphology is discussed in the context of modern sedimentary processes. A series of surficial sediment distribution maps are illustrated and sediment distribution patterns are discussed in terms of modern sedimentary processes and sedimentary features inherited from a previous stage of Lake Sibaya's evolution. The results of seismic profiling in Lake Sibaya are illustrated and analysed in terms of sequence stratigraphic principles. A stratigraphic interpretation of the seismic sequences is presented. A coring programme which was initiated to "ground truth" the seismic profiling investigations and to collect dateable material is discussed. Individual cores are described, illustrated and subdivided into a number of recurring sedimentary units. Radiocarbon dating of material from the sedimentary units permits the development of a lithostratigraphic framework which is compared to the results of the seismic profiling investigation. Finally the seismic sequences and sedimentary units are assigned to the lithostratigraphic framework of the proposed Maputaland Group and the geological evolution of the Lake Sibaya area is discussed.

# CHAPTER 2 : REGIONAL SETTING

## 2.1 CLIMATE

According to the Köppen Classification (Boucher, 1975), the Natal coastal belt has a humid subtropical climate with a warm summer; this climatic zone being dominated by the southern subtropical high pressure belt (STHP) (Hunter, 1988). Climatic data for this study were taken from the Lake Sibaya Research station (operational from 1965 to 1978) and from the Mbazwane forestry station.

Rainfall averages 900 mm per annum over the lake but varies between 1200 mm per annum in the southeast and 700 mm per annum in the west (Pitman & Hutchinson, 1975) (Fig.2.1). Forty three percent of the rain falls in the three month period from January to March (Wright & Mason, 1990). The mean wind speed measured at the Mabibi School (27° 19' 43" S 32° 43' 52" E) adjacent to Lake Sibaya was 4.6 $ms^{-1}$ for the period September 1994 to February 1996 with a maximum gust speed of 23.7 $ms^{-1}$ (Diab & Sokolic, 1996). Approximately 60% of the winds are in excess of 4 $ms^{-1}$ and 30% in excess of 6 $ms^{-1}$ (Diab & Sokolic, 1996). Dominant wind directions are NE and SW. The wind rose and frequency distribution of wind speed measured at Mabibi for the time period September 1994 to February 1996 are illustrated in Fig. 2.2 and Fig. 2.3.

Lake Sibaya has a small catchment area, measuring 536 $km^2$ and is fed by ground water flow and small streams (Pitman & Hutchinson, 1975) (Fig.2.1). The sandy substrate surrounding Lake Sibaya, limits the amount of surface runoff and consequently the water levels within the lake are maintained largely by ground water recharge (Pitman & Hutchinson, 1975). The water levels within Lake Sibaya constantly fluctuate in response to varying amounts of groundwater discharge into the lake, seepage loss through the coastal dunes and evaporation from the lake surface. Water levels in Lake Sibaya are very sensitive to local weather conditions and show direct responses to local rainfall conditions and seasonal cycles. Hill (1979) estimated the seepage loss through the coastal dune barrier at between 1 and 4 million $m^3$ per annum. Evaporation accounts for approximately 1420 mm per annum (Pitman & Hutchinson, 1975).

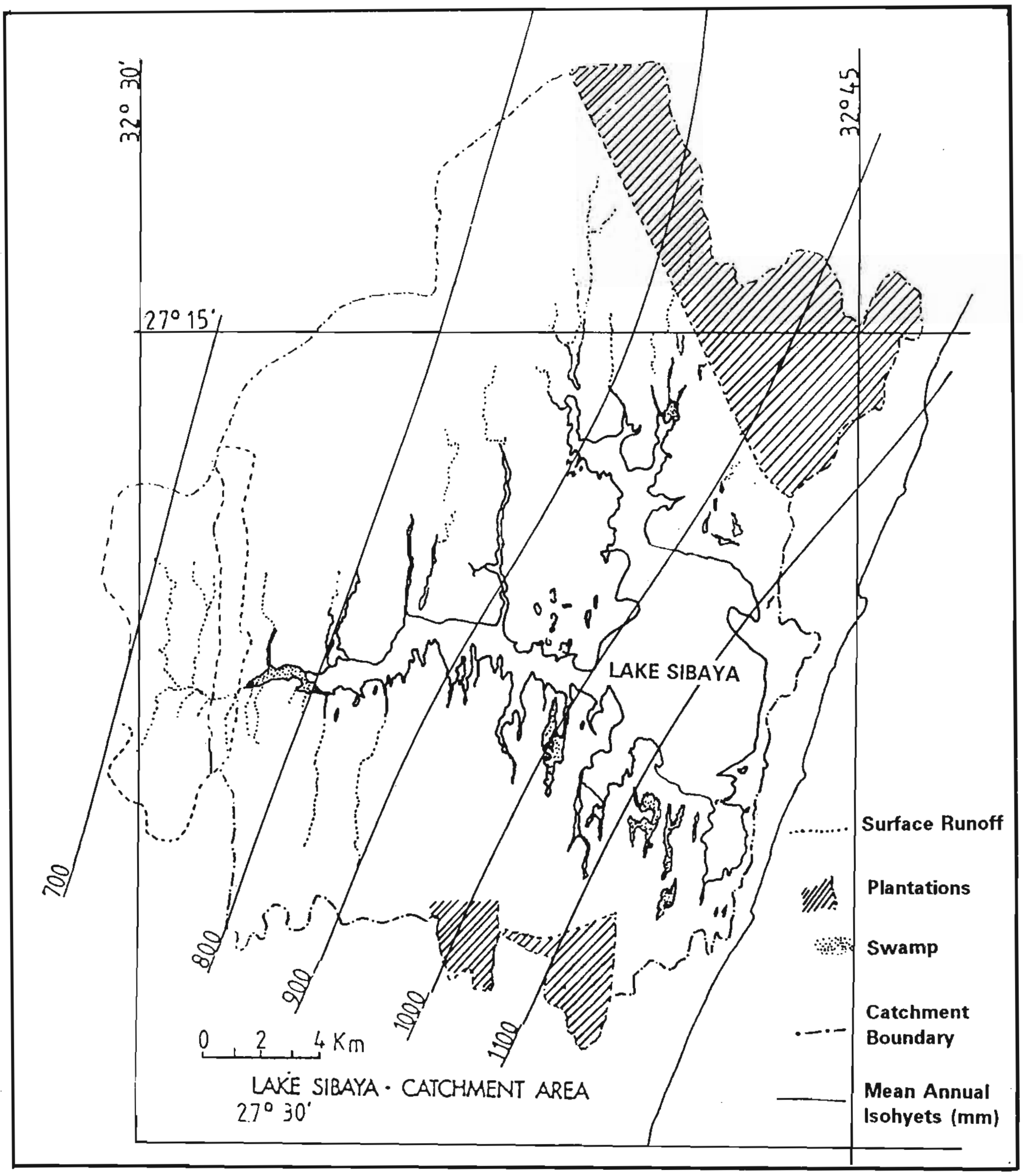


**Fig 2.1 Lake Sibaya catchment, showing surface runoff and rainfall distribution (After Pitman & Hutchinson, 1975).**

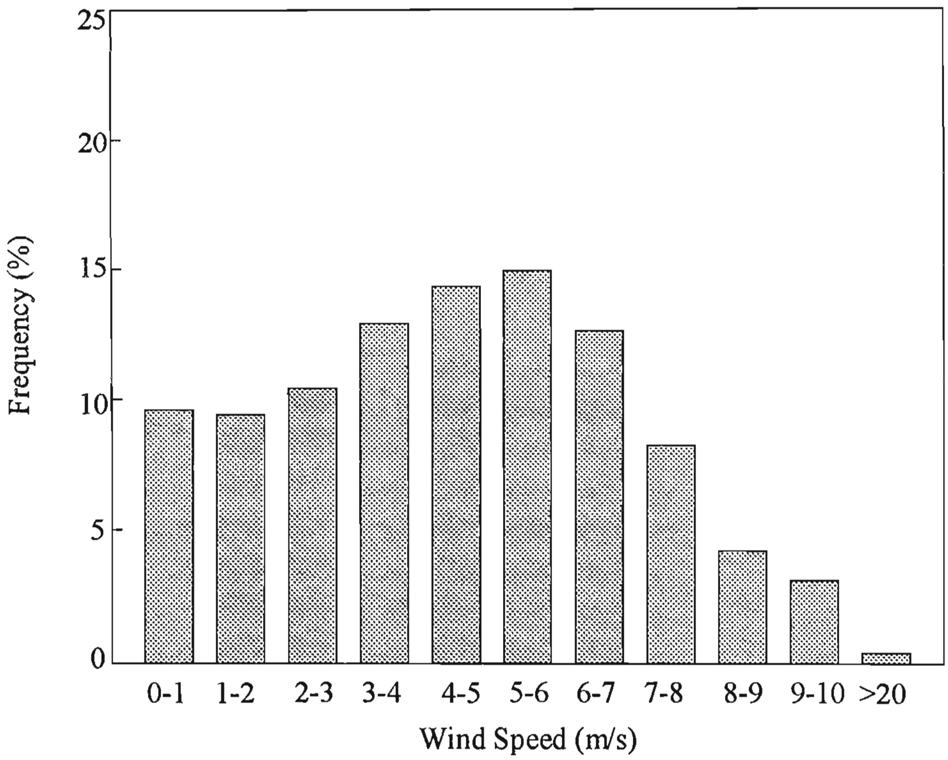


**Fig 2.2** Percentage distribution of wind speed at Mabibi School adjacent to Lake Sibaya for the period December 1994 to January 1996. (After Diab & Sokolic, 1998)

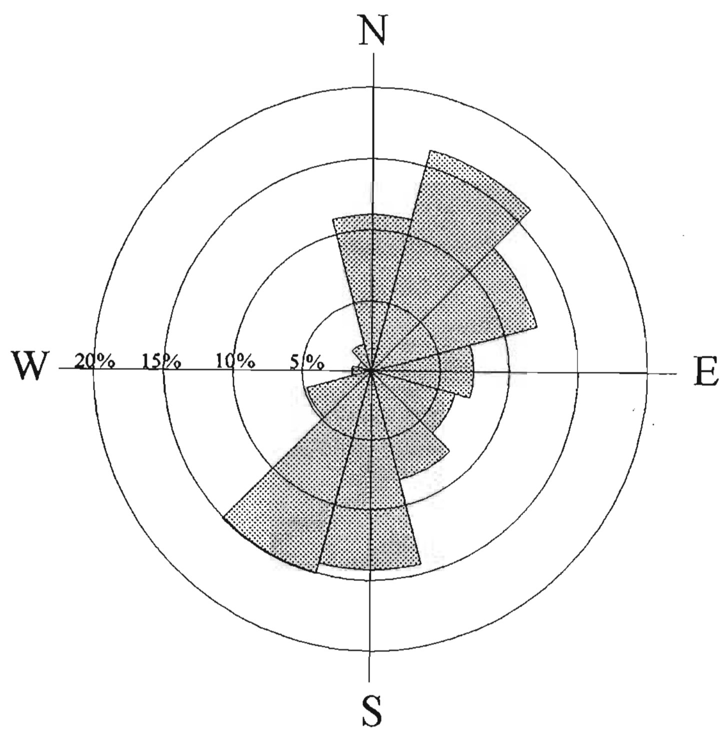


**Fig 2.3** Wind rose for the weather station at Mabibi School for the period December 1994 to January 1996. (After Diab & Sokolic, 1998)

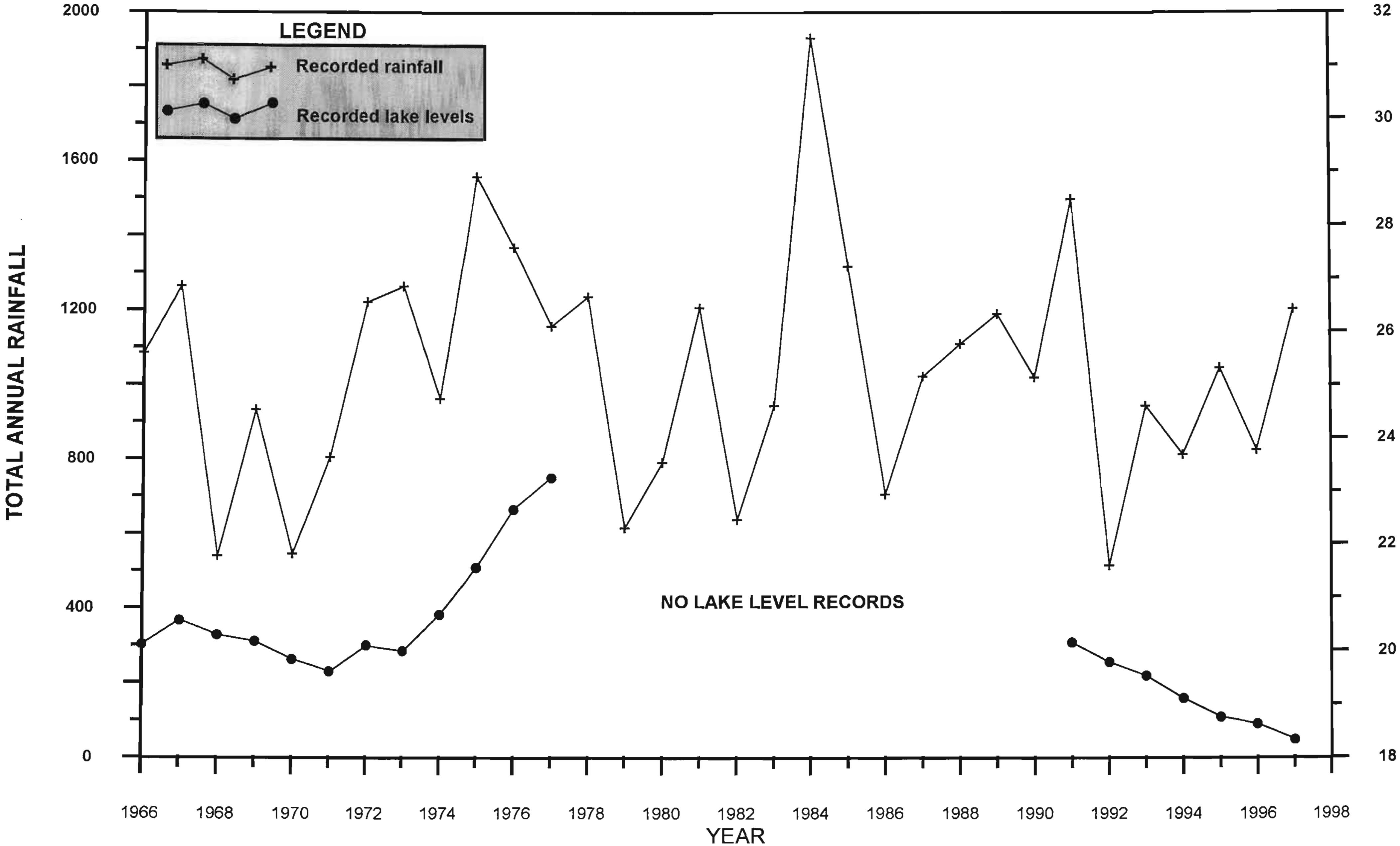


Fig 2.4 A plot showing the relationship between local rainfall (Mbazwane forest station) and recorded lake levels.

## 2.2 GEOLOGICAL SETTING

The Maputaland coastal plain is underlain by Mesozoic, Tertiary and Quaternary sediments and volcanic rocks (Fig. 2.5). The basement consists predominantly of volcanic successions extruded during the break-up of Gondwana. Overlying the basement is a thick succession of Cretaceous sediments (± 800m thickness at the coast) which is in turn overlain by a thin veneer of Cenozoic sediments.

### 2.2.1 Mesozoic

The oldest rocks outcropping in Maputaland are the 179 ± 7 Ma rhyolites of the Jozini Formation (Watkeys, 1993). These rocks outcrop to the west of the coastal plain as the Lebombo Range of mountains. Conglomerates of the Msunduze Formation overlie the Jozini rhyolites (Stratten, 1970) and are in turn overlain by basalts of the Movene and Mpilo Formations (Du Preez & Wolmerans, 1986; Wolmerans & Du Preez 1986). Pyroclastics, rhyolites and trachytes of the Bumbeni Complex form the upper part of the igneous basement (Allsopp *et al.*, 1984; Watkeys, 1994). The volcanic suite is draped over a major crustal fracture and dips eastward under the Cretaceous and Cenozoic sediments of the Maputaland coastal plain (Dingle *et al*, 1983).

The basement is unconformably overlain by the Cretaceous aged sediments of the Zululand Group (Table 2.1). The lower Cretaceous Makathini Formation consists of terrestrial sandstones and conglomerates which grade upwards into shallow marine clays (Kennedy & Klinger, 1975; Watkeys *et al*, 1993). The overlying Mzinene Formation consists of shallow marine glauconitic silts and sands (Kennedy & Klinger, 1975; Watkeys *et al*, 1993). The late Cretaceous St. Lucia Formation which unconformably overlies the Mzinene Formation consists of a basal conglomerate that is overlain by a succession of cross-bedded fine sands and silts. The top of the St. Lucia Formation is characterised by upward fining units of glauconitic silts and fine sands with interbedded hardgrounds. The St. Lucia Formation is richly fossiliferous and contains an abundance of calcareous concretions (Kennedy & Klinger, 1975; Dingle 1981; Watkeys *et al*, 1993). The elevation of the top of the St. Lucia Formation has been determined at 20 to 30 metres below mean sea-level in the Lake Sibaya area (Pitman & Hutchinson, 1975).

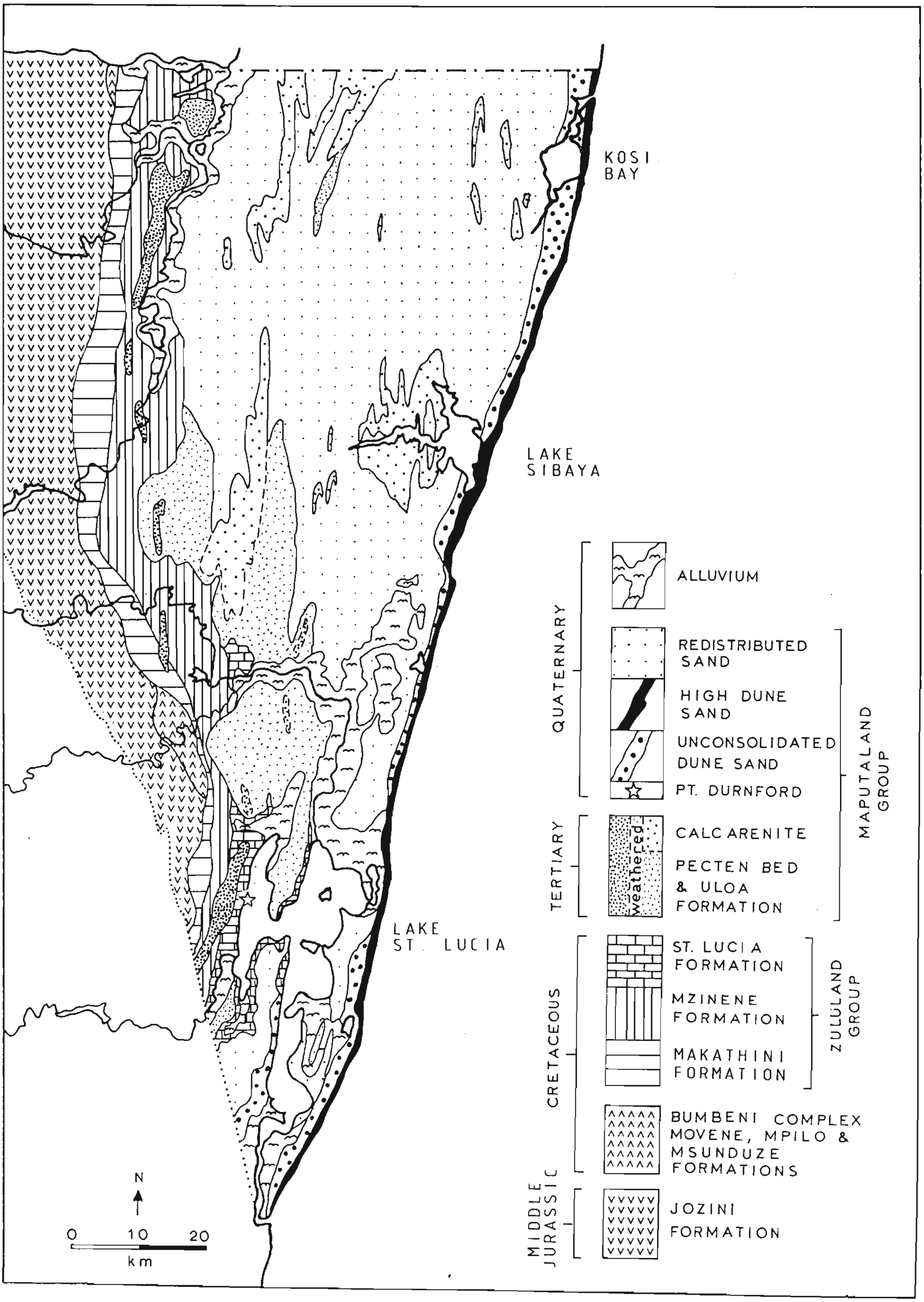


**Fig 2.5** Geological map of the Maputaland coastal plain. (After Watkeys *et al*, 1993).

| Era | Sub-Era | Period | Epoch | Group | Formation | Lithology |
|---|---|---|---|---|---|---|
| Cenozoic | Quaternary | Pleistogene | Holocene | Maputaland | Sibayi Formation | High coastal dune cordon; calcareous sand; lagoonal sands; lacustrine muds |
| | | | Pleistocene | | Kwambonambi Formation | Inland stabilised dunes and reworked sand; diatomite |
| | | | | | Kosi Bay Formation | Red sandy soil; cross-bedded sand; local calcarenite; lensoid carbonaceous sand |
| | | | | | Port Durnford Formation | Beachrock; coral bearing coquina; lignite; fossiliferous mudrock; calcarenite |
| | Tertiary | Pliocene to Miocene | Early to Late | | Umkwelane Formation | Red sandy soil; aeolian cross-bedded calcarenite |
| | | | | | Uloa Formation | Coquina (*Pecten* Beds); conglomerate |
| | | Palaeocene | Early | | | Fossiliferous shallow marine silts; thin clay lenses; hard concretionary horizons |
| Mesozoic | | Cretaceous | Late | Zululand | St. Lucia Formation | Fossiliferous shallow marine silts and fine sands; concretionary horizons; cross-bedded silts and fine sands; basal conglomerate |
| | | | Early | | Mzinene Formation | Fossiliferous shallow marine silts and sands |
| | | | | | Makathini Formation | Fossiliferous shallow marine clays; non-marine coarse fluviatile sandstone; conglomerate |
| | | | | | Bumbeni Complex | Pyroclastics; rhyolites; trachytes |
| | | | | | Mpilo & Movene Formations | Basalts |
| | | | | | Msunduze Formation | Conglomerate |
| | | Jurassic | Middle | Lebombo | Jozini Formation | Rhyolites |

Table 2.1 Stratigraphy of the Maputaland coastal plain. Note: the shaded nomenclature of the Maputaland Group has been proposed by G. Botha (1997) and is currently under review by the SACS Cenozoic Task Group.

### 2.2.2 Tertiary

Sediments of the Maputaland Group rest unconformably on the Upper Cretaceous sediments in northern KwaZulu-Natal (Botha, 1997). The Maputaland Group is a thin veneer of Cenozoic sediments which overlies the Zululand Group in northern KwaZulu-Natal. The Maputaland Group, as summarised in Table 2.1 and Fig. 2.6, has been proposed by G. Botha (Council for Geoscience - Pietermaritzburg) and is currently under review by the SACS Cenozoic Task Group.

The only known early Tertiary onshore strata are described from boreholes and excavations in the Richards Bay area. These consist of richly fossiliferous silts with thin lenses of clay and interbedded hard, calcareous, concretionary horizons (Maud & Orr, 1975). The sediments are lithologically similar to the underlying St. Lucia Formation but are separated from them by a hiatus spanning the Cretaceous/Palaeocene boundary (Dingle *et al.*, 1983). The elevation of the Palaeocene unconformity coincides with sea-level in the Richards Bay area (Maud & Orr, 1975). It is unknown whether Palaeocene sediments are preserved further north of Richards Bay in Maputaland.

The Uloa Formation consists of a thin basal conglomerate which is overlain by a 2 - 3 m thick coquina (Dingle *et al.*, 1983; Lui, 1995) which is considered to be late Miocene in age (Maud & Orr, 1975; Stapleton, 1977; Cooper & McCarthy, 1988; Watkeys *et al.*, 1993; Lui, 1995). The Miocene/Cretaceous unconformity was reported at elevations of -4 m to -13 m in the Richards Bay area (Worthington, 1978). The coquina is overlain by up to 20 m of aeolian cross-bedded calcarenites in places (pers. comm. G. Botha, 1996). Initially the calcarenites were regarded as upper Uloa Formation (Frankel, 1966; Maud & Orr, 1975; Cooper & McCarthy, 1988 & Lui, 1995). A marked lithological break exists between the calcarenites and the underlying coquina (Maud & Orr, 1975; Lui, 1995) a fact which has resulted in the proposal that this unit be given a separate formation status (G.Botha, 1997). This unit is assigned to the Umkwelane Formation in the proposed Maputaland Group nomenclature (Table 2.1; Fig. 2.6).

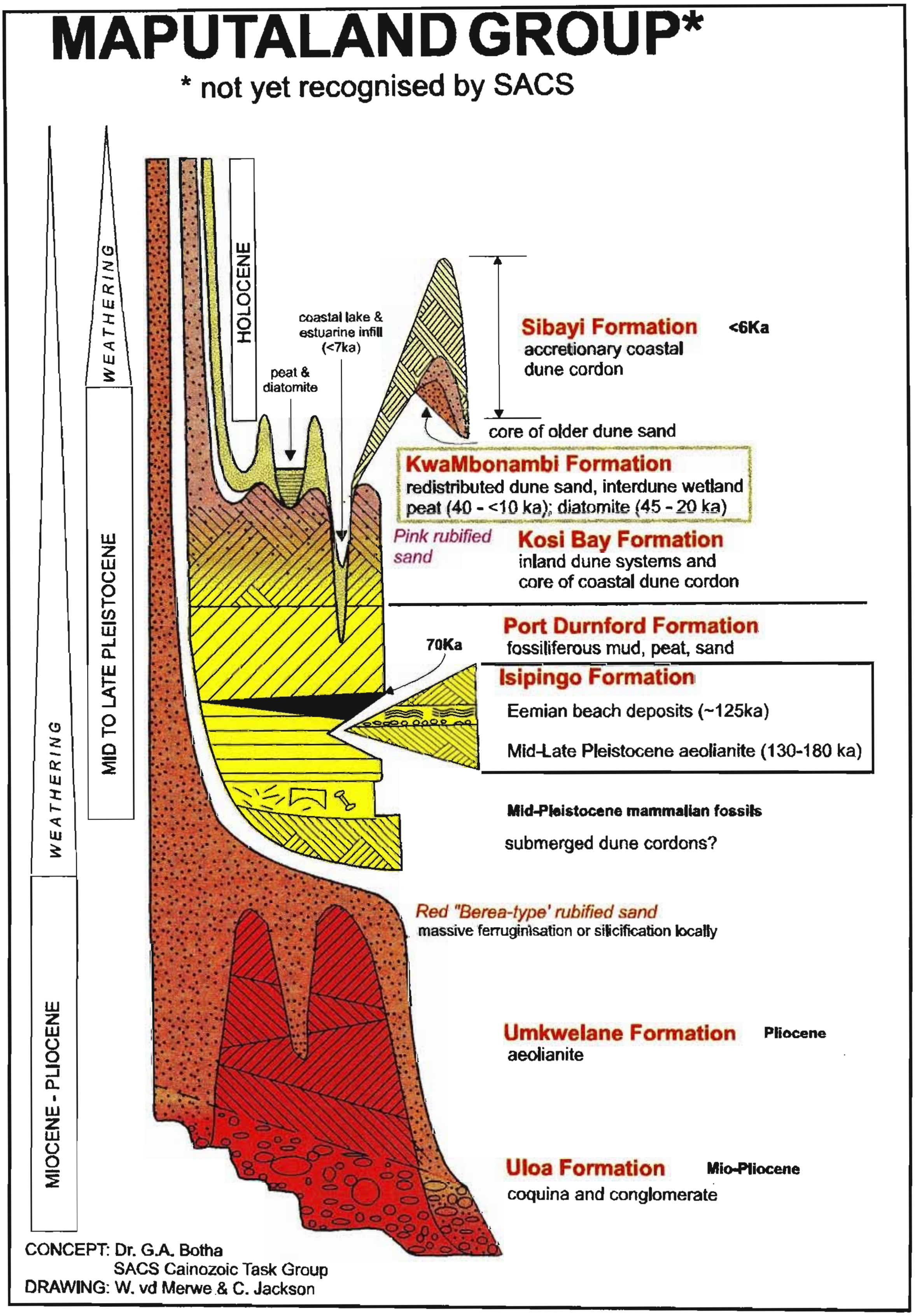


**Fig 2.6** Scematic composite section through the proposed **Maputaland Group** as proposed by Dr. G.A Botha. The subdivisions have been proposed by the SACS Cainozoic Task Group and are not yet recognised by SACS.

The lithology consists of a basal succession of beachrocks which are overlain by aeolian cross-bedded calcarenites (Maud & Orr, 1975; Lui, 1995). The upper surface of the Unkwelane Formation coincides with MSL in the Richards Bay area with minor fluctuations to between -10 m and +5 m above mean sea-level (Worthington, 1978).

**2.2.3 Pleistocene**

Pleistocene aged sediments of the Port Durnford Formation rest unconformably on eroded remnants of the Uloa and Umkwelane Formations. The sediments of the Port Durnford Formation to the north of Richards Bay, comprise a basal unit of discontinuous aeolian sediments which are unconformably overlain by fossiliferous shallow marine sands and organic-rich lagoonal clays (Hobday & Orme, 1974; Maud, 1993). The unit is ± 10 m thick and is overlain by a distinctive 1 - 1.5 m thick lignite horizon (Hobday & Orme, 1974; Maud, 1993). Hobday and Orme (1974) consider the Port Durnford Formation (their Lower Argillaceous Member) to be a transgressive barrier-lagoon complex which is related to the last interglacial highstand ± 120 000 BP. Fossiliferous beachrocks considered to be coeval with the last interglacial highstand are elevated ± 3.5 m above mean sea-level on the Ibella Peninsula at Lake St. Lucia (*pers. comm.* P. Ramsay 1996).

A thin bed of marine sands marks the base of a 15 m thick accumulation of arenaceous sediments which overlie the Port Durnford Formation. Hobday and Orme (1974) considered this unit (their Upper Arenaceous Member) to be part of the Port Durnford Formation. Sediments of this member constitute a thin basal unit of marine washover sands which are overlain by a thicker succession of predominantly medium-grained sands with characteristic large-scale cross-bedding (Hobday & Orme, 1974). This succession is punctuated occasionally with intermittent lenses of carbonaceous sand and occasional lignites (Hobday & Orme, 1974). This unit constitutes the Kosi Bay Formation of the proposed Maputaland Group (Table 2.1; Fig. 2.6).

Worthington (1978) reports an average thickness of 20 m (maximum of 40 m) for the Port Durnford Formation (his Middle Pleistocene Unit) reaching a maximum elevation of 40 m above MSL.

The KwaMbonambi Formation (proposed nomenclature of the Maputaland Group, Table 2.1; Fig. 2.6) consists of late Pleistocene decalcified dune sediments, redistributed sand, coastal wetland deposits and freshwater diatomite accumulations (Botha, 1997). Relic cordons of late Pleistocene dunes are evident in the Lake Sibaya region, forming a characteristic low undulating topography (Wright, 1995). Freshwater diatomite deposits banked up against the late Pleistocene dunes on the western shores of Lake Sibaya yield an age of more than 43 500 BP (Miller, 1996).

### 2.2.4 Holocene

Sediments of the Sibayi Formation (Proposed nomenclature for Maputaland Group - Table 2.1; Fig. 2.6) comprise a basal member of marine washover and lagoonal sediments which is developed in areas where the coastal dune barrier was breached during the Last Glacial Maximum (LGM). These deposits as well as late Pleistocene sediments are overlain by fine-grained, well sorted, aeolian sand of Holocene age. These sediments comprise the high coastal dune barrier which separates the modern beaches from the Maputaland coastal plain.

### 2.2.5 Recent Lake Sediments

The small catchment area (Fig. 2.1) and low runoff coefficient restricts the amount of fluvial sediment reaching the lake and accordingly Lake Sibaya has undergone very little sedimentation since its formation. The only new sediment collecting in the lake includes wind blown sediment and organic sediment that is added during high lake levels. During high water levels large areas surrounding the lake are inundated by water causing wholesale vegetation destruction and erosion of the surrounding dunes (Allanson, 1979) . Decaying vegetation is transferred rapidly into deeper areas of the lake by wave action where it contributes to the lake sediments in the form of an organic mud (gyttja). Aeolian sediment, which is stripped from surrounding dunes during high lake levels, accumulates in shallow areas near lake margins.

# CHAPTER 3 : RESEARCH METHODS

## 3.1 GEOPHYSICS

### 3.1.1 Navigation

Position fixes during the bathymetry survey were accomplished using two separate differential GPS systems on two separate cruises. The first cruise in May 1992 saw the use of the GPS *Pathfinder* differential system. This system is a non-real-time system which means that there is no data link between reference and mobile receivers, and therefore requires post processing on the *Pathfinder* differential correction program. The *Pathfinder* computer software automatically discards unreliable data during post processing enabling 2 m - 5 m resolution. A *Trimble* real-time differential GPS was used on all subsequent cruises including seismic profiling cruises. This system required no post processing as bathymetric data, time and corrected navigation data were downloaded directly into the survey computer in spreadsheet format. The accuracy of this system was tested on stationary points of known co-ordinates and it was found that the resolution varied between 0 m and 17 m with a mean accuracy of 8 m and a standard deviation of 9 m.

### 3.1.2 Bathymetry

The bathymetric survey for this study was carried out on board the Geological Survey Skiboat "Geocat" on three separate cruises over the period May 1992 to August 1993. Depth readings were taken with a 200 KHz Echotrac Model 3100 echo sounder with digital and paper output capabilities. Although the echo sounder is capable of recording depths with centimetre accuracy, decimeter resolution is a more realistic estimate when factors such as the roll and pitch of the survey vessel are considered. The echo sounder transducer was mounted in an "over the side" manner at the stern of the vessel in such a manner as to reduce flow turbulence. The echo sounder was calibrated using a "bar check" method whereby a bar or plate-like object was lowered to known depths below the transducer and the velocity of sound (in water) and draft values on the echo sounder were adjusted until the instrument recorded the correct values consistently over a range of depths. Depths were recorded at 2 - 10 second intervals depending on the complexity of the bathymetry in the area being surveyed. The digital output was downloaded into an integrated survey system package on a computer, together with a time and position fix. The paper output from the echo sounder was annotated every minute and was kept as a hard copy in the event of a digital output malfunction.

Bathymetric data were collected along predetermined north-south trending survey lines in the main basin of the lake. Random track lines were used to collect bathymetric data in other areas of the lake as well as around the circumference of the main basin. Tightly spaced random track lines were used to collect data in the Western Arm, Northern Arm and the northwestern part of the Main Basin where the bathymetry was more complex. Random track lines were run perpendicular to the bathymetric trend in the Northern Arm, Western Arm, Southwestern Bay and the Southern Basin. Approximately 420 line kilometres were surveyed for the compilation of the bathymetric map. The track line chart is shown in Fig. 3.1.

### 3.1.3 Seismic Profiling

The 3.5 KHz Edo-Western ("Pinger") sub-bottom profiling system was used in the first attempts at seismic profiling within the lake. This apparatus was largely ineffectual due to limited penetration achieved (7 m - 10 m) in the hard sands and to the rapid attenuation of the seismic signal in gyttja exposures.

Although the 3.5 kHz "Pinger" has high resolution capabilities (< 0.5m) (De Decker, 1987), this was of little consequence due to a lack of acoustically contrasting sediments lying within the penetrative range of this instrument. For seismic sources the resolution achievable in the vertical plane is roughly equal to one quarter wavelength of the dominant frequency of the propagated acoustic signal (Sheriff, 1985). The lower the frequency of the seismic source the greater depths of penetration that are achievable (Kennett & Ross, 1983). Consequently a more powerful "Boomer" seismic source with lower frequency output was used to achieve greater depths of penetration. Although the "Boomer" does not have the resolution capabilities of the "Pinger" system it is still considered a high resolution seismic profiling system.

The EG&G Uni-Boom seismic profiling system ("Boomer") was used with greater success, achieving up to 40 m of penetration and the capability to penetrate surface exposures of gyttja where accumulations were not too thick.

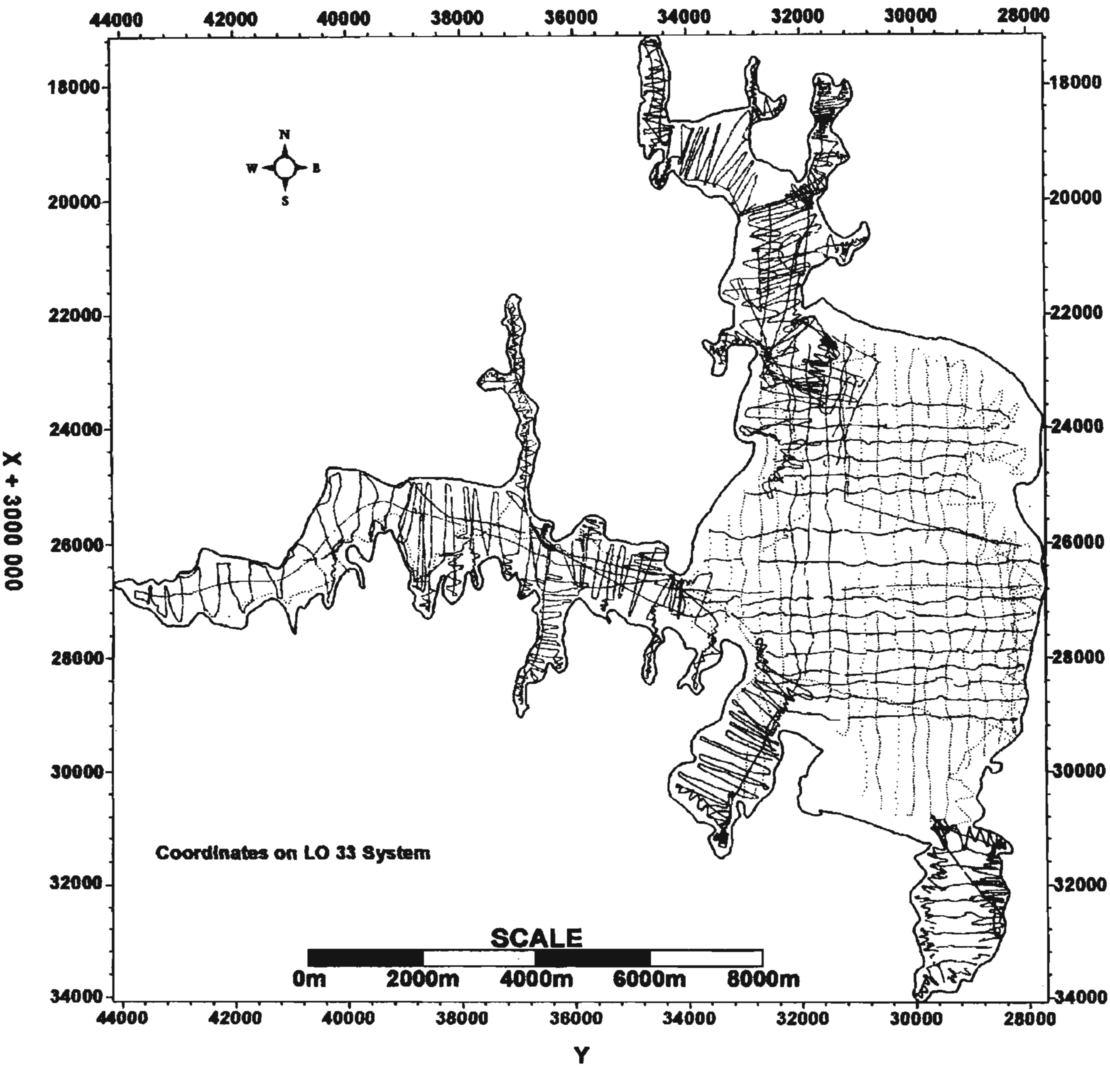


**Fig 3.1 Bathymetry trackline chart.**

The EG&G Boomer seismic profiling system consisted of;

- Model 234 seismic energy source,
- Catamaran mounted EG&G Model 230-1 source transducer,
- EG&G model 265 12 element hydrophone array,
- Model 4600 EPC graphic Recorder.

The EG&G Model 234 seismic energy source functions to convert AC at 230V to 3.5 KV DC and supply this on demand to the source transducer in 100, 200 or 300 joule pulses. The seismic energy source/transducer generates a broad-band (100Hz - 15KHz) pressure pulse into the water as a metal plate with attached rubber diaphragm is rapidly repulsed from an electro-magnetic coil. The transducer was "fired" at levels of 100 and 300 joules at a rate of 2 pulses per second (500 milliseconds). An EG&G 12 element hydrophone array with a frequency response of 0 - 20khz was used to detect arrival times of sub-bottom reflections from each "shot". Two types of low noise pre-amplifier were used in the hydrophone array namely the National 741 and the OP-07 by Analogue Divide. The EPC 4600 graphic recorder was used to produce the analogue by recording arrival times at 125 and 250 millisecond intervals.

Approximately 145 km of seismic traversing was undertaken with the "Boomer" seismic profiling system on two consecutive field trips to Lake Sibaya in August 1994 and February 1995. A survey grid consisting of north-south and east-west oriented survey lines spaced at 300 m intervals was generated using the NAVPCX software. Selected grid lines were surveyed by navigating with a *Trimble* differential GPS and the integrated NAVPCX programme which allows for steering at the helm by watching a monitor showing the boat position relative to the survey grid. The survey track chart is illustrated in Fig. 3.2. Surveying speed was kept between 3 and 6 knots which is the optimum range for producing "clean" records with the EG & G Uniboom seismic profiling system.

The hydrophone and the catamaran mounted transducer were towed on the opposite sides of the boat wake so as to minimize the direct pulse from the seismic source to the hydrophone array. When records were particularly "noisy" a motorcar tyre was towed in the boat wake to maximise this screening effect. Cleaner records were obtained when generators used for power supply

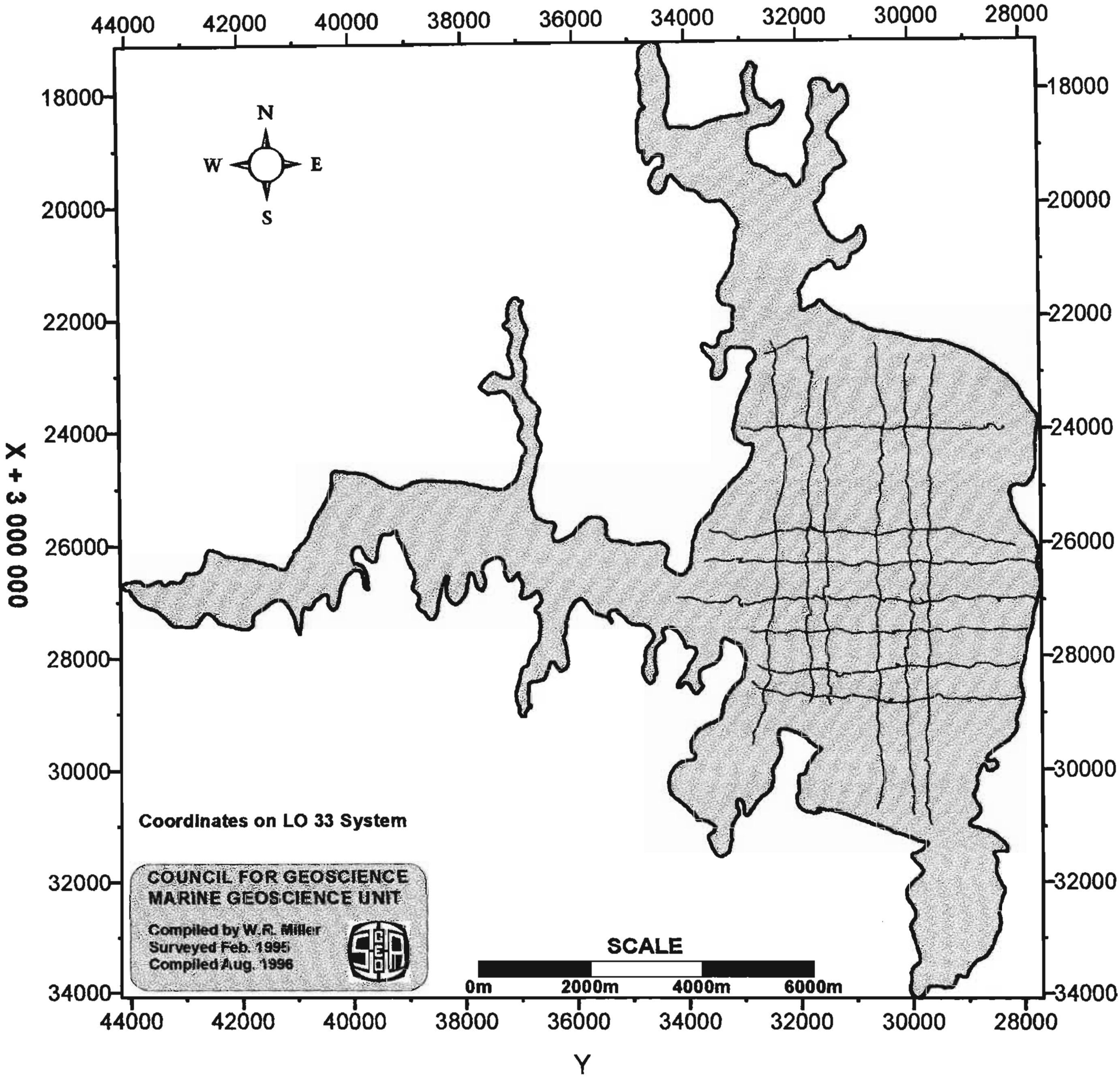


**Fig 3.2 Track chart of "Boomer" seismic survey lines.**

were mounted on a raised platform above the boat deck to minimize vibrations being transmitted to the water. The seismic records were annotated at 2 - 5 minute intervals. All data processing routines such as amplitude gain functions, and band-pass filtering were recorded in a logbook. Positional information from the differential GPS and bathymetry data were downloaded in X, Y & Z format to the NAVPCX survey package on a 386 notebook computer at 4 second intervals.

There was a marginal increase in penetration achieved when "firing" the seismic energy source at an output level of 300 joules as apposed to 100 joules. The 741 low noise pre-amplifier gave markedly cleaner records than records gathered with the OP-07 pre-amplifiers. The 741 pre-amplifiers were however less resilient, and some burnt out in shallow water when reflections from the sediment-water interface became too intense. The best seismic records in terms of depth of penetration and resolution of seismic reflectors were obtained for shot intervals of 0.5 milliseconds and for sweep-rates of 125 milliseconds.

## 3.2 SEDIMENT ANALYSIS

### 3.2.1 Sediment Sampling

A total of 515 grab samples were collected on consecutive field trips between August 1994 and February 1995. The samples were collected with a Van Veen grab which samples the top 2 cm to 10 cm of the bottom sediment. In addition to the grab samples, 22 sediment cores ranging in length from 2.4 m to 4.6 m were collected from the bottom of Lake Sibaya. The upper layer of sediments (the top 6 cm) from each core were analysed and added to the data set. Several of the grab samples were collected along traverses to investigate the changes in sediment grain-size statistical parameters with increased depth. All sample sites were fixed with a Lowrance hand held GPS unit that is capable of 10 m to 70 m accuracy (average 50 m). This precision was deemed adequate for this study. The sample sites are illustrated in Fig.3.3.

An outcrop of diatomite exposed on the western shore of Lake Sibaya was excavated, sampled and logged. After excavation of the basal section of the diatomite deposit a total thickness of more than 2.80 m was exposed. The outcrop was carefully logged according to sedimentology principles and was then sampled at 10 cm intervals. An organic rich horizon which was exposed at the base of the diatomite was sampled for radiocarbon dating.

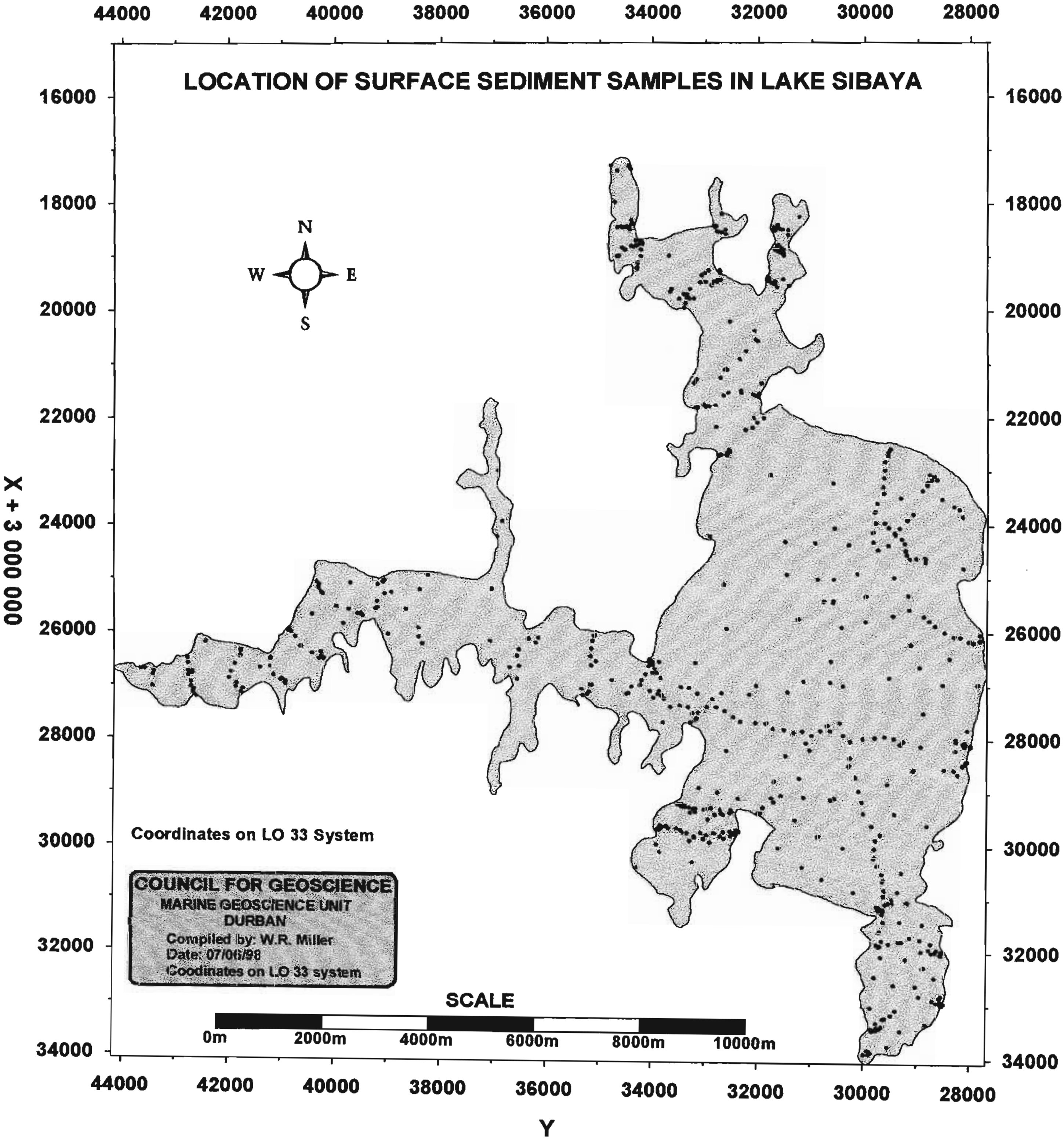


Fig 3.3 Grab sampling sites in Lake Sibaya.

All samples were stored in clearly marked 100 ml sample containers and transported back to the MGU offices in Durban for laboratory analysis. The laboratory preparation of samples is outlined in the flow diagram (Fig. 3.4) and aims to determine the relative percentages of mud, sand & gravel, carbonate content, organic content and sand grain-size statistical parameters.

### 3.2.2 Sediment Coring

The coring system used to collect sediment cores from Lake Sibaya was built by Peter Bova of the Council for Geoscience Bellville office. The coring system was based on the VK 300 Marine Kiel Vibracorer which was originally designed to take 4 m box cores. The system was modified from a vibracoring system to one that used a hydraulic jackhammer to drive 6 m core barrels into the substrate. The core barrels consisted of 6 m lengths of class 16 PVC tubes with an outer diameter of 63 mm and a wall thickness of 4.5 mm. Core catchers were cut from 1.5 mm pliable plastic sheets and inserted in the bottom of each core barrel to prevent sediment loss. The coring apparatus, which consists of a 6 m collapsible aluminium tripod, a specially adapted hydraulic jackhammer, hydraulic power supply, hydraulic hoses, and a hydraulic winch are mounted aboard a 5 m x 6 m coring barge. The barge which was built by Mr. Peter Bova consists of 4 large polystyrene blocks wrapped in heavy-duty industrial plastic and netting, bound together by a rigid framework of wooden planking held in position by galvanised metal clamps. The barge supports the aluminium tripod over an open "moonpool" at the centre of the barge. The tripod complete with jackhammer and core barrel are lowered to the lake floor by means of a hydraulic winch and cable. On arrival at the lake floor at least 6 m of cable is spooled off the winch, and two divers are deployed to activate the hydraulic jackhammer. The divers task is to assist the hydraulic jackhammer by applying added weight, and to monitor the coring process until the core barrel is driven to the maximum penetration or until point of refusal.

Once extracted the cores were stored in an upright position to allow for drainage and consolidation of the sediments. The cores were then cut into manageable lengths and transported to Durban for further analysis. The cores were split and logged according to sedimentology principles which included recording sediment type, grain-size, colour and the presence of fossil material within the sediments. Dateable materials were extracted and sent away for radiocarbon dating, textural analysis was undertaken on core samples and graphic core logs were produced.

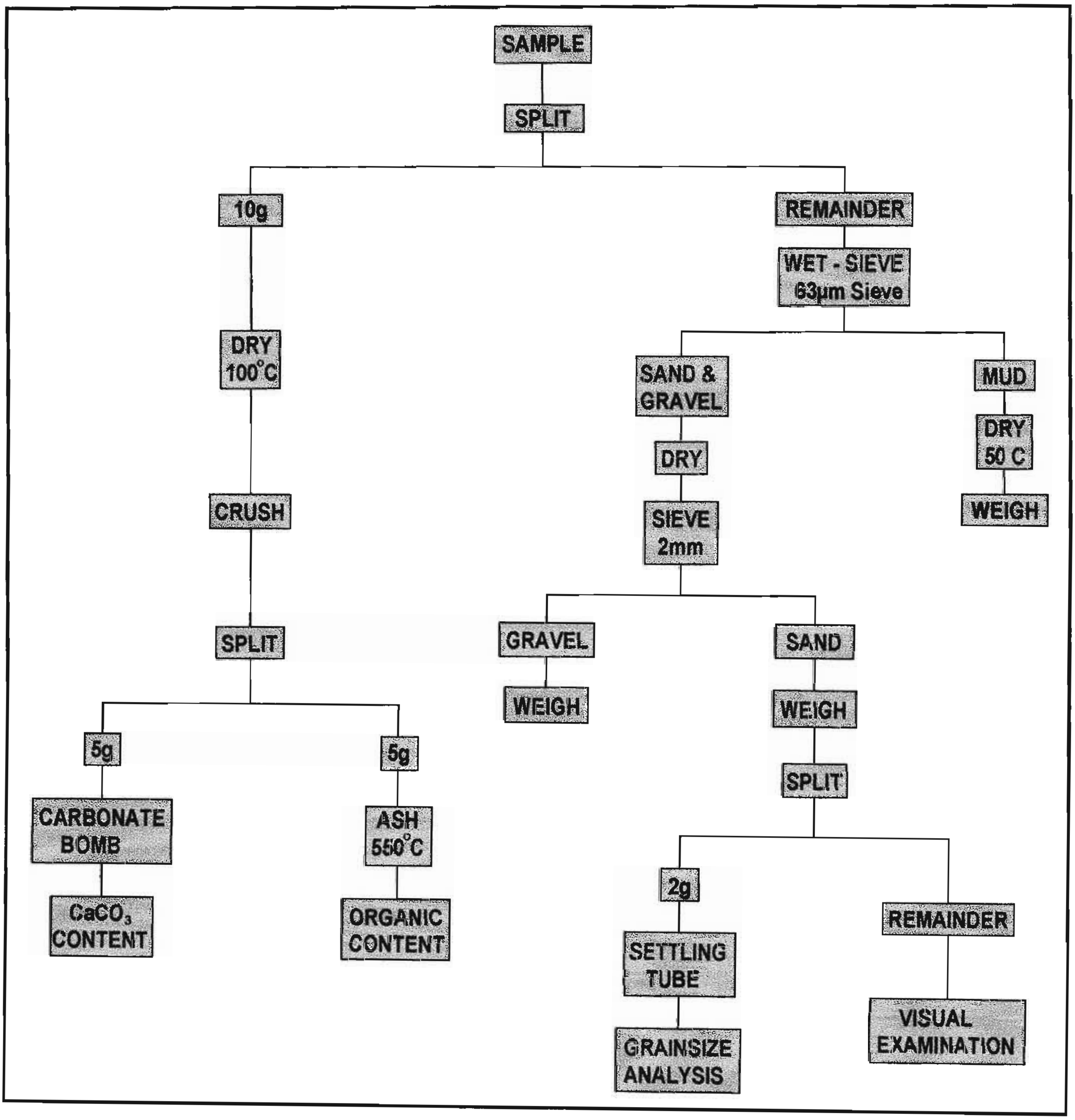


**Fig 3.4 Flow diagram showing laboratory treatment of sediment samples. (After Cooper & Mason, 1987).**

## 3.3 DATA REDUCTION

### 3.3.1 Bathymetry

Navigation data collected with the GPS *Pathfinder* differential system were stored as Geographical Co-ordinates (latitude and longitude) on the Clarke's 1880 spheroid after post-processing with the *Pathfinder* software. These data required a further conversion from Geographical Co-ordinates to the Lo 33 system (Longitude Origin). The Lo system is more practical for surveys since the X- and Y-axis are equal (orthogonal) making it easier to measure distance and calculate scales (De Decker, 1987). The conversion from Geographical co-ordinates to the Lo 33 system was accomplished using software obtained from the Department of Land Surveying at the University of Natal. The resulting data consisting of X- co-ordinates, Y- co-ordinates and time annotations were then imported as ASCII text files into the *Quattro Pro* software where depth values were manually added to the spreadsheet from the echo sounder records. The final spreadsheets consisting of X- and Y- co-ordinates with corresponding depth values were exported as ASCII files for gridding. A total of 9636 data points were processed in this manner.

The data collected with the *Trimble* real-time differential GPS were downloaded along with depth and time values, in a binary spreadsheet format onto a computer at the Geological Survey offices. A subroutine in the integrated survey package was used to convert the binary data to ASCII text. The data were then imported into the *Quattro Pro* package for manipulation in spreadsheet format. The data in the spreadsheet required editing for dilution of precision spikes (dop spikes), anomalous depth readings and for times when the differential link between receivers was lost. When the differential link is lost, the geodetic datum reverts from Clarkes 1880 to WGS 84 since no correction is being transmitted to the mobile receiver. This causes inaccuracies of up to 100m in the fixing of the boat's position. Once dop spikes, anomalous depth readings and non-differential data were edited out, the spreadsheets were exported in ASCII format ready for gridding. A total of 73846 usable data points were collected with the real-time GPS. A digitized outline of Lake Sibaya was prepared from thirteen separate 1 : 10000 orthophotos using the *Digitize* software and an A0 digitizing tablet. A total of 23644 digitized points were used to define the lake margins.

A total of 154 data files (99 bathymetry files and 55 digitized files) containing 107126 data points were merged into one ASCII file and imported into the Surfer ver. 6.02 software. The Surfer software grids data using weighted average interpolation algorithms. This means that the closer a data point is to a grid node, the more weight it carries in determining the Z value of that particular grid node. The data was gridded with a krigging method, using an octant search, a grid interval of 50m and a search radius of 500m. Krigging is a geostatistical gridding method that is recommended for most bathymetric investigations (Ramsay, 1990).

### 3.3.2 Seismic Profiles

The speed of sound in water was fixed at 1500 $ms^{-1}$ and the speed of sound through saturated sediment was estimated at 1750 $ms^{-1}$ (Browne, 1994). The resolution of the "Boomer" seismic profiling system, as determined from the analogue records, varies from 0.5 m - 1.5 m in the vertical plane. Sequence stratigraphic methods were employed to interpret the analogue records. Although sequence stratigraphy is usually applied to regional basin analysis surveys, facies analysis and depositional sequence studies can also be applied to high resolution seismic data by considering seismic events in terms of "packages" bounded by unconformities or laterally persistent disconformities (Mitchum *et al.* 1977).

The seismic records were analysed and a series of seismic overlays were prepared by tracing seismic reflectors from the analogue records on to drafting film. The seismic overlays/records which displayed the greatest depth of penetration and best resolution of the various seismic reflective packages were selected for presentation as fence diagrams. Principle reflectors were identified and used to delineate sequences and sequence boundaries.

# CHAPTER 4 : MORPHOLOGY OF LAKE SIBAYA

Lake Sibaya can be subdivided into 5 regions: Main Basin, Northern Arm, Western Arm, Southwestern Bay and Southern Basin (Hill, 1979) (Fig.4.1).

## 4.1 MORPHOLOGY

### 4.1.1 Main Basin

The Main Basin is the largest of these comprising almost 60% of the surface area of the lake. This water body is roughly oval in shape with the long axis measuring 8.75 km and trending north - south and the short axis measuring 6.5 km and trending east - west. The Main Basin is characterised by straight or gently curving shorelines which are punctuated by prograding sand bodies or by prominent dune ridges which encroach on the lake margins. Straight sections of the shoreline are located at the northern and southern extremities of the Main Basin in a downwind direction of the dominant northeasterly and southerly winds. A linear section of lake shoreline is located on the eastern shores of the Main Basin where the lake encroaches on the foot of the Pleistocene/Holocene dune complex.

### 4.1.2 Western Arm

The Western Arm has a roughly dendritic shape. The Western Arm is ± 10 km long and has an average width of ± 1.5 km. The southern bank of the Western Arm has an irregular shoreline which contrasts markedly with the more linear shoreline of the northern bank. The southern bank of the Western Arm has an irregular appearance due to back flooding of inter-dune hollows, whereas the dune topography of the northern bank has been truncated by fluvial processes (Fig. 4.2). Numerous non-perennial streams drain into the Western Arm along north - south oriented interdune marshes, the only exception is the Mseleni River which is oriented in an east - west direction and truncates dune cordons before draining into the Western Arm (see Fig.4.2).

### 4.1.3 Northern Arm

The Northern Arm measures a little over 4 km at the longest point and has an average width of ± 1km. The Northern Arm has three subsidiary arms which measure between 1.5 km and 2 km in length which give the shoreline a dendritic appearance. The subsidiary arms represent drowned

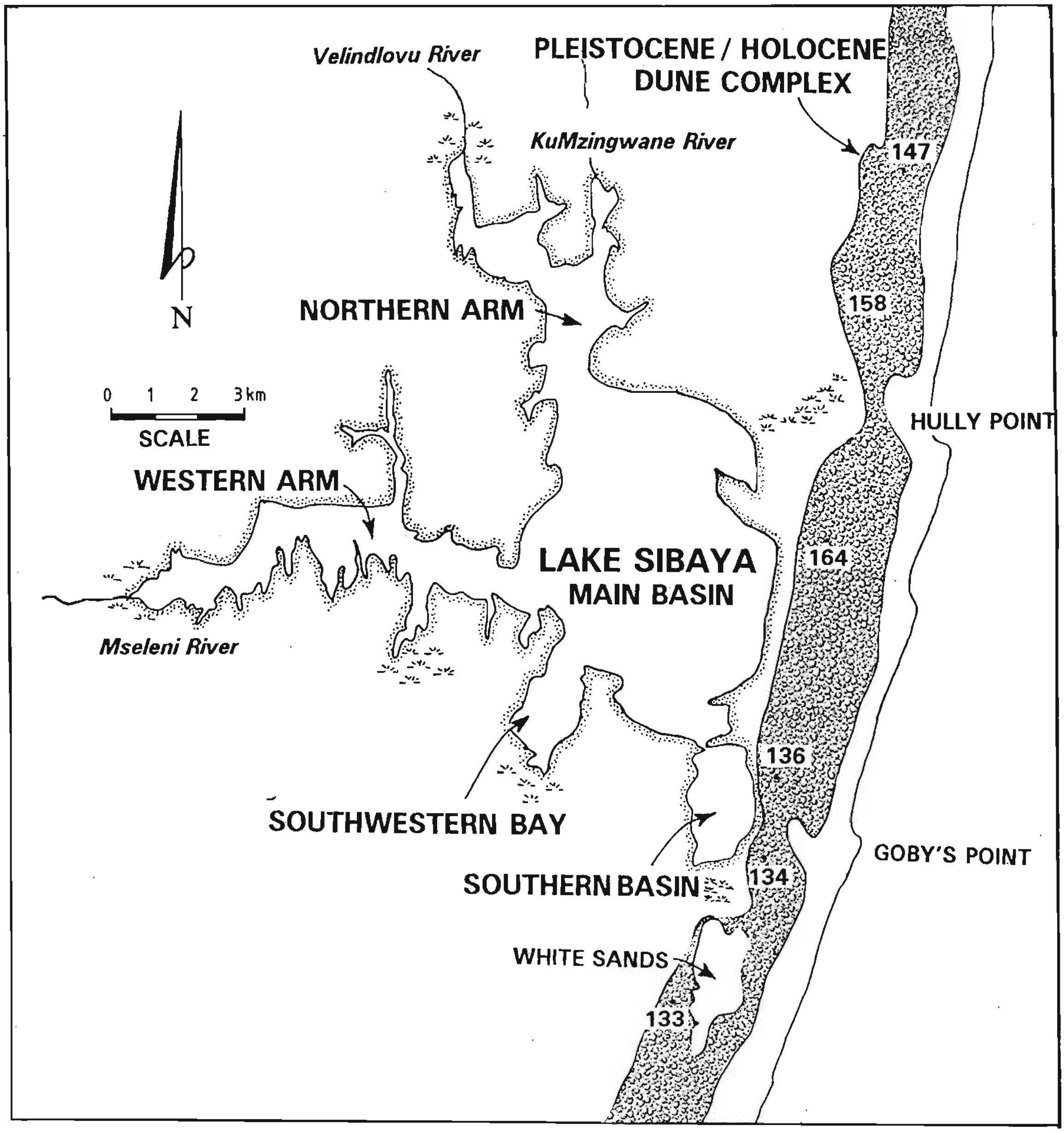


**Fig 4.1** Morphology of Lake Sibaya showing the Pleistocene/Holocene dune complex and some of the larger non-perennial streams that feed the lake.

**Fig 4.2** An oblique aerial photograph of the Western Arm of Lake Sibaya showing the backflooded dune topography of the southern bank in contrast to the truncated (linear) nature of the northern bank (foregound).

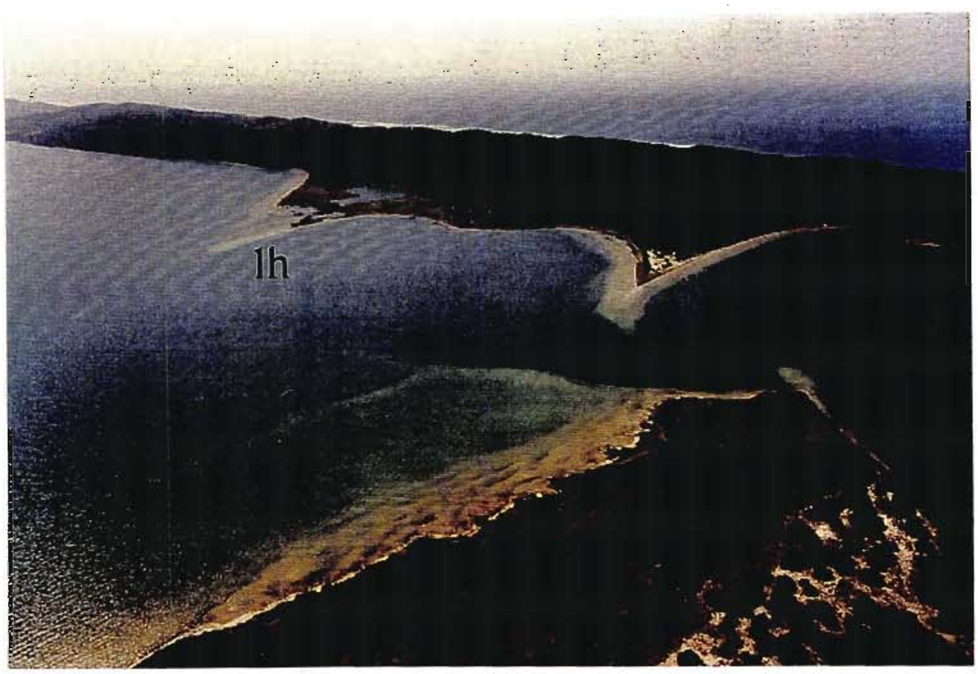


**Fig 4.3** An oblique aerial photograph showing the prograding sand spits 1h, 1i & 1j at the confluence between the Main Basin and the Southern Basin. Note the palaeoshoreline defined by the vegetation change in the bottom right section of the photograph. A drowned palaeoshoreline is also evident in the shallow water in the foreground.

dune topography and are fed by small non-perennial streams which drain along inter-dune marshes.

### 4.1.4 Southwestern Bay

The Southwestern Bay is enclosed between two prominent dune ridges which strike northeast - southwest and attain heights of 54 m in the east and 33 m to the west. The Southwestern bay is roughly oval in shape measuring 2.2 km in length and 1.5 km in width. The southwestern shore is exposed to wave activity driven by the strong northeasterly winds and is consequently more linear than other sections of shoreline in the Southwestern Bay. Small non-perennial streams drain into the Southwestern Bay along inter-dune hollows from the southwest.

### 4.1.5 Southern Basin

The Southern Basin is an oval shaped body of water that measures 2.75 km in length and 1.8 km in width. and 1.7 km in breadth. The Southern Basin is separated from the Main Basin by three prograding sand spits located at the confluence of the two water bodies (Fig. 4.3: 1h, 1i & 1j & Fig 4.4). A low lying sparsely vegetated area to the south testifies to the fact that the Southern Basin was much larger in extent in the recent past.

## 4.2 PROGRADING BEDFORMS

Prograding sand bodies in the form of sand spits and cuspate forelands are common along the shoreline of Lake Sibaya (Fig. 4.3 - Fig. 4.6). The prograding bedforms are the driving force behind lake segmentation processes, whereby sedimentary processes attempt to separate a large water body into a series of smaller, round or oval water bodies (Orme, 1973). The bedforms prograde during periods of high wind stress when wind-driven currents are operative. The size of the prograding bedforms is therefore dependent on sediment availability, wind speed and wind fetch. The largest of these bedforms are found in the Main Basin where large expanses of water are exposed to the dominantly northeasterly and southerly winds and where large amounts of sediment have been made available from the erosion of aeolian dunes during high lake levels. Four large-scale cuspate forelands are evident in the northern part of the Main Basin, two occurring on the western shore and two on the eastern shore (Fig. 4.4: 1b, 1c, 1f & 1g; Figs.4.5 & 4.6). All of these features prograde when the southerly wind stress is active. Two medium-

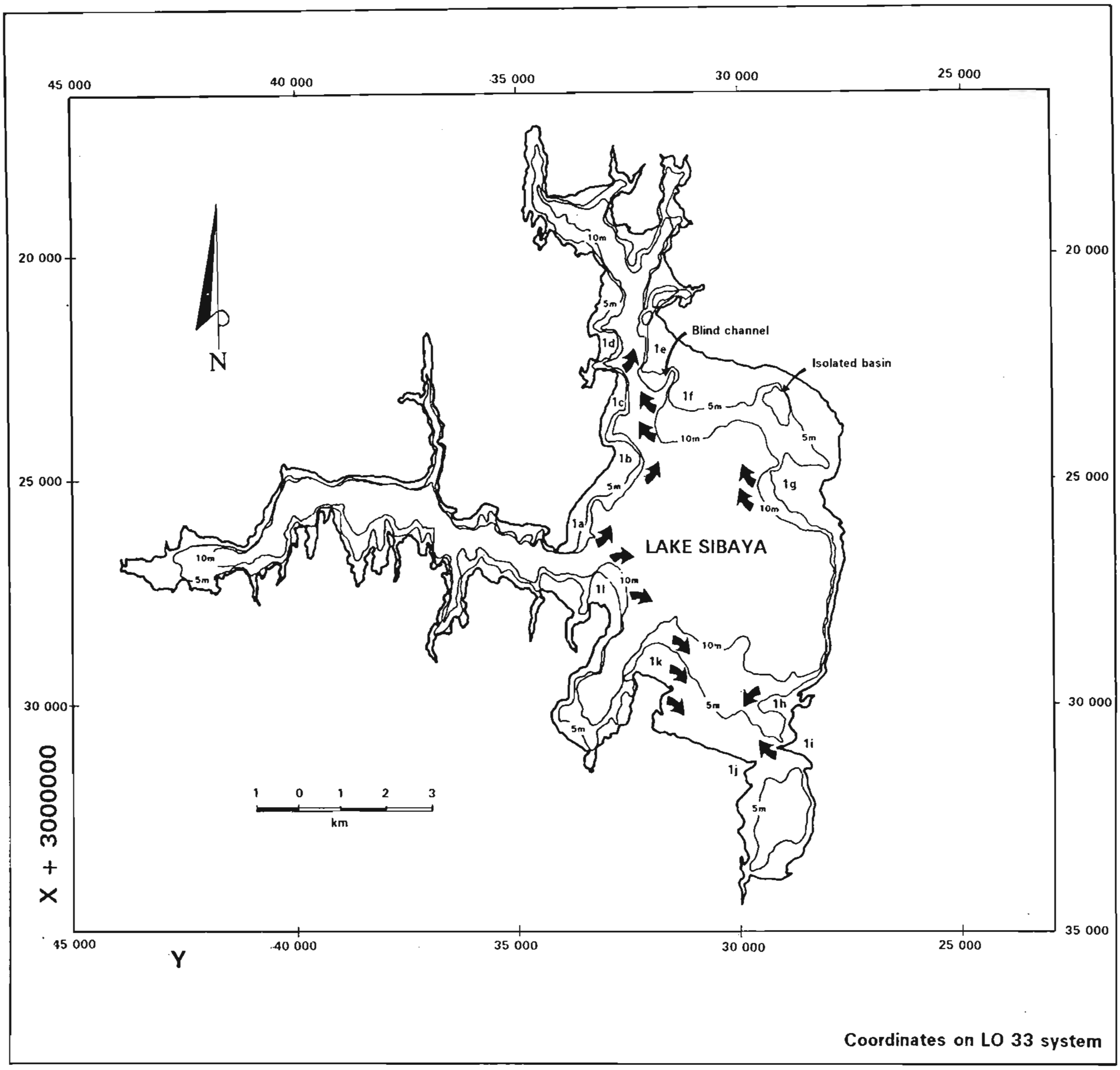


Fig 4.4 Lake Sibaya showing prograding sand bodies (1a - 1j) which are defined by tne 5 m and 10 m isobaths. Progradation of bedforms 1e - 1g from lake margins has led to the formation of remnant features such as the blind channel and isolated basin at the northern end of the Main Basin. Sand bodies 1k and 1l represent subaqueous extensions of aeolian dunes. Northerly facing arrows indicate sediment transport direction during periods of southerly wind stress, whereas the southerly facing arrows are indicative of sediment transport directions when the northerly winds blow. Note that the sediment from the drowned dune 1k has been reworked and has infilled the area to the east to create a large shallow terrace at the southern end of the Main Basin.

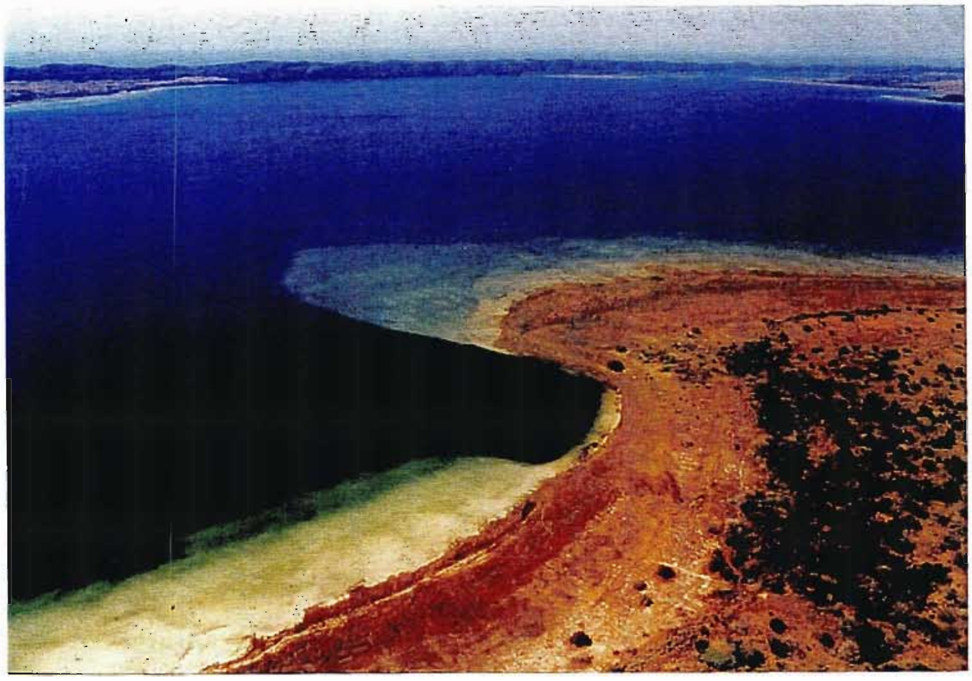

**Fig 4.5** An oblique aerial photograph showing cuspate foreland 1b. Note the development of underwater terraces which are related to older lake level lowstands. The tree line which mimics the lake shore is related to an older lake level highstand.

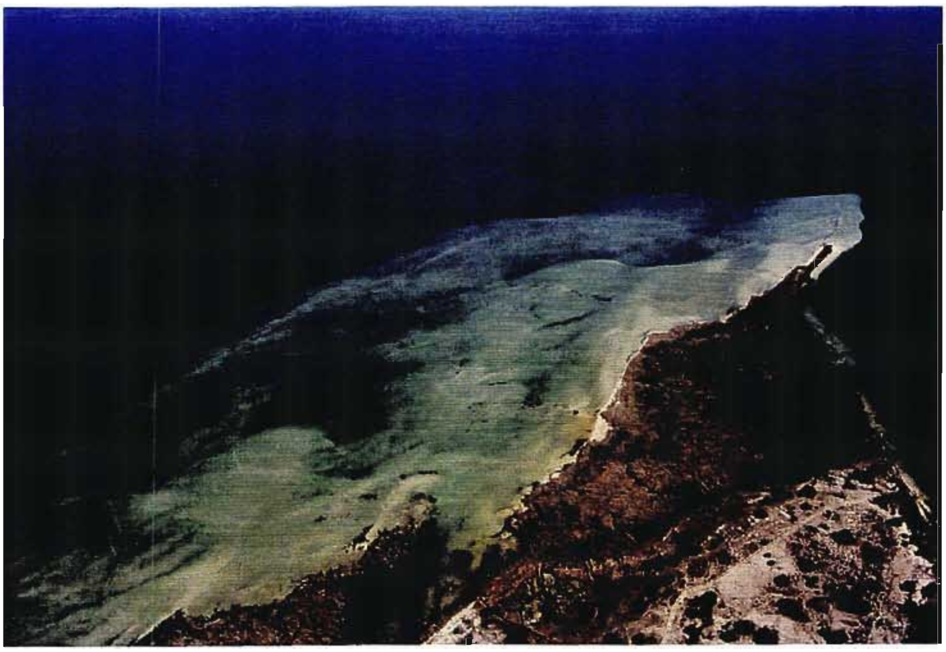

**Fig 4.6** An oblique aerial photograph showing cuspate foreland 1g. Note the presence of medium scale subaqueous dunes on the shallow terrace (1 - 2 m deep) and small scale subaqueous dunes on the deeper (2 - 3 m deep) terrace.

scale prograding sand spits are located on the southern shores of the Main Basin in the vicinity of the Southern Basin (Fig.4.3 & Fig.4.4: 1h & 1i:). The northerly sand spit (Fig.4.3 & Fig.4.4: 1h) progrades when the southerly wind stress is active and the southerly sand spit (Fig.4.3 & Fig. 4.4: 1i) progrades during periods of northeasterly wind stress. The "blind channel" and "isolated Basin" in the northern area of the Main Basin are late Pleistocene drainage features that are being infilled by sedimentation associated with the prograding of bedforms 1e, 1f and 1g (Fig.4.4) .

The Southern Basin and the Southwestern Bay show the development of small-scale, cuspate forelands which occur at regular intervals along the western shores of these water bodies. The eastern shores of the Southern Basin and the Southwestern Bay show less evidence of shoreline progradation than the western shores of these water bodies. This is probably a function of the larger dune ridges to the east which protect these shorelines from the strong southerly winds. The sand spits found in the Western Arm and Northern Arm are more proximal to the areas of sediment supply and occur as subaqueous extensions of aeolian dune ridges.

Although the northeasterly winds dominate for most of the year it is the southerly winds which generally have the highest speeds and are more effective sediment movers (Hunter, 1988). The dominance of sand bodies that prograde during southerly wind stress in the Main Basin, and the larger size of these features, compared with sand bodies which prograde during the periods of northeasterly wind stress, testify to this fact.

## 4.3 DISCUSSION

The morphology of Lake Sibaya is a product of a late Pleistocene drainage system that was incised during the LGM event and subsequently dammed by the development of a coastal dune barrier. Most of the features preserved in Lake Sibaya's morphology are directly related to this erosional event while others are related to modern lacustrine sedimentary processes. Sedimentary processes, driven by fluctuating water levels and wind driven currents are in the process of modifying Lake Sibaya's morphology by processes of infilling and shoreline progradation associated with the lake segmentation process.

# CHAPTER 5 : BATHYMETRY OF LAKE SIBAYA

The first bathymetric chart of Lake Sibaya was produced by B.J. Hill in 1969. The study was undertaken by running echo sounder traverses between prominent features on the shoreline of the lake. No GPS navigation was available at this time and the only echo sounders that were available were the type that produced an analogue record. The results (see Appendix 1) which although being of questionable accuracy by modern standards, are remarkably similar to those of the present study. The bathymetric data for this study have been corrected to the May 1992 level (19.82m above MSL.) which was determined from the water-level recorder operated by the Department of Water Affairs in the Southern Basin.

The dendritic forms of the Western and Northern Arms and the fact that a large proportion of the lake floor is located below sea-level indicate that Lake Sibaya represents a series of drowned river valleys that were cut when sea-level was appreciably lower (Hill, 1969). Fluvial incision probably took place during the Penultimate Glacial Maximum ± 150 000 BP and again during the LGM event ± 18000 BP when sea-level was ± 130 m lower than present (Ramsay, 1991; Wright & Mason, 1988). The lake has undergone little sedimentation since formation, the palaeodrainage pattern is thus preserved and is clearly visible on the colour bathymetric chart (Fig. 5.1).

## 5.1 MAIN BASIN

The most striking features of the Main Basin bathymetry are the extensive shallow areas located to the north and south, large-scale progradational sand bodies and a deep trough which is aligned roughly northwest-southeast (see Fig. 5.1). The shallow sand flats located at the northern and southern end of the Main Basin are areas that underwent lesser amounts of erosion during the LGM event. In the northerly area, the extensive sand flats are punctuated by an “isolated basin” and a “blind channel”. These are small-scale erosional features related to the LGM event that are currently being infilled by sedimentary processes. The asymmetrical profile of the "blind channel" (Fig. 5.2: cross section Q-R) and the geometry of sand lobes 1f and 1g (Fig. 5.3), suggests that infilling of these features is more rapid from the east. The "blind channel" is currently being infilled by sedimentary lobes 1e and 1f whereas the isolated basin has been formed by the progradation of sand lobe 1g ( Fig.5.3).

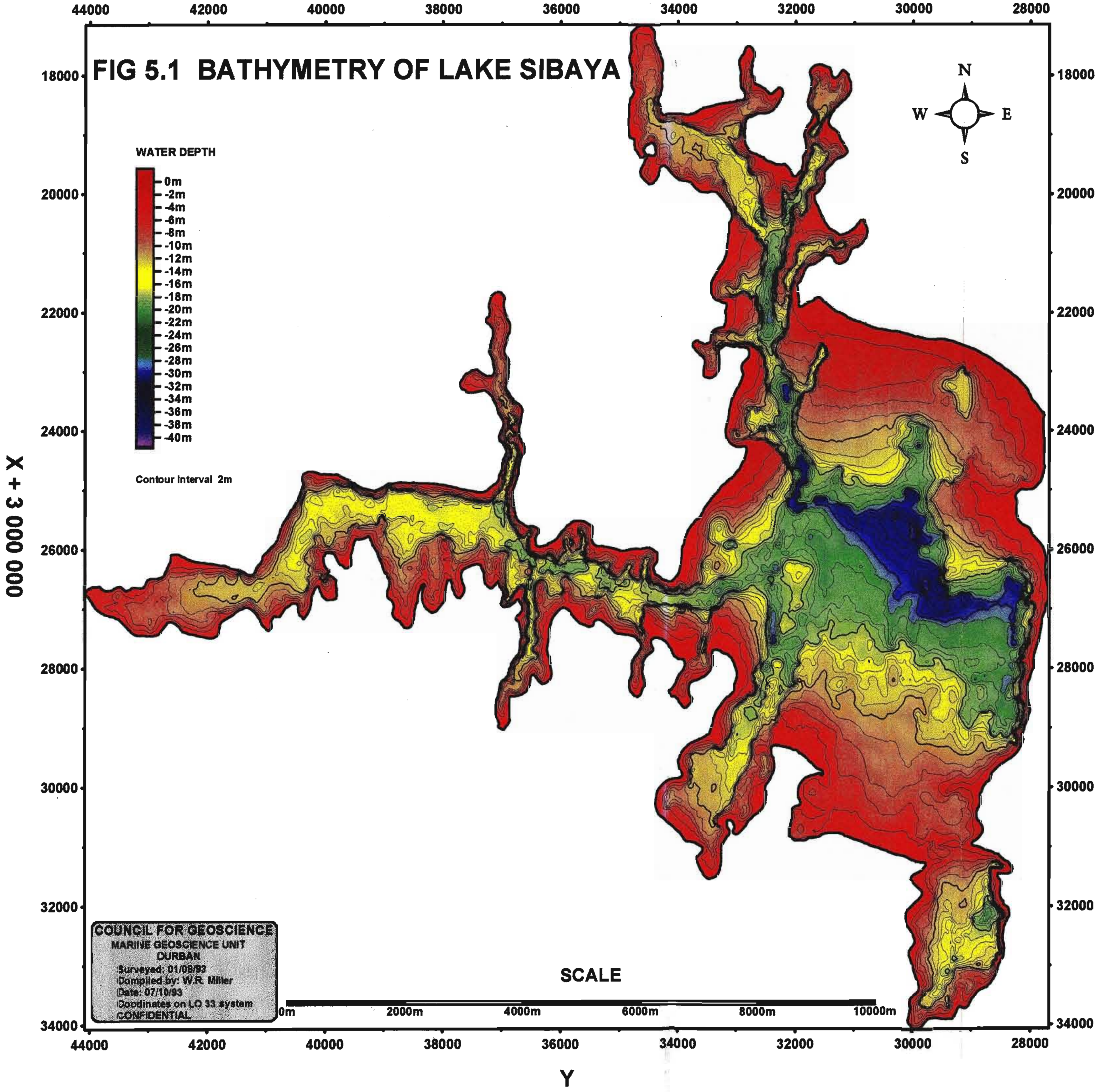


FIG 5.1 BATHYMETRY OF LAKE SIBAYA

FIG 5.2 BATHYMETRIC CROSSECTIONS

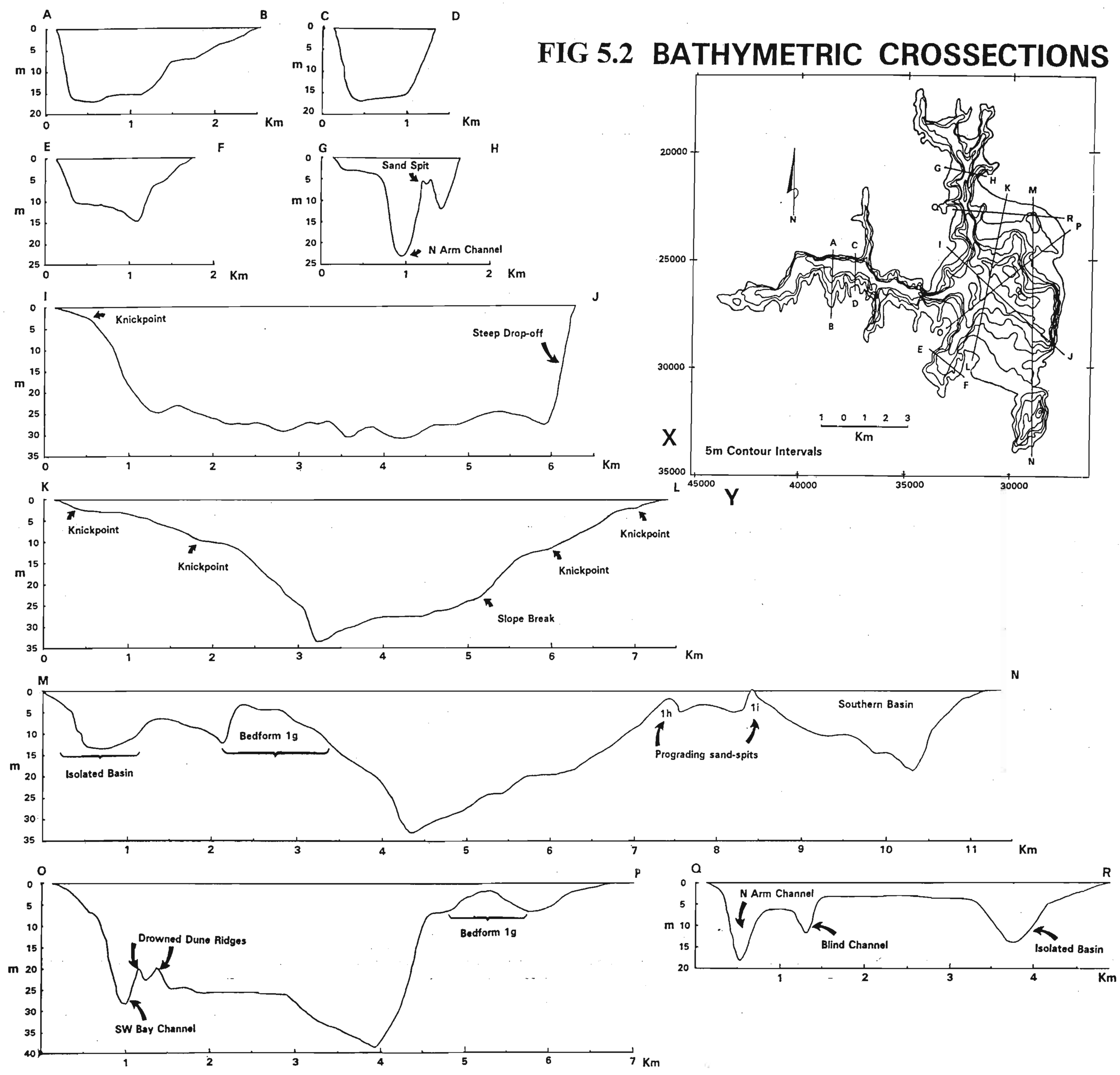

Two partially drowned aeolian dunes are evident at the southern end of the Main Basin (Fig.5.3: 1l & 1k, ). The extensive shallow area located at the southern end of the Main Basin has probably been infilled to some extent with sediment derived from the drowned dune 1k during periods of northerly wind stress. Progradation, which is characterised by convex shaped sand lobes, has progressed to depths of 10 m in the Main Basin and is more pronounced in the northern areas (see Fig.5.1 & Fig. 5.2). Subtle knickpoints occur in the Main Basin at -2.5 m, -9 m and -12 m and are related to previous lake stillstands ( Fig.5.2: cross sections I-J & K-L). The -2.5 m terrace is related to the lake levels observed in the early 1970's which was later drowned by a 2 m to 3 m rise in lake levels in 1975 (see Fig. 2.4). The -9 m and -12 m terraces are related to a more ancient lake level lowstands. A slope break occurs at the -20 m isobath in the Main Basin indicating the depth at which ancient dune topography is preserved (Fig.5.2: cross-section O-P; Fig. 5.1). The -20 m isobath probably defines the ancient landscape at the time of lake closure and the beginning of back flooding of the ancient topography.

The drowned valleys which originate in the Northern Arm, Western Arm and the Southwestern Bay can be traced for considerable distances along the floor of the Main Basin. The valleys are interrupted by a slight shallowing trend where the peripheral water bodies meet the Main Basin, due to infilling associated with lake segmentation processes. The drowned valley originating in the Northern Arm is deepest at the confluence with the Main Basin. The palaeovalleys emerging from the Western Arm, Southwestern Bay and Northern Arm converge in the western area of the Main Basin and continue as one valley to form the deep northwest - southeast oriented trough.

A steep drop off on the eastern shores adjacent to the Pleistocene/Holocene dune complex indicates that the dune development has encroached on the lake margins since the lake became an isolated system (Fig.5.2: cross-section I-J). The eastern shores of the Main Basin are characterised by a narrow wave cut terrace which has a maximum width of 20 m - 30 m and reaches depths of ± 3 m before dropping away steeply into deeper water. This wave cut terrace experiences high energy wave conditions during periods of wind stress. Wave fronts break obliquely across the terrace and, in doing so, generate longshore sediment transport to areas of deposition where the wave-cut terrace widens.

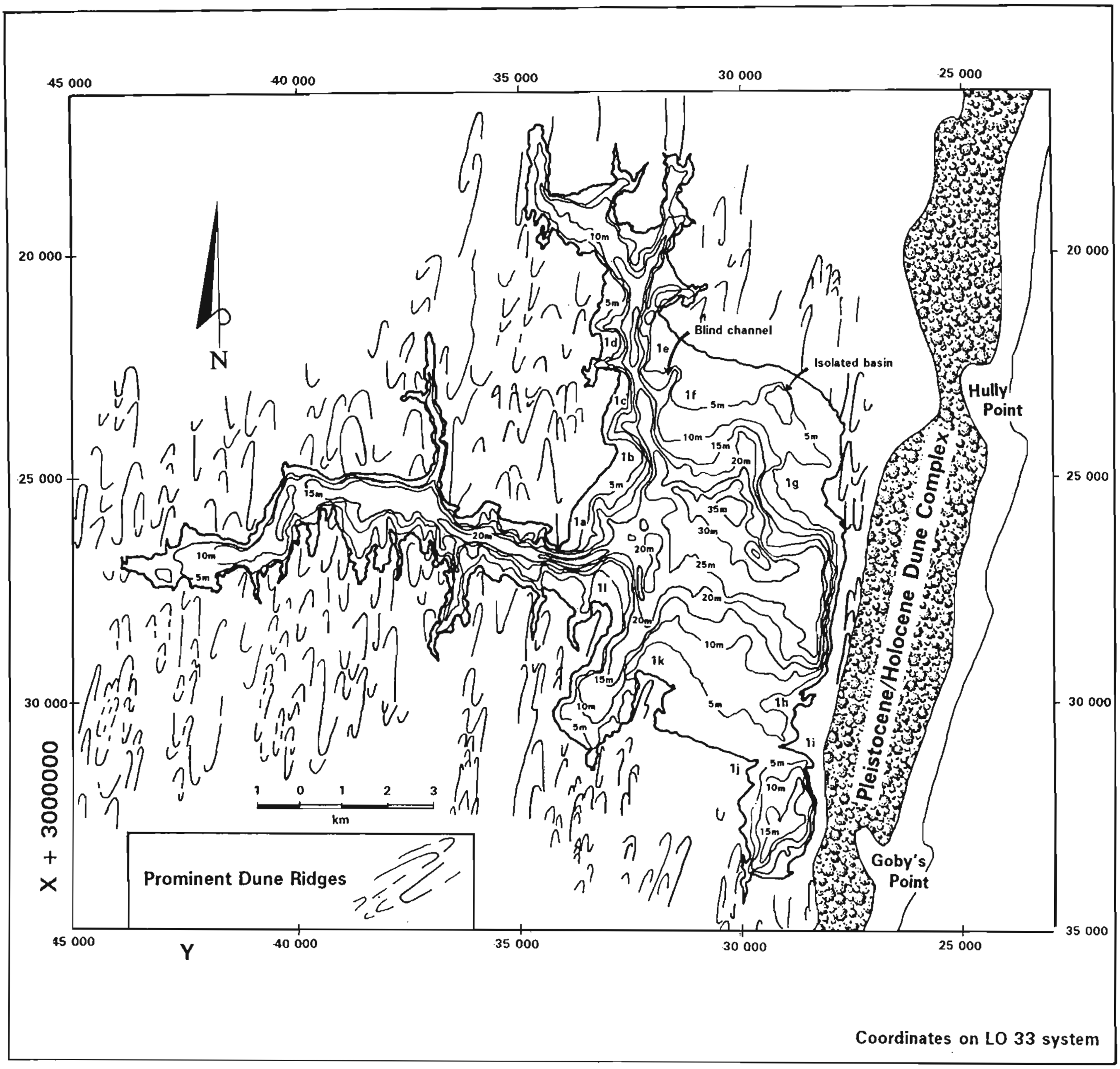


Fig 5.3 Bathymetry of Lake Sibaya contoured at 5m contour intervals. Areas of the shoreline that are prograding are indicated by symbols 1a - 1g (cuspate forelands) and 1h - 1j (sand spits). Note that progradation in the Main Basin has encroached to depths in excess of 20m. The bedforms 1k and 1l represent subaqueous extensions of aeolian dunes that have been partially reworked by sedimentary processes within the lake. Note that the original dune topography is preserved to water depths of 20m. Subaerial exposures of prominent dune ridges which occur near the lake margins are also illustrated.

## 5.2 WESTERN ARM

The Western Arm is a drowned river valley which deepens to 22 m at the confluence with the Main Basin. The Western Arm has a pronounced asymmetrical profile due to the fact that the northern bank of this feature drops away steeply into deep water (Fig.5.2: sections A-B & C-D). In contrast, the southern bank is characterised by back flooded dune topography, sand spits and a more gentle gradient. The northern bank of the Western Arm is a product of fluvial incision which manifests itself as straight sections of shoreline that truncate dune topography, show steep gradients and show little shoreline progradation. The otherwise straight sections of shoreline of the northern bank are interrupted by a long back flooded interdune hollow, located two thirds of the length along the Western Arm, and by prograding sand spits located closer to the Main Basin. The back flooded interdune hollow deepens to 10m at the confluence with the Western Arm and has a symmetrical underwater profile. The bathymetry of the southern bank of the Western Arm is complex, due to back flooding of interdune hollows and subaqueous extensions of aeolian dune ridges (see Fig.4.2). The back flooded interdune hollows have symmetrical profiles which deepen uniformly towards the confluence with the Western Arm. Sand spit development is dependent on sediment availability and therefore these features, unlike the spits in the Main Basin, are restricted to areas where dune ridges encroach on lake margins. The size and mobility of these features increases towards the Main Basin because of increased exposure to the prevailing winds.

## 5.3 NORTHERN ARM

The Northern Arm comprises three drowned valleys which merge just above the confluence with the Main Basin. Two smaller valley forms merge with the Northern Arm valley at the confluence with the Main Basin. These features are smaller scale palaeodrainage features. The Northern Arm deepens to a maximum of 25 m but the bathymetric trend narrows and shallows at the confluence with the Main Basin. This "narrowing and shallowing" results from lake segmentation processes whereby prograding sand bodies infill the confluences between water bodies in an attempt to isolate the smaller water bodies (Orme, 1973). The bathymetric trend shows that infilling in the region between the Northern Arm and the Main Basin is mainly from the east, where large amounts of sand are reworked into prograding bedforms under conditions of southerly wind stress. Small scale progradation of the shoreline in the Northern Arm is evident where small sections of the shoreline are exposed to the southerly winds. Sand spit development is also observed where large amounts of sediment have been made available from the erosion of dune ridges during past highstands of the lake.

### 5.4 SOUTHWESTERN BAY

The Southwestern Bay has an elongate shape that resembles a drowned valley and is locally modified by prograding sand bodies from lake margins. The small-scale drainage which joins the Southwestern Bay from the southwest testifies to the fact that fluvial processes have played a part in the formation of this water body. The Southwestern Bay gradually deepens to 20 m at the confluence with the Main Basin where the "narrowing and shallowing" trend associated with lake segmentation is once again evident.

### 5.5 SOUTHERN BASIN

The Southern Basin is an oval-shaped water body that has a basin-like geometry. The confluence between the Southern Basin and the Main Basin narrows markedly due to the presence of two sand spits which are prograding towards one another from opposite banks (Fig.4.3: 1i & 1j). The bathymetry shallows to less than 4 m indicating high sedimentation rates and an advanced stage of lake segmentation processes in this area. The eastern shore of the Southern Basin, which encroaches on the base of the Pleistocene/Holocene dune complex, is characterised by a narrow wave cut terrace which drops away rapidly from -3 m to a depth of -15 m. Small-scale shoreline progradation is evident on the gentler gradients of the western shore where prograding bedforms have encroached to a water depth of ± 5 m. A deep trough extends roughly northeast-southwest across the Southern Basin reaching a maximum depth of 25 m in the southwest. This trough represents a remnant of the original bathymetry of the Southern Basin which is being infilled from the north and west. The Southern Basin is in advanced stages of the lake segmentation process.

# CHAPTER 6 : SEDIMENT DISTRIBUTION IN LAKE SIBAYA

## 6.1 SEDIMENT TYPE

Five sediment types are evident in and around Lake Sibaya namely; ground-water ferricrete, diatomite, red consolidated dune sand, quartz sand, and gyttja.

### 6.1.1 Ground-water Ferricrete

Ground-water ferricrete is intermittently exposed around the periphery of Lake Sibaya and outcrops in places below lake level. This sediment type is the only lithified material exposed in the vicinity of the lake. The ferricrete consists of numerous sub-angular to rounded nodules with an ochre to dark brown coating of ferrous oxides. The ferricrete nodules vary in size from 0.02 m diameter up to as large as 2.0 m diameter (see Fig 6.4). The ferricrete nodules are irregular in appearance with some having symmetrical channels running into or through them. These channels may represent solution features or ancient root structures that were present in the unlithified sediment.

The ferricrete is dusky red when viewed on a freshly broken surface and the texture varies from massive to finely laminated. The ground water ferricrete is fine to coarse-grained with subangular to angular grains. The modal proportions of minerals which comprise the ground water ferricrete are; 66 % quartz, 17 % feldspar, 12 % heavy minerals and 5 % lithic fragments. The feldspars are evident as white kaolinized flecks on freshly broken surfaces of the ferricrete. The ferricrete exposures probably represent an ancient deflation surface where heavy minerals were concentrated by wind winnowing. The heavy mineral content of this sediment which consists of magnetite, ilmenite and rutile, is above background for the area, as late Pleistocene and Holocene dune sands have a heavy mineral content of less than 2 %. The genesis of the ferricrete is a result of the interplay between slightly acidic ground water, and heavy mineral enriched sediments. The distribution of ground water ferricrete in the Lake Sibaya area is illustrated in Fig.6.1.

### 6.1.2 Diatomite

Diatomite is a siliceous deposit made up of microscopic diatom cell walls (frustules). A freshwater diatomite is intermittently exposed along the western shores of Lake Sibaya and along the

Western Arm of the lake. The diatomite exposures occur as terrace deposits backed up against older aeolian sediments of the Kosi Bay Formation (Fig 6.2 & Fig 6.3) (Botha, 1997; Miller, 1996). The diatomite is strongly laminated and light to dark grey in colour when moist and fades to a very pale grey to white powder upon desiccation. These subaerial diatomite exposures are punctuated by black horizons rich in organic material and sparsely developed lenses of bottle green chert. The diatomite deposits are late Pleistocene lacustrine deposits that accumulated under variable climatic conditions between ± 43500 BP and ± 25500 BP (Miller *et. al.*, 1997). The distribution of diatomite exposures around Lake Sibaya is illustrated in Fig. 6.1.

Diatomite sediments are also located beneath Lake Sibaya where they blanket the drowned dune topography of older aeolian sediments. These sediments represent shallow interdune lake deposits which accumulated during early to mid-Holocene times (see Chapters 7 & 8).

### 6.1.3 Red Consolidated Dune Sand

This sediment type is informally known as the "Berea type" red sand which occurs as isolated exposures along ± 500 km of coastline along the east coast of southern Africa. The "Berea type" sand is a fine-grained, mottled, red-brown semi-consolidated clay rich sand (see Fig 6.5). The sand was originally deposited as a free flowing dune sand during late Tertiary to early Pleistocene times and has undergone alteration in the post depositional physico-chemical environment to produce the semi-consolidated nature of this sediment (Botha, 1997; Dunlevy, 1997). The sand fraction of the "Berea Type" red sand is dominated by quartz (75 - 90 %) with smaller amounts of heavy minerals (2 - 20 %) and traces of feldspar (< 3 %). The mud fraction (<63 μm) which comprises 10 - 15 % of the sediment, consists predominantly of quartz grains, kaolinite and an amorphous aluminium-iron hydroxide (Dunlevey, 1997). These ancient dune sediments are easily set apart from the younger dune sands by virtue of their colour, consolidated nature and an increase in clay content. One exposure of this sediment type is located in the Northern Arm of Lake Sibaya (Fig. 6.1 & Fig 6.5).

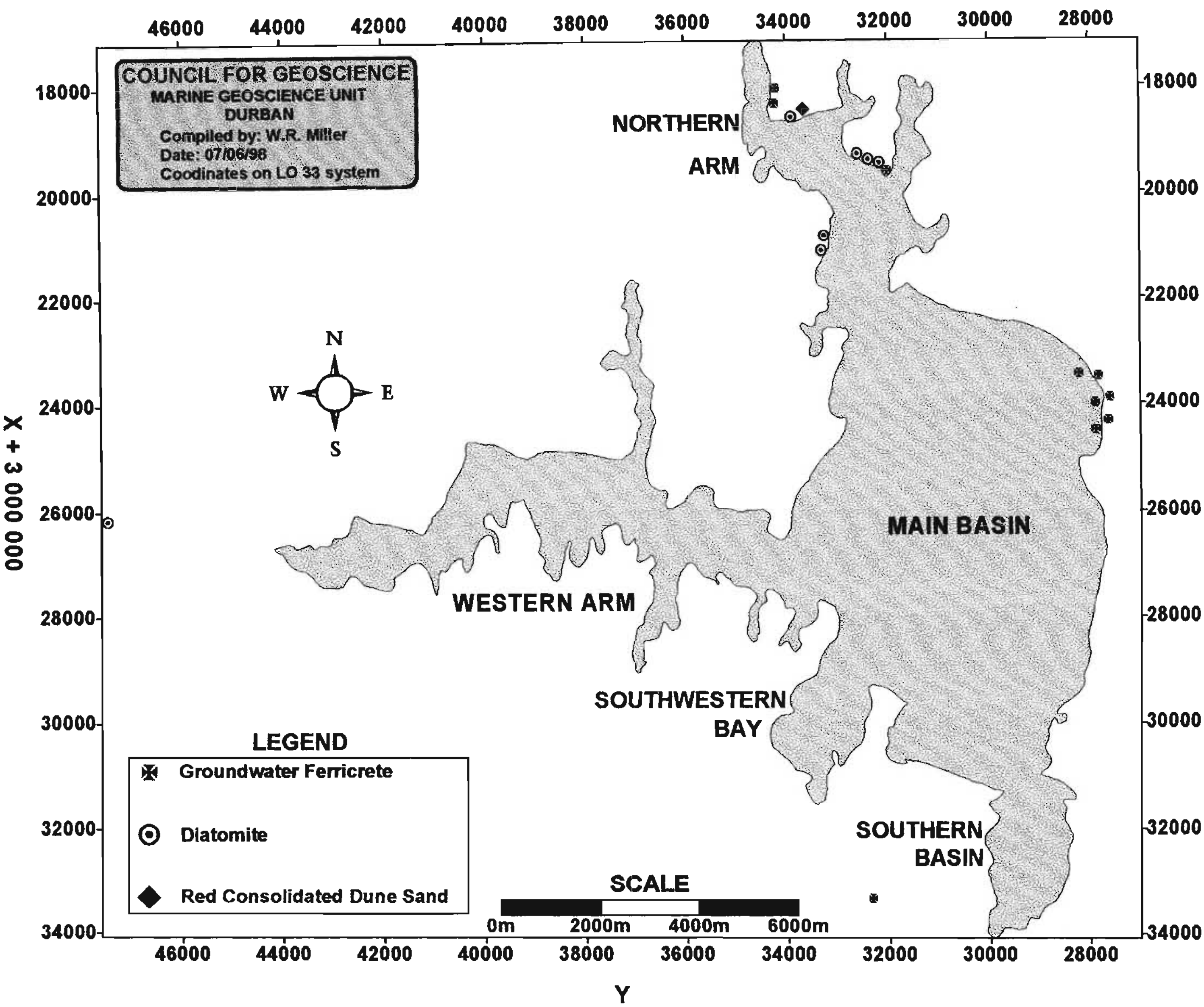


**Fig. 6.1 The distribution of known outcrops of ferricrete, diatomite and consolidated red dune sand in the vicinity of Lake Sibaya.**

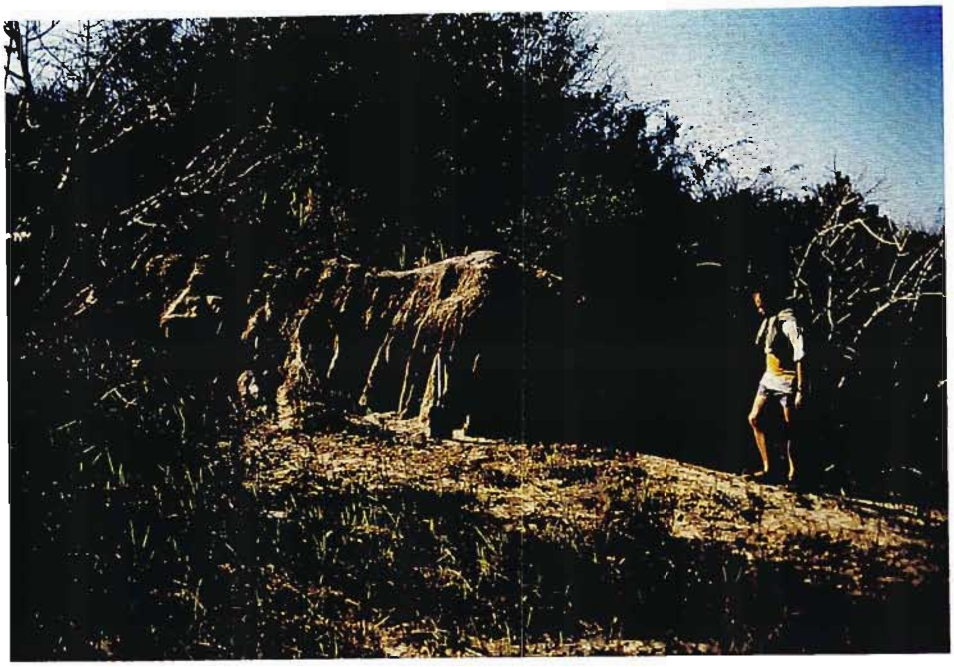

**Fig 6.2** A diatomite exposure located in the Northern Arm vicinity of Lake Sibaya. The deposit is backed up against an older vegetated dune ridge seen in the background of this photograph.


**Fig 6.3** A photograph of the ochre coloured clay rich sand which forms the base of the diatomite deposit. This sediment type is thought to represent an ancient weathering profile in older aeolian sediments.

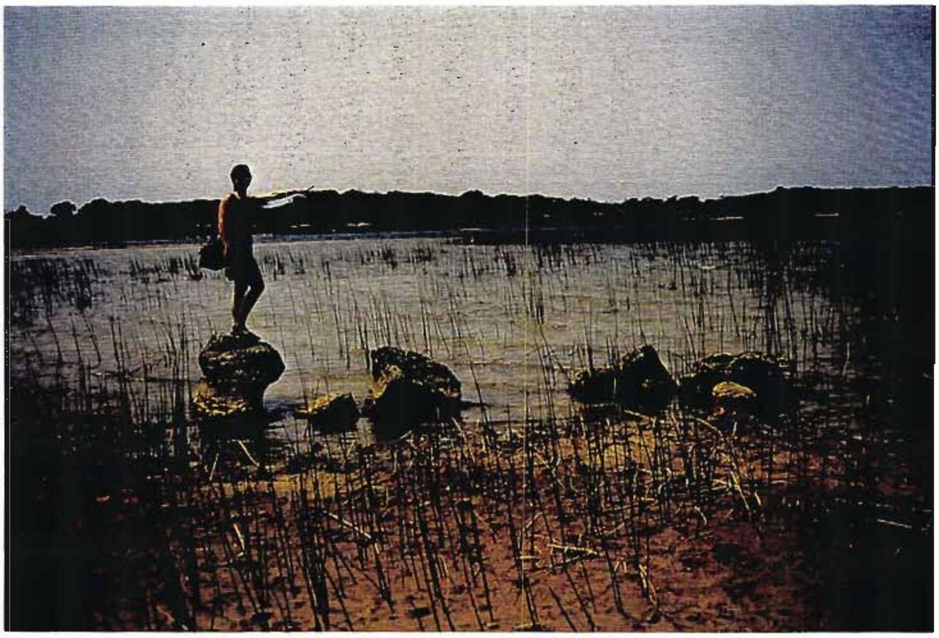

**Fig 6.4** An example of the nodular ground-water ferricrete which is intermittently exposed near the margins of Lake Sibaya. This exposure is located on the shoreline of the Northern Arm.

**Fig 6.5** A photograph of the red consolidated dune sand located on the shoreline of the Northern Arm (see Fig 6.1). Note the highly mottled appearance of this sediment type.

### 6.1.4 Quartz Sand

The sand varies from white to light olive in colour and ranges in grain size from very fine-grained to medium-grained. The rounding of the sand grains ranges from angular to rounded. The mud content of the sand is characteristically less than 2 % but can be as high as 20 %. The organic carbon content of the sand is low (typically less than 1 %) but can be as high as 8 %. The sand fraction comprises ± 99 % quartz with minor amounts of feldspar, heavy minerals, organic matter and shell fragments. The heavy mineral concentrations are highest along the eastern shores of the main basin adjacent to the Pleistocene\Holocene dune complex and in the Northern Arm adjacent to an exposure of red Tertiary\Pleistocene dune sand. Shell fragments are concentrated along the lake shoreline in the shallow areas as well as in shallow lagoons above water level. The preservation potential for the shell fragments is low due to the acidity of the lake water and the thin shelled nature of the freshwater gastropods and bivalves.

Binocular microscope studies indicate that there is more than one population of sand grains lying at the sediment-water interface below Lake Sibaya. The sand grains are derived from different generations of aeolian dunes of which there are at least four in the Lake Sibaya area (Wright, 1995; Miller, 1996). Wind generated currents and waves, as well as lake level fluctuations are responsible for the reworking and sorting of the lake floor sediments. The surface distribution of quartz sand in Lake Sibaya is illustrated in Fig. 6.6.

### 6.1.5 Gyttja

Gyttja is a dark grey to black organic-rich mud that is found in the deeper and more sheltered areas of Lake Sibaya. The gyttja is derived from the breakdown of the fringing vegetation that is destroyed during periods of high lake levels. Dune vegetation also contributes to gyttja development where the canopy is proximal to the lake on the eastern shores. The decaying vegetation is gradually broken down and carried in suspension to the deeper areas of the lake where current velocities are low enough to facilitate its deposition. Gyttja deposits have a high methane content and consequently have a characteristic domed shape on the lake floor (Miller, 1996). This sediment type contains on average 22 % sand (>63 μm) and has a mean organic carbon content of 27 %. The surface distribution of gyttja in Lake Sibaya is illustrated in Fig. 6.6.

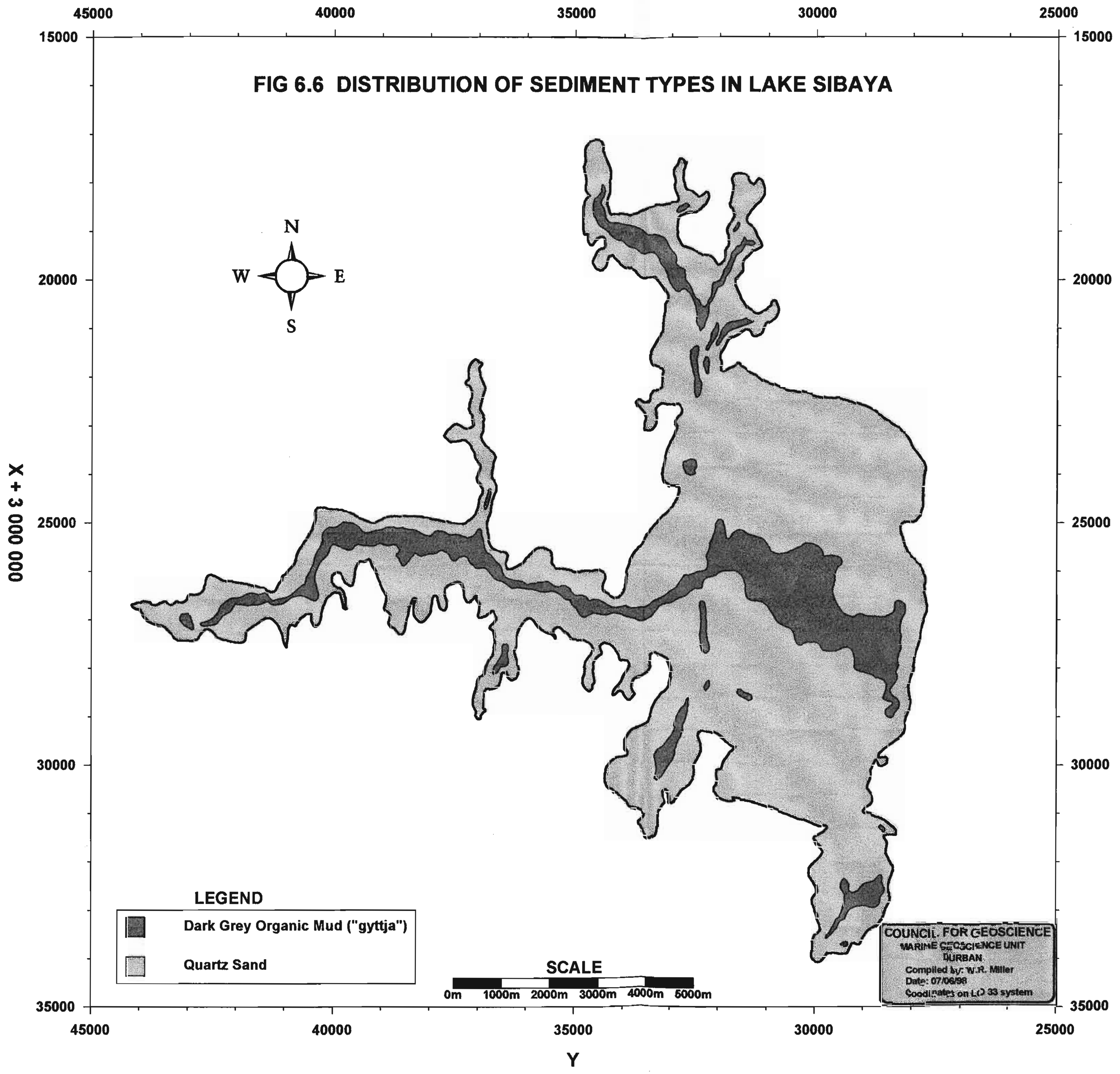


FIG 6.6 DISTRIBUTION OF SEDIMENT TYPES IN LAKE SIBAYA

## 6.2 SAND STATISTICAL PARAMETERS

The basic descriptive element of all sediments is grain-size, which can be characterised in terms of mm or phi units ($\varphi$). A geometric scale was devised by Wentworth in 1922 to subdivide sediments into a number of classes based on grain-size measurements in mm. The phi unit ($\varphi$) is the logarithmic transformation of this scale and is used in most grain size studies since it has the advantage of making mathematical calculations much easier (Tucker, 1991). A number of statistical parameters can be deduced from grain-size distribution curves or directly from grain-size data, these are: mean grain-size, mode, median grain-size, kurtosis, sorting and skewness. The statistical parameters are calculated using the Folk & Ward formulae given in Table 6.1 below (Folk & Ward, 1957). Some of the statistical parameters are more useful than others, consequently the mean grain-size is used in preference to the mode and median grain-size. Kurtosis has no geological significance and is consequently ignored (Tucker, 1991). The statistical parameters were calculated with a BASIC based software package and a computer linked settling tube which yields results comparable to standard sieving techniques (Wright & Mason, 1990).

| PARAMETER | FOLK & WARD FORMULA |
|---|---|
| Median | $Md = \varphi_{50}$ |
| Mean | $M = \frac{\varphi_{16} + \varphi_{50} + \varphi_{84}}{3}$ |
| Sorting | $\sigma\varphi = \frac{\varphi_{84} - \varphi_{16}}{4} + \frac{\varphi_{95} - \varphi_{5}}{6.6}$ |
| Skewness | $Sk = \frac{\varphi_{16} + \varphi_{84} - 2\varphi_{50}}{2(\varphi_{84} - \varphi_{16})} + \frac{\varphi_{5} + \varphi_{95} - 2\varphi_{50}}{2(\varphi_{95} - \varphi_{5})}$ |

**Table 6.1** Formulae for the calculation of sediment grain-size parameters from grain-size data.

The statistical parameters are not only useful in describing sediments but can also yield valuable information on sediment provenance, movement and depositional processes (Lewis, 1984). The relationship between the various sand statistical parameters has also been used to distinguish between different sedimentary environments (Dyer, 1986).

A study of sediment distribution was undertaken at Lake Sibaya in 1990 (Wright & Mason, 1990) and the results are available in Appendix 2 for comparison.

### 6.2.1 Sorting

Sorting is a measure of the spread of the grain-size distribution and is one of the most useful parameters, as it gives an indication of the efficiency with which a depositional medium is able to separate sediment grains of different size classes (Tucker, 1991). Sediment sorting is dependent on several factors which includes; sediment source, grain-size and depositional mechanism. The sediment sorting in Lake Sibaya varies from very well sorted (< 0.35) to moderately sorted (0.71 to 1.00). The distribution of sand sorting is illustrated in Fig. 6.7 and is summarised in Table 6.2 below.

| SORTING | φ VALUE | SURFACE AREA |
|---|---|---|
| Very well sorted | < 0.35 | 5.46 $Km^2$ |
| Well sorted | 0.35 to 0.5 | 46.91 $Km^2$ |
| Moderately well sorted | 0.51 to 0.7 | 20.16 $Km^2$ |
| Moderately sorted | 0.71 to 1.00 | 1.47 $Km^2$ |

**Table 6.2** A summary of the area covered by the various categories of sand sorting in Lake Sibaya.

The surface sediments of Lake Sibaya comprise well sorted (63.4%), moderately well sorted (27.2%), well sorted (7.4%) and moderately sorted (2%) sand fractions. Very well sorted, fine-grained sand forms a thin veneer around the lake margins. These grain-size parameters are consistent with aeolian sand suggesting that surrounding dune sediments are contributing to lake sediments during periods of high water levels. Moderately well sorted sand has a complex distribution pattern on the floor of Lake Sibaya and is confined to the area between the -2 m and -20 m isobaths (Fig. 6.7). In the Main Basin of the lake the moderately well sorted sand distribution is located in the shallow areas to the north and south and a smaller area in the west. The distribution pattern (Fig. 6.7) suggests that the moderately well sorted sand population was deposited in areas between the -2 m and -4 m isobath and the -10 m and -20 m isobath. Subsequent reworking has led to mixing of these populations in areas to the north and south of the Main Basin. Moderately sorted sand is confined to the northern eastern area of the Main Basin and to isolated areas in the Northern Arm ( Fig. 6.7).

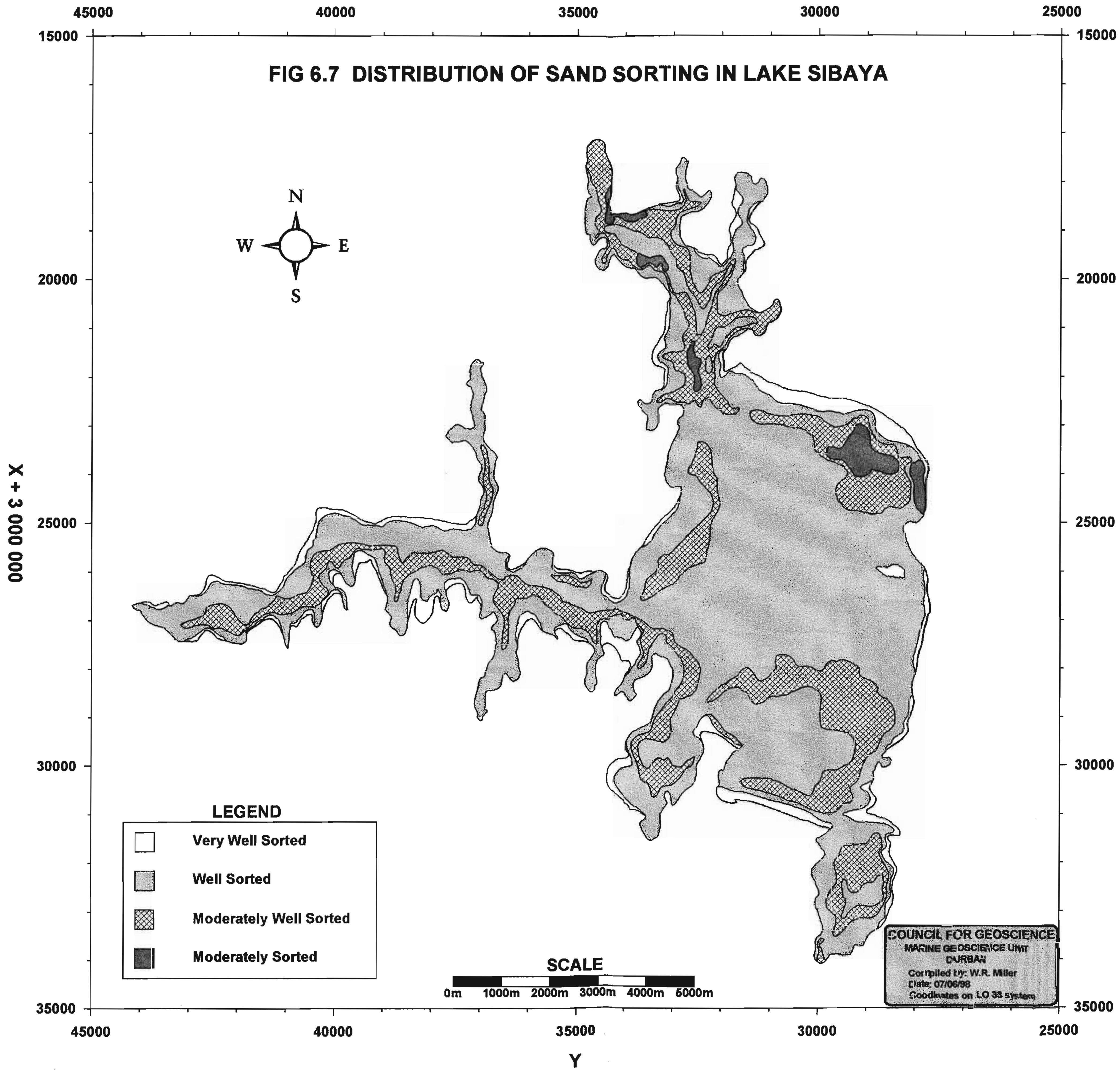
FIG 6.7 DISTRIBUTION OF SAND SORTING IN LAKE SIBAYA
45000
40000
35000
30000
25000
15000
20000
25000
30000
35000
X + 3 000 000
Y
N
W
E
S
LEGEND
Very Well Sorted
Well Sorted
Moderately Well Sorted
Moderately Sorted
SCALE
0m 1000m 2000m 3000m 4000m 5000m
COUNCIL FOR GEOSCIENCE
MARINE GEOSCIENCE UNIT
DURBAN
Compiled by: W.R. Miller
Date: 07/06/98
Coordinates on LO 33 system

### 6.2.2 Mean Grain-size

The mean grain-size is an average value calculated from the 16th, 50th and 84th percentiles of the grain-size distribution (Table 6.1). Trends in mean grain-size in large water bodies can be used to infer sediment transport direction, as a decrease in grain-size is related to decrease in wave and current energy and an increase in water depth. The sand fraction of the surface sediments of Lake Sibaya range from very fine-grained to medium-grained. The surface distribution of the various sand fractions are illustrated in Fig. 6.8 and summarised in Table 6.3 .

| GRAIN-SIZE | φ VALUE | SURFACE AREA |
|---|---|---|
| Very fine-grained sand | > 3.0 | 4.0 $km^2$ |
| Fine-grained sand | 2.0 to 3.0 | 56.5 $km^2$ |
| Medium-grained sand | 1.0 to 2.0 | 13.5 $km^2$ |

**Table 6.3** A summary of the mean grain-size surface coverage in Lake Sibaya.

Fine-grained sand comprises 76.3 % of the surface sediments, with medium sand comprising 18.4% and very fine sand comprising 5.3% (see Fig. 6.8). The mean grain-size distribution pattern is generally in keeping with expected lake sedimentation in that there is generally a decrease in grain-size with an increase in water depth. A large area of very fine sand is associated with gyttja deposits in the centre of the Main Basin. Medium grained sand is located in shallower water in the northern and southern areas of the Main Basin. Isolated areas of medium grained sand also occur in the Southern Basin, Southwestern Bay, Western Arm and the Northern Arm.

The medium-grained sand exposures occur in areas that are most exposed to the northerly and southerly prevailing winds, suggesting that wind induced current and wave activity may be responsible for winnowing the finer sand fraction from these areas.

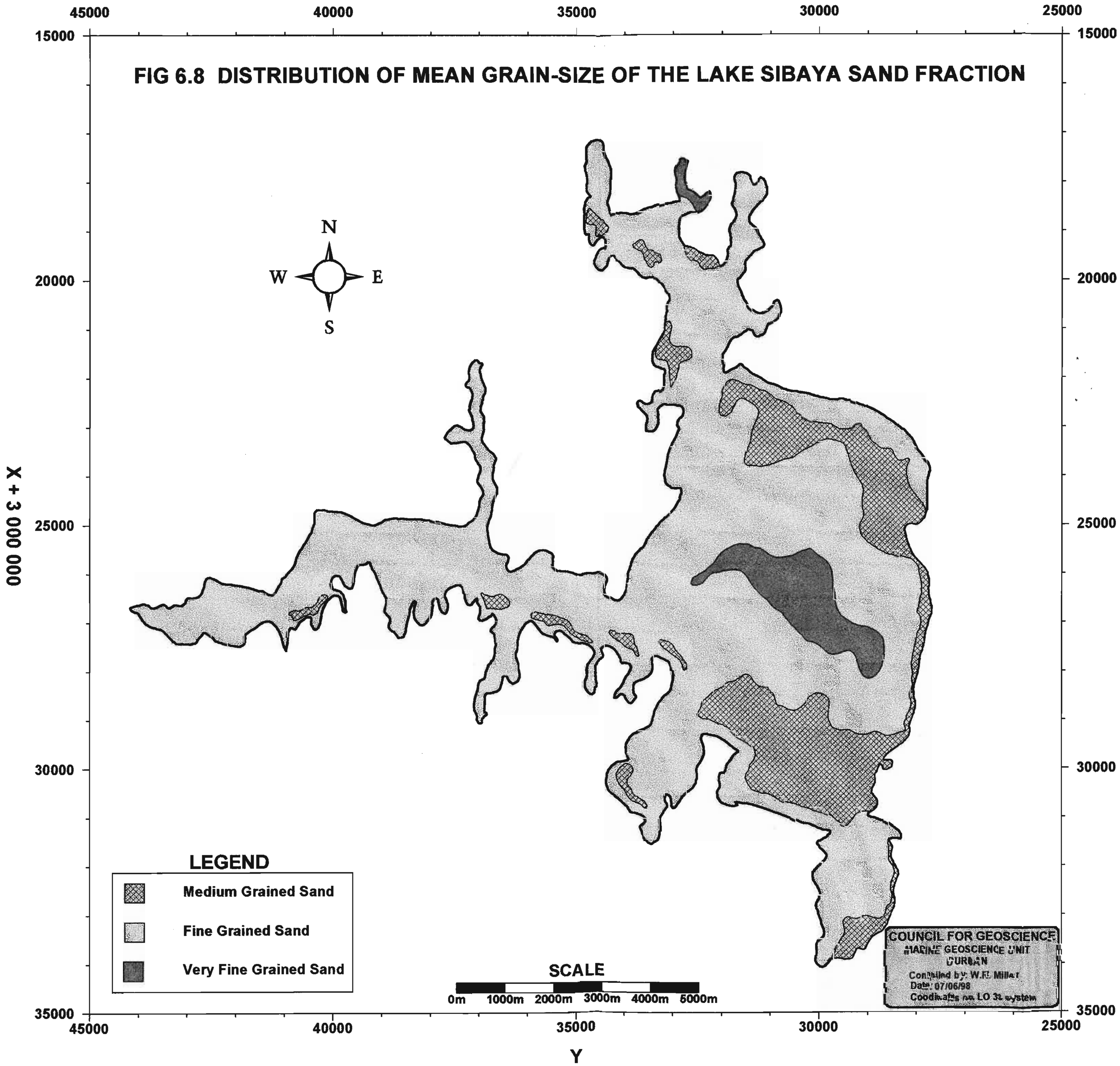


FIG 6.8 DISTRIBUTION OF MEAN GRAIN-SIZE OF THE LAKE SIBAYA SAND FRACTION

### 6.2.3 Skewness

Skewness is the measure of the coarse or fine bias of a grain-size distribution. Apart from being useful to describe a sediment sample, skewness is also a reflection of the depositional process. In general sediment becomes more fine skewed (finer grained) along its sediment transport path whereas the source sediment (lag) becomes more coarse skewed (coarse grained) as the finer sediment is winnowed from it (McLaren & Bowles, 1985). The skewness surface distribution pattern is illustrated in Fig. 6.9 and summarised in Table 6.4.

| SKEWNESS | φ VALUE | SURFACE AREA |
|---|---|---|
| Near symmetrical | -0.10 to 0.10 | 26.3 $km^2$ |
| Coarse skewed | -0.10 to -0.30 | 42.7 $km^2$ |
| Strongly coarse skewed | < -0.30 | 5.0 $km^2$ |

**Table 6.4** A summary of surface coverage of skewed sand populations below Lake Sibaya.

Near symmetrical sand accounts for 35.5% of the surface area of Lake Sibaya and large deposits are located to the south of the Main Basin and in the Southern Basin (see Fig 6.9). Roughly 90% of the lake shoreline is characterised by sand with near symmetrical grain-size distributions which have accumulated in shallow water. Near symmetrical sand distributions are characteristic of aeolian sediments, this suggests an input of sediment from the surrounding dunes.

Coarse skewed sediment accounts for 57.7 % of the surface area of Lake Sibaya. This is surprising since the lake is situated on sediments which are predominantly of aeolian origin, and implies that winnowing of the finer material must have occurred during the lake's development. Strongly coarse skewed sand accounts for the remaining 6.8% of the surface area of Lake Sibaya.

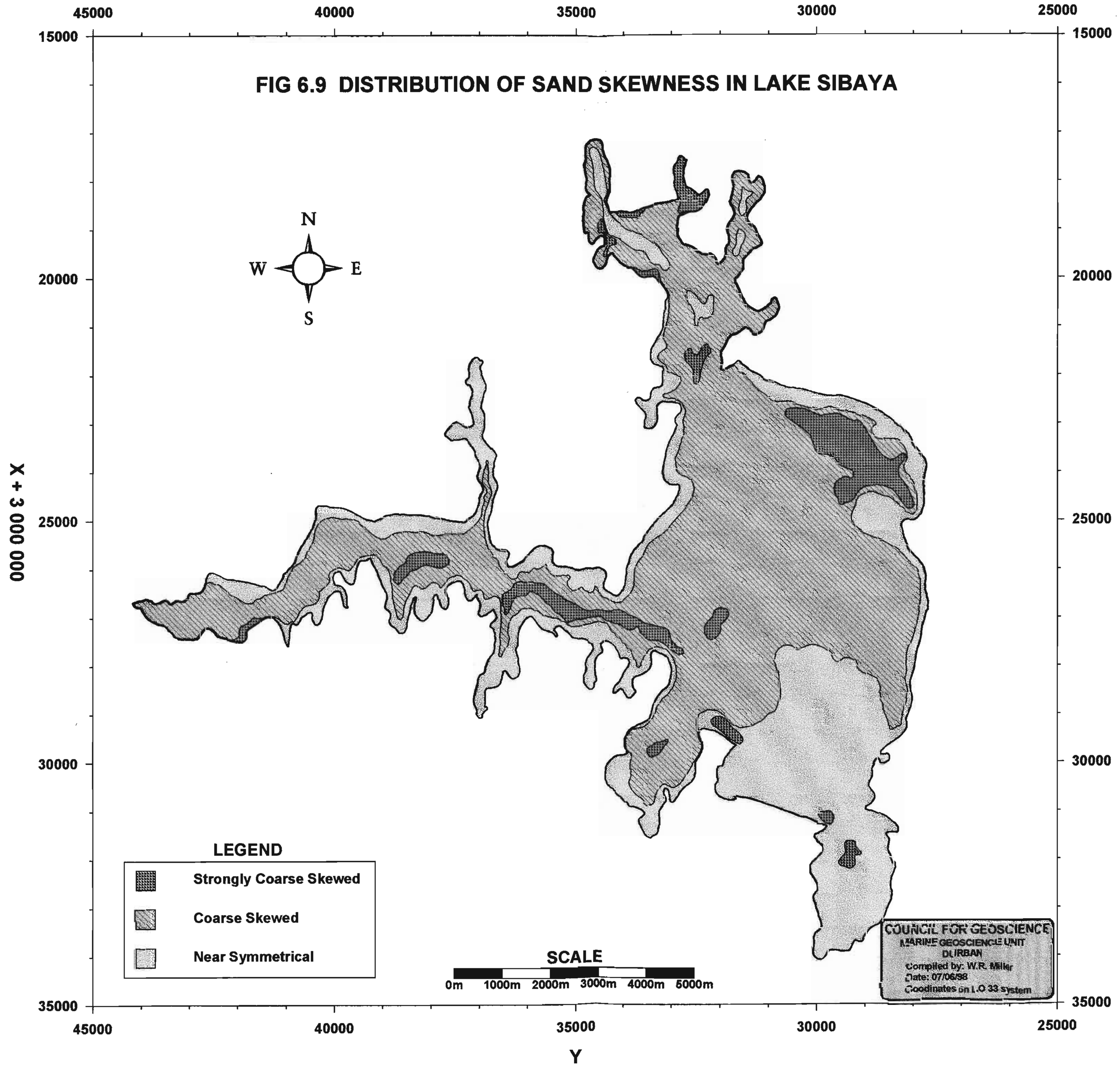


FIG 6.9 DISTRIBUTION OF SAND SKEWNESS IN LAKE SIBAYA

## 6.3 SEDIMENT DISTRIBUTION

Although the sedimentation of Lake Sibaya roughly conforms with normal lake sedimentation i.e. a decrease in grain-size with increased water depth, there are several factors which complicate the sediment distribution pattern on the lake floor. The most important factors in this regard are the very low sedimentation rate and the modern sedimentary processes operative in the lake. The sediment input into Lake Sibaya is restricted to the deeper areas where gyttja accumulates and shallow marginal areas where eroded dune sediment and wind blown sediments accumulate. Sedimentary processes in the lake are driven by water level fluctuations and wind generated currents and are active in reworking sediments in the shallower areas of the lake. The majority of the clastic sediments on the lake floor have therefore been inherited from a previous stage of the lake's development. The present sediment distribution within Lake Sibaya has therefore been dictated by three major factors namely; (1) the inherited sedimentary framework, (2) modern lake processes and (3) aeolian processes.

During the LGM erosive event large volumes of sandy sediments of mid to late Pleistocene age were reworked during the draining of the proto Lake Sibaya. These sediments were predominantly aeolian sediments of the Kosi Bay Formation and the Port Durnford Formation (Botha, 1997). The erosional chasm left after the draining of the proto Lake Sibaya was infilled by a large volume of aeolian sediment during the early Holocene and smaller amounts of lagoonal sand during early to mid-Holocene times. The coastal dune barrier was reestablished ± 5030 BP to form the modern Lake Sibaya. The only sediments which have accumulated in the lake since its formation includes small amounts of gyttja and aeolian sand reworked from the fringing dunes during high water levels. It would be expected therefore, that the majority of the sediments in Lake Sibaya should have aeolian characteristics.

The majority of the surface sediments of Lake Sibaya are well sorted, fine-grained sands with a coarse skewed grain-size distribution (Figs. 6.7, 6.8 & 6.9). The coarse skewed grain-size distribution sets these sediments apart from modern aeolian sediments which are evident around much of the lake's periphery. This suggests that winnowing of the finer sand fraction occurred during the development of Lake Sibaya. The coarse skewed grain-size populations probably have some aspect in the erosion associated with the draining of the proto-Lake Sibaya and subsequent reworking of the newly exposed sediments. The LGM erosion episode eroded an incised valley into the coastal plain thereby creating a conduit for newly exposed shelf sands to be transported inland. Large amounts of aeolian sediments were transported inland to supply the low undulating dune fields adjacent to Lake Sibaya during the Pleistocene - Holocene transition (see Fig. 5.3). During this time period a significant thickness (>15 m) of aeolian sediments accumulated in the topographic low created by the LGM erosion event (see Chapters 7 & 8). As sea-level recovered to near present levels ± 7000 BP, the coastal dune barrier began to be reestablished forming a coastal lagoon (Miller, 1996). This event halted the inland transport of aeolian sand and induced a sediment starved status to the region. Prior to the flooding of the area to form the modern Lake Sibaya, it is speculated that a deflation basin developed on the lake site as the finer sand fraction was winnowed from the exposed aeolian sediments. The filling of the lake, in mid-Holocene times, preserved the now coarse skewed grain-size populations of the dune fields as part of the lake floor. The slow sedimentation rate in Lake Sibaya has not altered this inherited sedimentary framework and explains the dominance of coarse skewed grain-size distributions on the lake floor.

Fine to medium-grained, moderately sorted to moderately well sorted, strongly coarse skewed sand forms small isolated areas amongst the more dominant sediment distributions (Figs. 6.7 & 6.9). The largest of these occurrences is located in the northeast corner of the Main Basin in the vicinity of the ground water ferricrete exposures (Fig. 6.1). The ground water ferricrete marks the unconformity which separates the older Port Durnford Formation from younger aeolian sediments of the Kosi Bay Formation (Botha, 1997; Miller, 1996). The coarser grain-size and concentration of heavy minerals above background values suggest that this was a deflation surface prior to the deposition of the Kosi Bay Formation during the late Pleistocene. The isolated exposures of the strongly coarse skewed sediments might be explained as areas where the top of the Port Durnford Formation outcrops below lake level.

Modern lake processes are active in modifying inherited sediment distribution patterns in the shallow areas (<10 m) of Lake Sibaya. The lake processes include water level fluctuations and currents generated by wind stress. These processes have been responsible for the development of wave cut terraces, eroding sediment from proximal dune cordons and for reworking sediment in the shallower areas of the lake. During periods of high water levels in Lake Sibaya, aeolian sediment is eroded from surrounding dune cordons and added to the lake sediments. Lake Sibaya beach profiles (wave cut terraces) are developed during lake level still-stands and are characterised by moderately well sorted sediments with a fine to medium grain-size. There are numerous wave cut terraces preserved above and below present water level in Lake Sibaya. The wave cut terraces are particularly noticeable in the northern and southern areas of the Main Basin where the wind fetch is exaggerated (Miller, 1994). These areas are delineated by medium-grained, moderately well sorted sand in shore parallel lenses (Figs. 6.7 & 6.8). This suggests that the action of currents and waves in shallow water reworks the sediment removing the finer sand fraction. The concentration of aeolian sand in the shallow water proximal to the shoreline of Lake Sibaya indicate that the surrounding dunes are supplying sediment to the lake.

A large area in the south of the Main Basin and almost the entire southern basin are characterised by fine to medium-grained, moderately well sorted to well sorted sand with near symmetrical grain-size distributions (Figs. 6.8 & 6.9). These statistics are consistent with aeolian sediment and suggest a more recent input of aeolian sediment into this area of the lake. This hypothesis is supported by the existence of the "White Sands" parabolic dune system to the south of Lake Sibaya. "White Sands" was until the 1960's an active dune field which transported sediment from the beach environment inland to the southern area of Lake Sibaya (Fig. 6.10). A study of the aerial photographs suggests that "White Sands" has probably been active since at least mid-Holocene times. A dune stabilisation initiative undertaken by the Department of Agriculture in the 1960's saw the extensive planting of *Casuarina* trees to halt sand movement into the "White Sands" dune field (Fig. 6.11). This undertaking halted sediment movement into the Southern Basin areas of Lake Sibaya and has induced a sediment starved status to "White Sands".

While the results of this study might seem significantly different to the Wright & Mason study of 1990 (see Appendix 2) this is more a function of sample density rather than research techniques or changing sedimentation patterns in Lake Sibaya. In fact it is highly unlikely that patterns of sediment distribution changed much during the time period between the two studies. The results merely reflect the perceived sediment distribution patterns based on the available samples. It follows that the more dense the sample pattern is, the more accurate the perceived sediment distribution patterns will be.

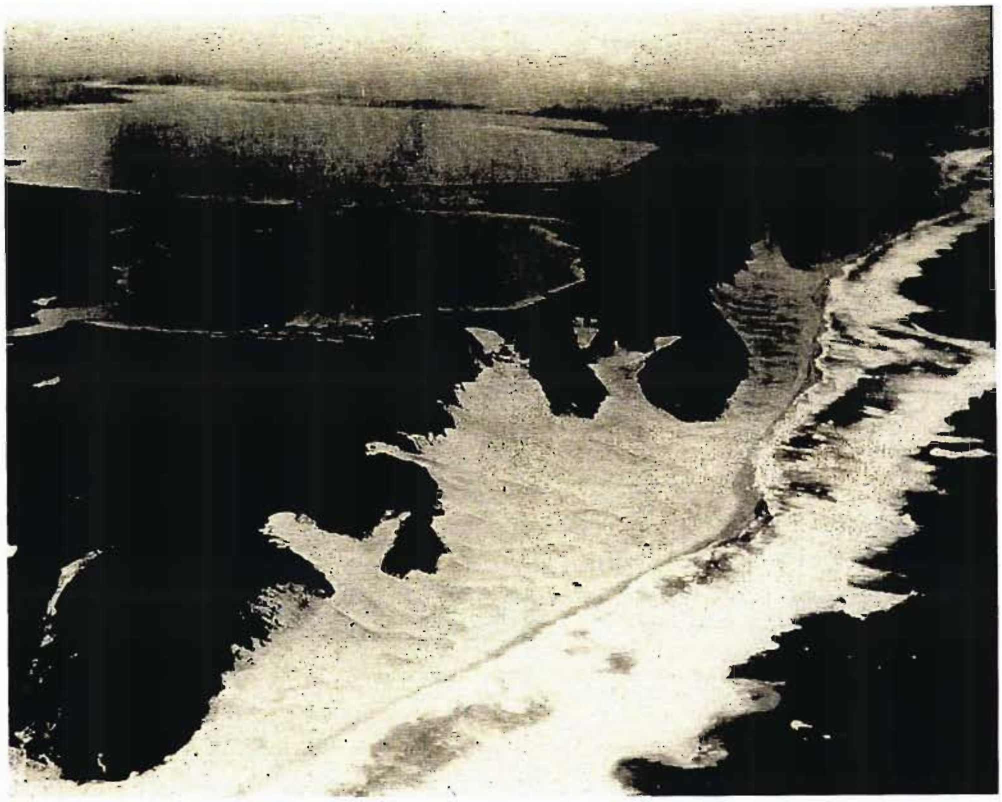

**Fig 6.10** An oblique aerial photograph of "White Sands" dunefield and Lake Sibaya in the 1960's. Note the transverse dune systems which transported sediments from the beach, to the Southern Basin area of the lake. Photograph supplied courtesy of John McCarthy.

**Fig 6.11** An oblique aerial photograph showing the "White Sands" dunefield after stabilization of the foredunes with *Casuarina* trees. The photograph was taken by Dr. P.J. Ramsay in August 1987.

# CHAPTER 7 : SEISMIC PROFILING

## 7.1 SEISMIC SEQUENCE STRATIGRAPHY

Seismic sequence analysis involves the recognition of principle reflection packages known as seismic sequences. This process involves the delineation of fundamental depositional units which are bounded by unconformities or equivalent conformities (Vail *et al.*, 1977; Browne & Fisher, 1979). A depositional sequence is composed of a relatively conformable succession of genetically related strata, and by virtue of the fact that it is bounded by unconformities at its upper and lower extremities, represents a time stratigraphic unit (Browne & Fisher, 1979).

A seismic profile is a montage of thousands of seismic reflections generated by reflections within the sedimentary succession from an incident acoustic pulse. Seismic reflections are generated when the acoustic signal encounters unconformities or stratal surfaces which have significant density\velocity contrasts. Consequently, attitude, continuity and geometry of reflections enable the researcher to use the seismic profile to infer superposition, depositional topography, erosion, non-deposition and other stratigraphic aspects.

A seismic overlay is prepared by tracing seismic reflectors from the analogue records (seismic profiles) on to drafting film, to get a clearer representation of the internal geometry of the sedimentary succession which has been traversed with the seismic profiling equipment.

## 7.2 DESCRIPTION OF SEISMIC SEQUENCES

A series of west - east and north - south oriented seismic overlays were prepared from the analogue records and are illustrated in Figs. 7.2 & 7.3. The seismic overlays (Figs. 7.2 & 7.3) were interpreted according to sequence stratigraphic principles, whereby the sedimentary succession is subdivided into a number of sequences bounded by unconformities or laterally persistent disconformities. Unconformities and disconformities were defined by identifying principle reflectors on seismic records and reproducing them on seismic overlays (Figs. 7.2 & 7.3). These surfaces were then extrapolated to produce seismic sequence diagrams (Figs. 7.4 & 7.5).

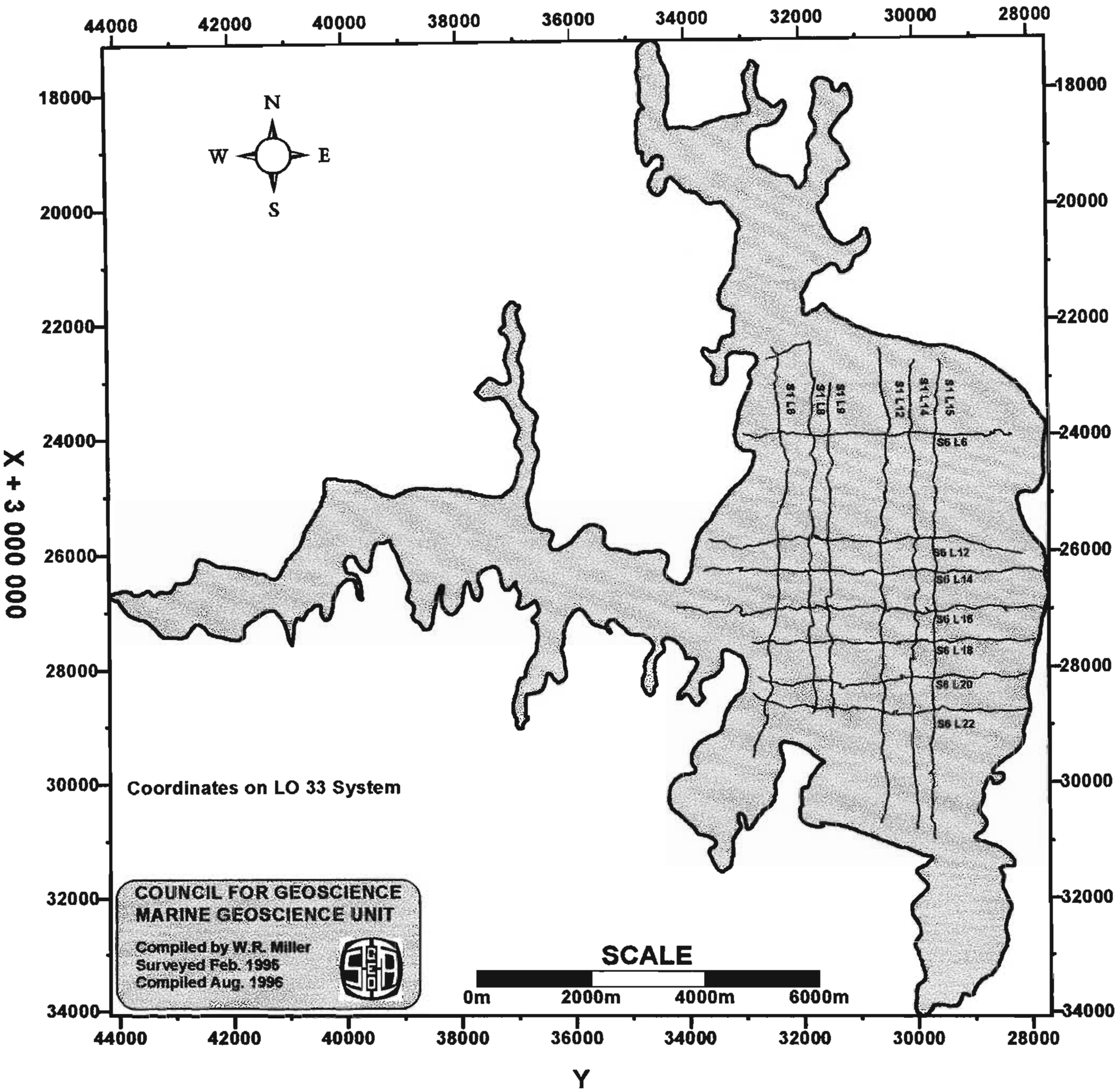


**Fig. 7.1 Track chart of selected seismic survey lines**

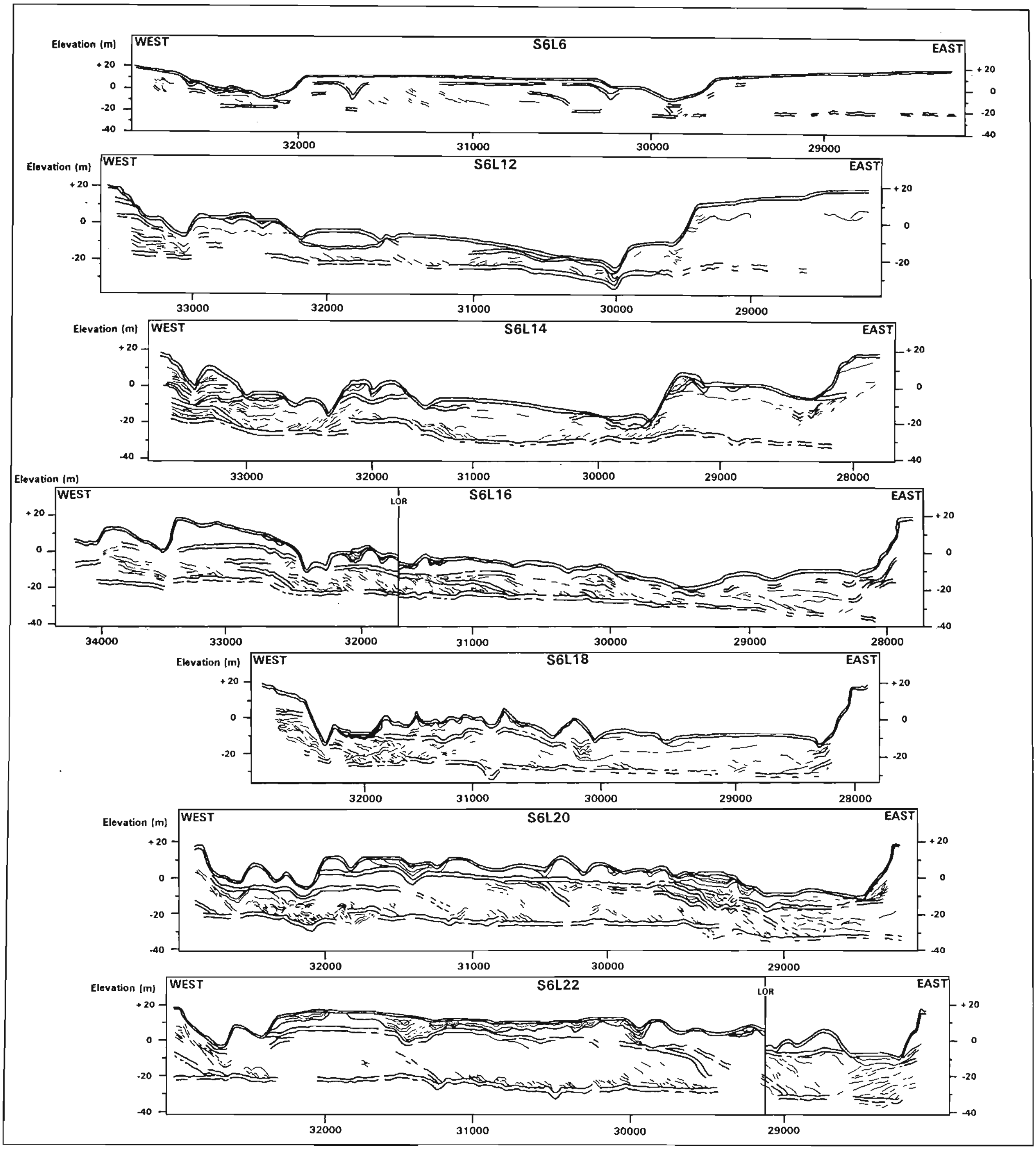


**Fig 7.2** Selected west - east seismic overlays.

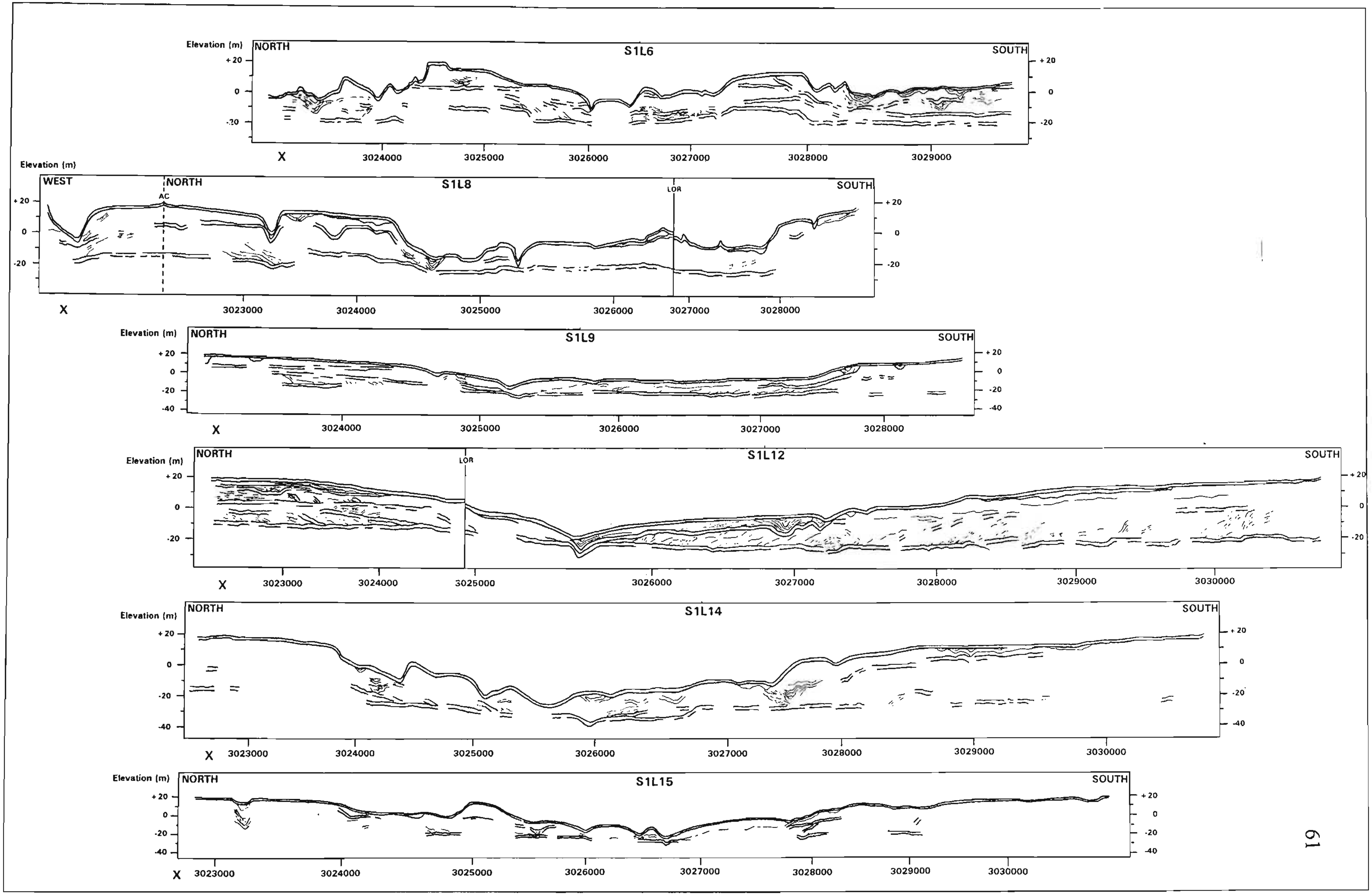


**Fig 7.3** Selected north - south seismic overlays.

### 7.2.1 Sequence 1

The acoustic basement for the geophysical survey is defined by a regionally developed reflector with a strong density contrast to overlying sediments. This reflector is assigned a sequence boundary status (sequence boundary SB1). The reflector defining the sequence boundary (SB1) shows the highest amplitude and continuity of all reflective surfaces below Lake Sibaya. Surface SB1 dips gently from west to east and has a saucer shaped geometry when viewed in a north-south orientation on the sequence diagrams (Figs. 7.4 & 7.5). A contoured plot of surface SB1 shows that the geometry of this surface is far more complex (Fig. 7.6). A relict drainage pattern appears to be etched into surface SB1 with palaeochannels underlying the northern and western arms of the lake. Further east a third palaeochannel enters the Main Basin from the north (Fig. 7.6). The palaeochannels coalesce from the north and east, in the central area of the Main Basin. The juncture of the palaeochannels is almost at right angles which implies a deeper seated structural control to the palaeodrainage (Fig. 7.6). The point of juncture of the palaeochannels is also coincident with the deepest point on the modern bathymetry of Lake Sibaya (Fig. 5.1).

There is evidence for faulting of sequence boundary SB1 (Fig. 7.4: lines S6L16, S6L18, S6L20 & S6L22; Fig. 7.5: lines S1L9 & S1L12; Fig 7.8). The faults are situated in the south west area of the Main Basin and show apparent throws of less than 10 m. The west - east oriented palaeochannel which underlies the Western Arm of the lake is deflected by what appears to be a horst structure which has an apparent upward throw of ± 6 m (see Fig. 7.6).

### 7.2.2 Sequence 2

Sequence 2 downlaps on to sequence boundary SB1 from the west, north and south and is characterised by strong reflectivity and chaotic internal reflections ( Fig 7.4: lines S6L18 & S6L20). Sequence S2 reaches a maximum thickness of ± 20 m in the south, but the thickness averages 10 - 15 m. Sequence 2 pinches out towards the east and no evidence of this sequence occurs east of the 30 000 Y coordinate. The highly irregular appearance of sequence boundary SB2 testify to the fact that Sequence 2 has been subject to prolonged periods of erosion. Apart from being totally stripped away in the east, there is also evidence of channel erosion into sequence boundary SB2 under the western margin of the Main Basin. Sequence boundary SB2 does not show any evidence of faulting.

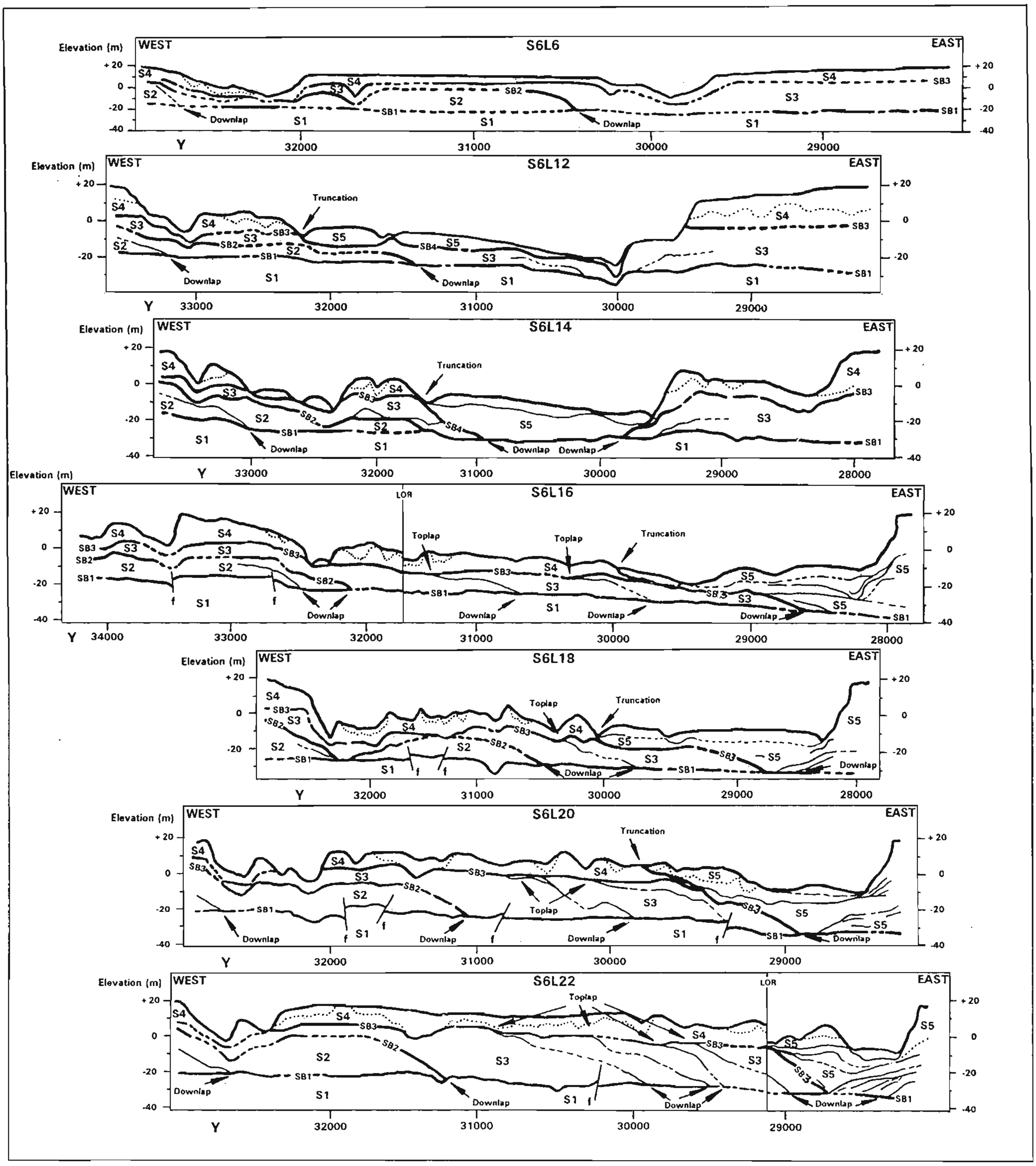


Fig 7.4 Interpretation of west -east seismic overlays.

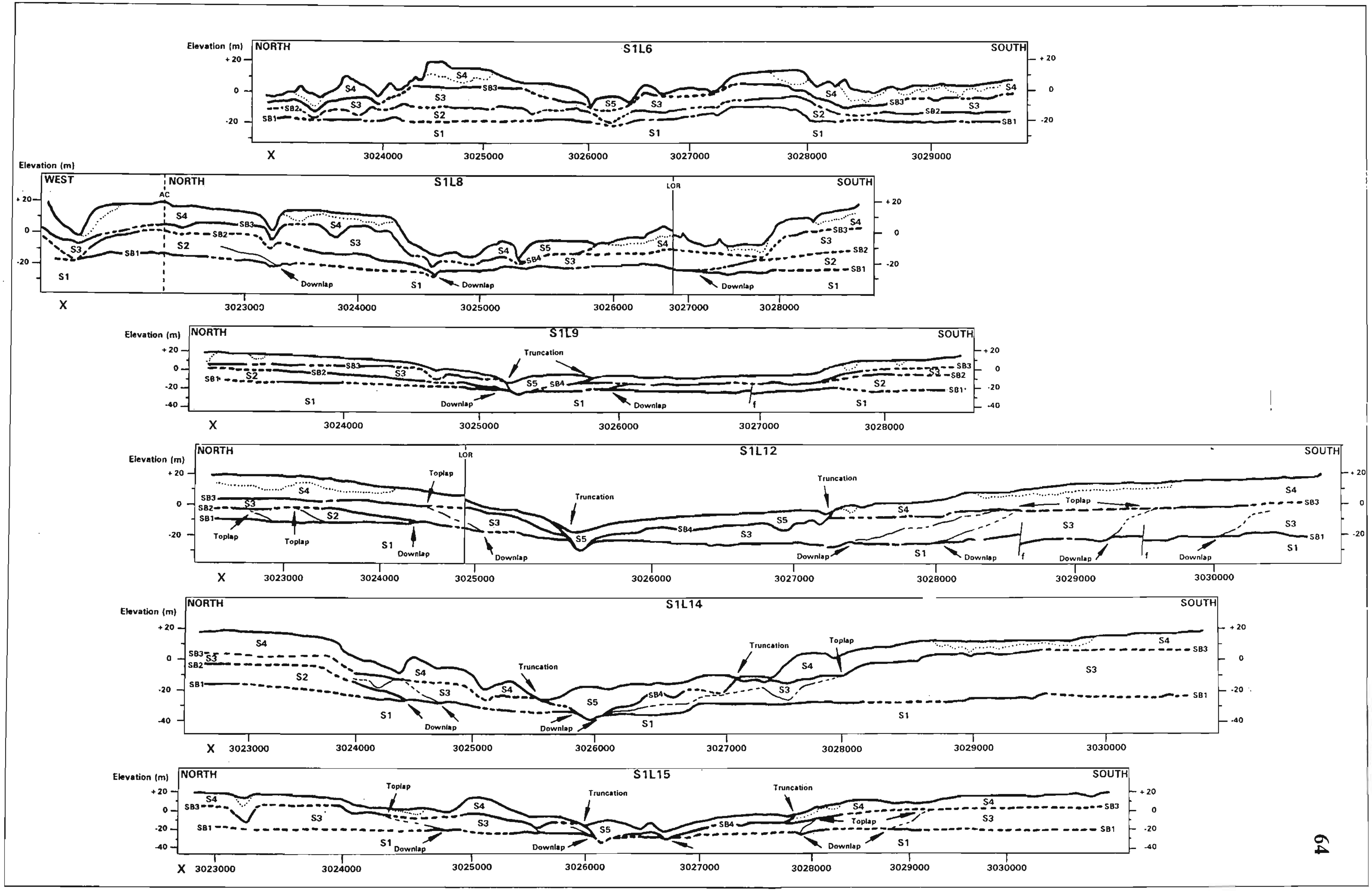


Fig 7.5 Interpretation of north - south seismic overlays.

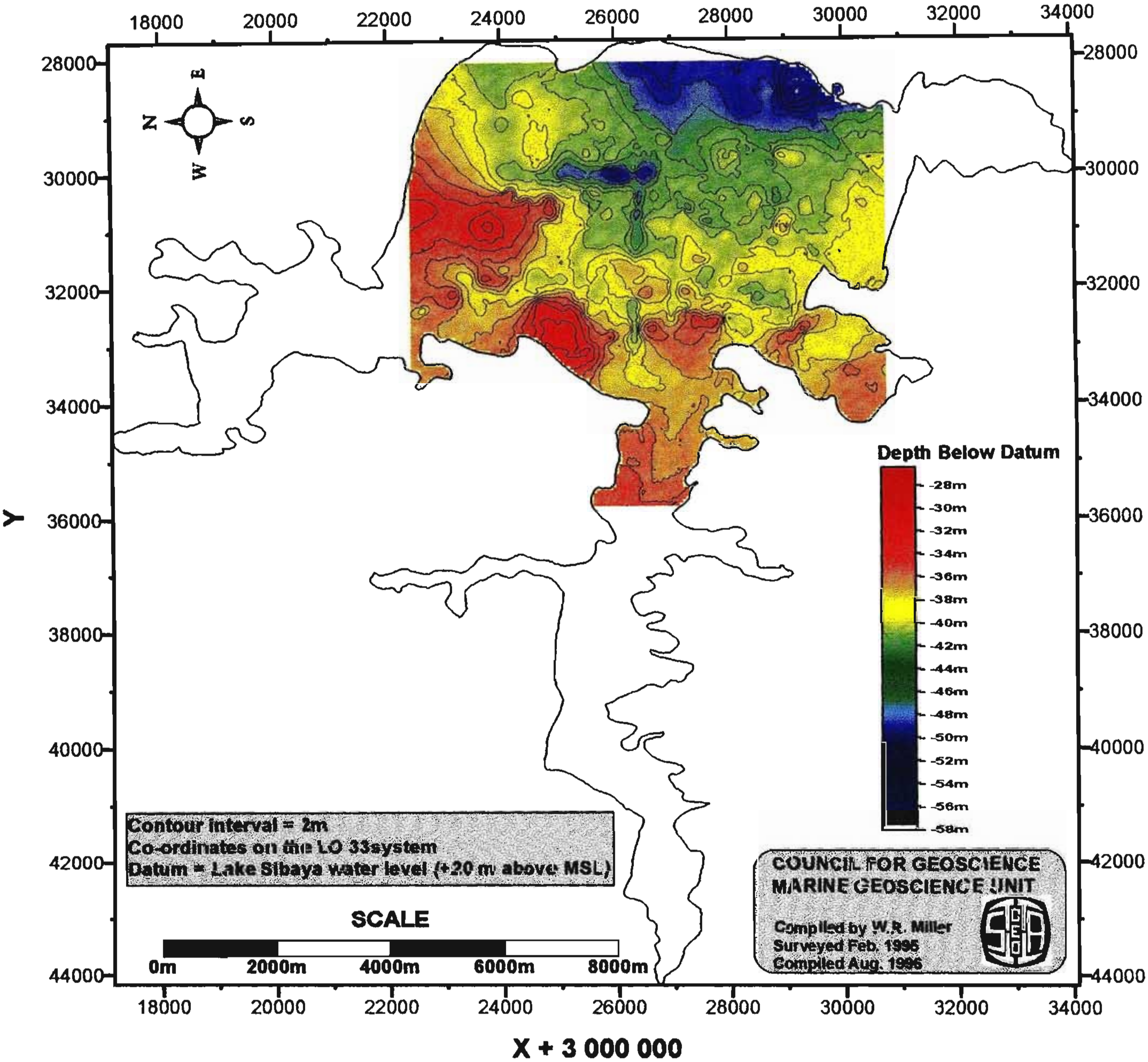


Fig. 7.6 Contoured surface of the elevation of sequence boundary SB1 as measured from seismic sections.

### 7.2.3 Sequence 3

Sequence 3 unconformably overlies sequence boundaries SB1 and SB2 and thickens from 2 m - 8 m in the west to ± 30 m in the east. This thickening tendency is only evident in the shallow areas of Lake Sibaya (areas not incised to elevations below sea-level) at the northern and southern end of the Main Basin (Fig. 5.1). In the deeper areas of the lake (below MSL), sequence 3 is truncated by sequence 5 and consequently downlaps onto sequence boundary SB1. The base of Sequence 3 is located at an elevation near sea-level in the west, but further east where it downlaps onto sequence boundary SB1 it is located as much as 35 - 40 m below MSL.

A number of parasequences defined by weakly reflective surfaces that display low continuity are evident in Sequence 3. These parasequences show a toplap configuration with sequence boundary SB3 and downlap onto sequence boundary SB1 (Fig. 7.4: lines S6L20 - S6L22; Fig. 7.5: lines S1L12 - S1L15). At least 5 of these parasequences are evident on some seismic sections. The parasequences downlap on to sequence boundary SB1 predominantly from the west and south with fewer examples being evident downlapping from the north and east. This geometry is suggestive of prograded basin fill with each of the parasequences representing a prograded sediment wedge, and each parasequence boundary representing a hiatus in sedimentation. Some of the parasequence boundaries show evidence of erosion (Fig. 7.4: line S6L20; Fig. 7.5: line S1L14).

Below the shallow plateau like areas of the lake, Sequence boundary SB3 forms a flat, gently eastward dipping surface located ± 5 m above present sea-level (Fig 7.4: lines S6L6, S6L20 & S6L22). Sequence boundary SB3 shows a more subdued and irregular topography below the deeper areas of the lake (see Fig 7.7). Possible relict channel deposits which are post sequence 3 in age, occur in the area proximal to the Western Arm and Southwestern Bay (Fig. 7.4: lines S6L18 & S6L20). At least two cycles of erosion are recorded in Sequence 3 namely;

(1) erosion of some of the parasequences, which occurred during minor erosional phases during the accumulation of sequence 3 (Fig. 7.5: line S1L14).

(2) incision into sequence boundary SB3 by isolated channels underlying shallow areas of the lake, and by the denuded nature of the same sequence boundary in deeper areas of the lake. This cycle of erosion is post sequence 3 but pre sequence 4.

### 7.2.4 Sequence 4

Sequence 4 rests unconformably on Sequence 3 in the context of the study area. Sequence 4 blankets the incised topography delineated by sequence boundary SB3 dipping gently from west to east and varies in thickness from less than 1 m to ± 15 m. A reflector characterised by low amplitude and continuity is evident in Sequence 4 (dotted line). The reflector is observed intermittently on most of the seismic lines and is characterised by a gently undulating surface that appears to outcrop in places on the lake floor (see Fig 7.7). The fact that this reflector appears to be truncated in places (where it outcrops) by the existing lake bathymetry (Fig. 7.4: lines S6L12 - S6L22; Fig. 7.5: lines S1L6 - S1L15) suggests that sequence 4 underwent erosion prior to or during the formation of the lake. The undulating reflector (dotted line) in the author's opinion did not show the regional development necessary for it to constitute a sequence boundary.

### 7.2.5 Sequence 5

Sequence 5 truncates all other sequences in the study area and can be shown to incise down into the top of Sequence 1 (Fig. 7.5: lines S1L9 to S1L15). Sequence 5 has a typical channel morphology that coincides with NW - SE trending deep channel of Lake Sibaya's bathymetry (Fig. 5.1). Sequence boundary SB4 defines the palaeovalley incised during the last erosional event that saw the erosion of the sediments underlying Lake Sibaya. Sequence 5 represents the sediments which infilled the palaeovalley once sea-level stabilised near its present elevation. The sediments of this sequence consist of a basal sediment wedge which infills the palaeovalley from the east (Fig. 7.4: lines S6L18, S6L20 and S6L22) and two successions of valley fill.

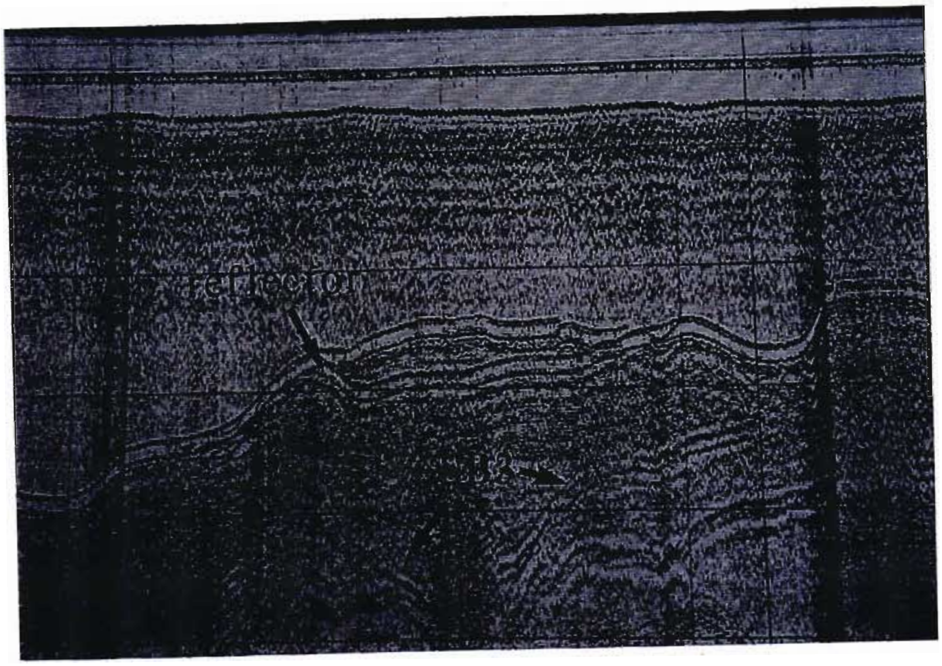


**Fig 7.7** An example of the "Boomer" seismic records collected from below Lake Sibaya. This seismic profile shows sequence boundary SB3 and the undulating reflector in Sequence 4 which outcrops in places on the lake floor. This surface marks the base of the diatomite deposits (see Chapter 8).

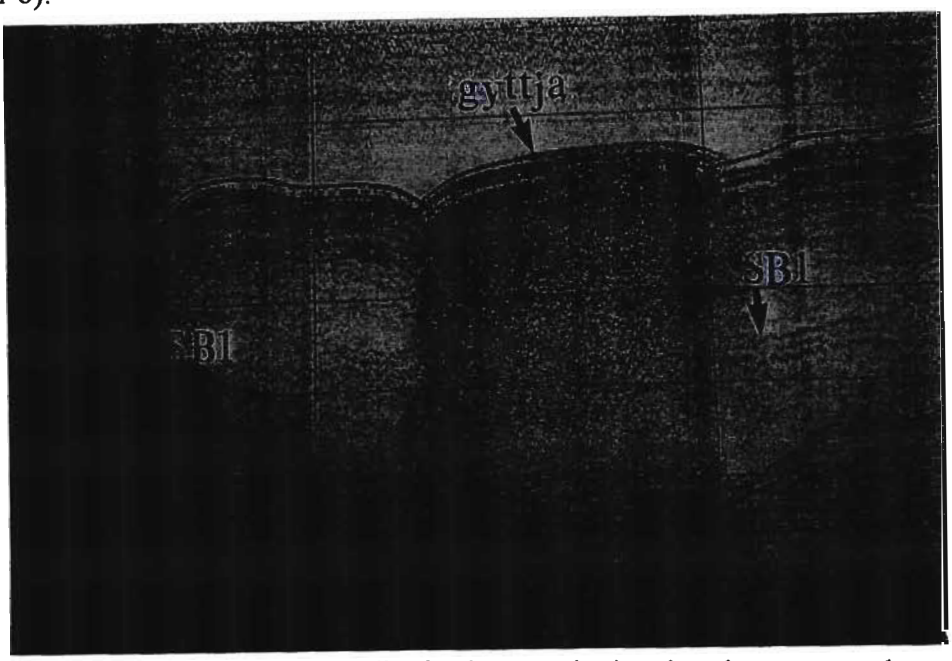


**Fig 7.8** An example of the "Boomer" seismic records showing the sequence boundary SB1 and a domed exposure of gyttja. Note the vertical displacement of sequence boundary SB1 to the left of the gyttja exposure, which implies faulting of this surface. Note also the acoustic impedence of the gyttja exposures which gives a characteristic saturated record and masks the underlying seismic stratigraphy.

## 7.3 STRATIGRAPHIC INTERPRETATION OF SEISMIC RECORDS

### 7.3.1 Sequence 1

Sequence boundary SB1 is preserved at elevations ranging from -15 m to -40 m below present sea-level. This surface shows strong reflectivity and lateral continuity on the seismic records. This suggests a strong density/velocity contrast between two superimposed sediment types. It is therefore most likely that this sequence boundary probably represents the Palaeocene unconformity which separates the predominantly sandy sediments of the Maputaland Group (Botha, 1997) from the underlying Cretaceous siltstones. Cretaceous aged sediments have been confirmed at elevations of -20 m to -30 m in the Lake Sibaya area (Pitman & Hutchinson, 1975).

### 7.3.2 Sequence 2

Sequence 2 is characterised by strong reflectivity and chaotic internal reflection configurations suggesting that sediments of this sequence are more dense/lithified than the overlying sequences. Sequence 2 is preserved at elevations slightly higher than sea-level down to -30 m. From the seismic sequence diagrams (Figs. 7.4 & 7.5) it can be seen that sequence boundary SB2 rises to elevations near present sea-level in the east. A calcarenite with karst solution features has been proved at similar elevations in the Lake Sibaya area by a drilling programme conducted by the Industrial Development Corporation (pers. comm. G. Botha, 1996). This lithotype is characteristic of the cross-bedded calcarenite of the Umkwelane formation (Frankel, 1966; Maud & Orr, 1975; Cooper & McCarthy, 1988; Lui, 1995; Botha, 1997).

Sequence 2 probably represents the Tertiary aged sediments of the Uloa and Umkwelane formations. The lithological break between the Umkwelane and Uloa formations is not evident on the seismic records, therefore these formations are treated as a single sequence.

### 7.3.3 Sequence 3

Sequence 3 forms a seaward thickening wedge of sediment composed of numerous parasequences. The downlapping geometry of the parasequences on to sequence boundary SB1 is suggestive of a prograded regressive sequence. Sequence boundary SB3 has a plateau-like geometry below the shallow areas of Lake Sibaya (not incised to elevations below sea-level) and shows strong evidence of erosion in the central and eastern areas of the Main Basin.

The planation event which is evident below the shallow areas of Lake Sibaya was probably initiated by a marine transgression to elevations not much higher than present sea-level. The "soft" nature of this coastline by virtue of the abundance of easily erodible sandy sediments, suggests that if more than one marine transgression took place on this part of the coastline, the last of these would be the most likely to be preserved intact. It follows that this planation event is most likely to be the last interglacial highstand which reached elevations of ±5 m above present sea-level 120 000 BP (Ramsay, 1996). This highstand is believed to be responsible for the deposition of the Port Durnford Formation (Hobday & Orme, 1974). Sequence 3 shows strong evidence of erosion and has been totally stripped in the central and eastern areas of the Main Basin where sequence boundary SB3 downlaps on to sequence boundary SB1. The incision which was responsible for the denudation of sequence boundary SB3 is probably related to the regression following the last interglacial highstand.

All the evidence suggests that sequence 3 represents the Port Durnford Formation and that sequence boundary SB3 represents the LGM erosion surface.

### 7.3.4 Sequence 4

Sequence 4 rests unconformably on sequence 3 and is characterised by an undulating upper surface, which is suggestive of palaeo-dune topography. A weak reflector with the same undulatory nature is intermittently observed on the seismic records (Figs. 7.4 & 7.5: dotted line - sequence 4; Fig 7.7). This is believed to represent an ancient landsurface which marks a hiatus between underlying aeolian sediments and younger freshwater lake\wetland deposits.

If the evidence suggesting that sequence boundary SB3 represents the LGM erosion surface is accurate, it follows that the sediments of sequence 4 represent late Pleistocene to Holocene aged aeolian sediments which accumulated after the draining of the proto-Lake Sibaya. A coring programme in Lake Sibaya and surrounding areas has shown that late Pleistocene and Holocene aged freshwater diatomite deposits exist in the Lake Sibaya area (Miller, 1996; Chater 8). Diatomites of the KwaMbonambi Formation accumulated in depressions on aeolian sediments of the Kosi Bay Formation beneath the waters of the proto-Lake Sibaya for the time period ±43 500 BP to ±25 500 BP. The late Pleistocene diatomites are not found within the bounds of the modern Lake Sibaya and having been totally stripped from this area during the LGM erosion event. The Holocene diatomite deposits accumulated in interdune depressions on late Pleistocene to Holocene dune topography during the development of the modern Lake Sibaya and are still preserved on the lake floor (Chapter 8). Radiocarbon dating places a maximum possible age of 7060 ± 80 BP for the Holocene diatomite deposits (Chapter 8).

Sequence 4 therefore represents a thick accumulation of latest Pleistocene to Holocene aged aeolian sand with intercalated deposits of Holocene diatomite. These two sediment types can be differentiated from one another when the palaeo-landsurface (dotted line) can be identified from the seismic records (Fig 7.7).

### 7.3.5 Sequence 5

Sequence boundary SB4 represents an erosional surface which post dates the LGM erosion event and is probably related to normal coastal drainage during the late Pleistocene and early Holocene, following the draining of the proto-Lake Sibaya. As sea-level recovered to its present elevation ± 7000 BP (Ramsay, 1996), the erosional chasm created by LGM event and subsequent early Holocene coastal drainage, was infilled by sediments of sequence 5. The sediments of sequence 5 represent valley fill sediments which accumulated during the Holocene, initially as marine washover sediments, later as lagoonal sediments and finally as freshwater lacustrine sediments (Miller, 1996; see Chapter 8). Coring of the lake sediments has revealed a thin veneer (up to 5 m) of lacustrine muds (gyttja) overlying marine lagoonal sediments of undetermined thickness (Miller, 1996; see Chapter 8). Gyttja accumulations, the Holocene diatomites of sequence 4 and bedforms composed of reworked sediments located in shallow areas around the lake margins, represent the only truly lacustrine sediments underlying Lake Sibaya.

The stratigraphic interpretation of the sedimentary succession below Lake Sibaya is highlighted and illustrated in Figs.7.9 &7.10.

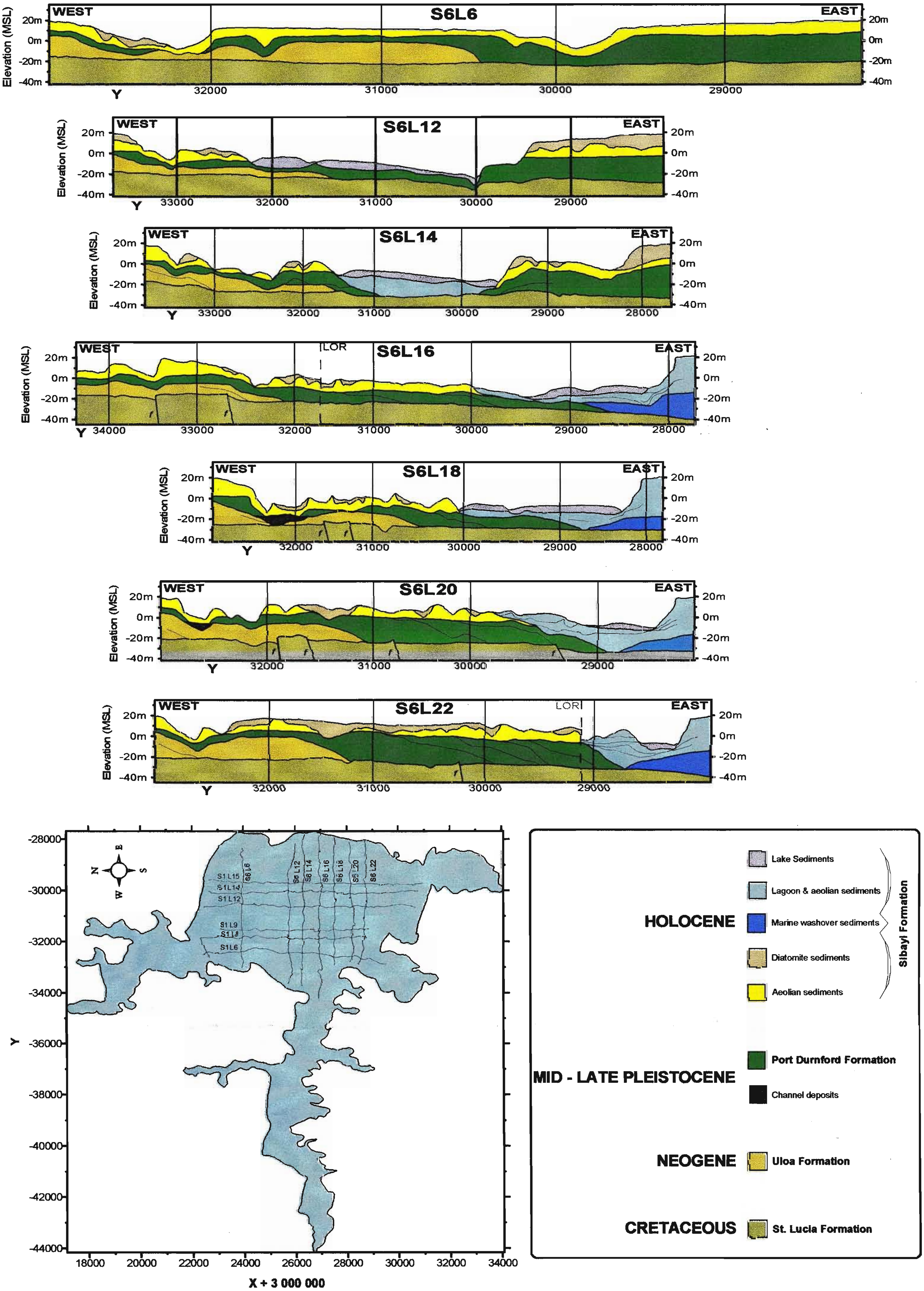


Fig 7.9 Stratigraphic interpretation of west - east seismic survey lines.

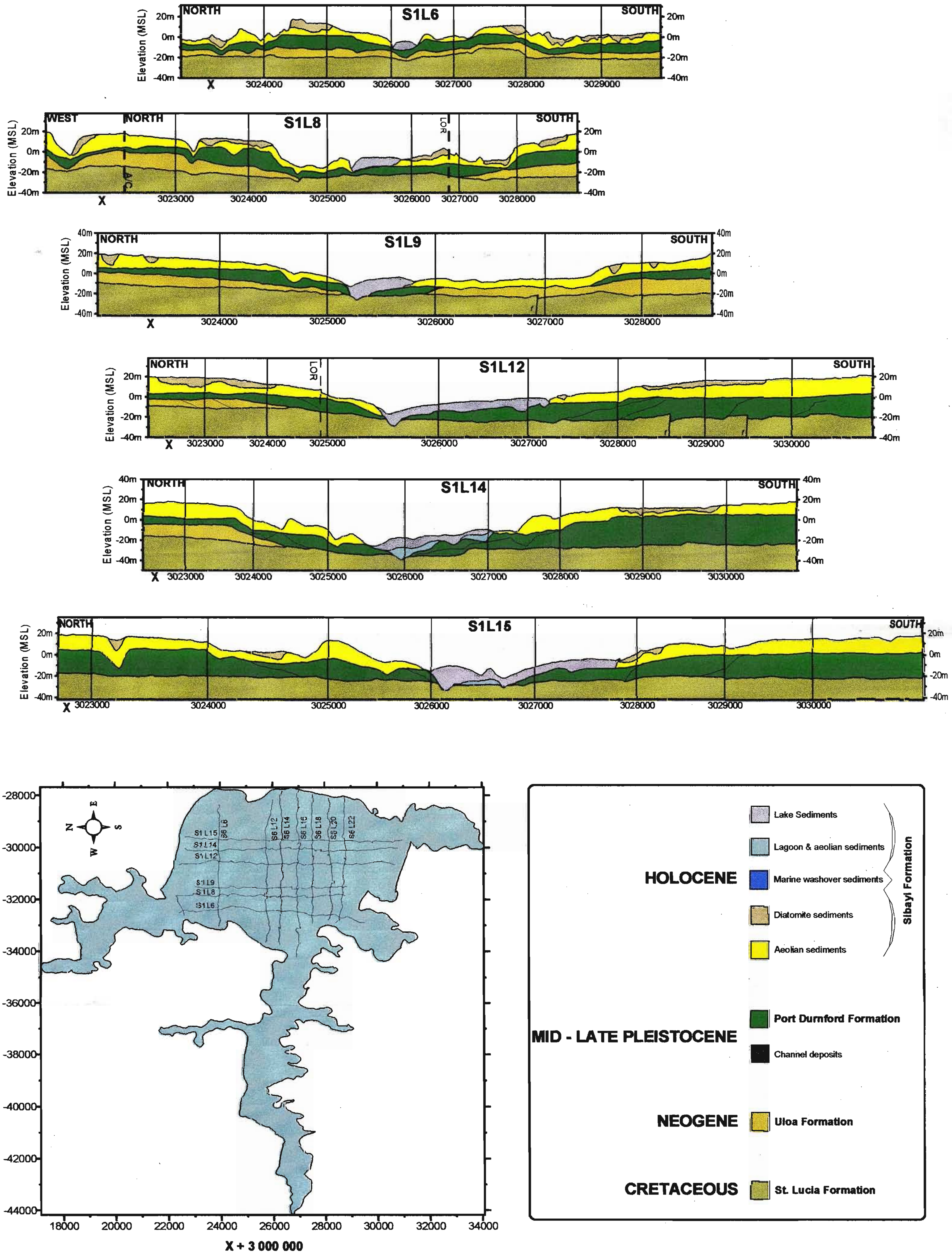


Fig. 7.10 Stratigraphic interpretation of north - south seismic survey lines.

# CHAPTER 8 : SEDIMENT CORING

Twelve sediment cores measuring between 2.4 m and 4.4 m were collected from the bottom of Lake Sibaya following the seismic profiling investigation. The cores were collected to investigate the sedimentary stratigraphy, for textural analysis, to investigate seismic reflectors below the lake floor and to collect dateable material. In addition to the subaqueous sediment coring, an exposure of diatomite was excavated on the western shores of the lake to sample the stratigraphy of this sediment type, to collect dateable material and to investigate the basal sediments underlying the diatomite. The location of each of the cores sites is illustrated in Fig.8.1 and the coring barge is shown in Fig 8.2.

## 8.1 DESCRIPTION OF SEDIMENT CORES

### 8.1.1 Core D

Core D comprises an excavated diatomite exposure on the western shores of Lake Sibaya. The diatomite is exposed in a 1 - 1.5 m high terrace where the Main Basin merges with the Northern Arm (Fig. 8.1). The core site is located at 27° 18.253 S, 32° 39.855 E. The diatomite deposit was excavated to reveal a total thickness of ± 2.45 m and was logged according to sedimentology principles (Cooper & Mason, 1987). The exposure consists of a light to dark grey laminated diatomite with intermittent horizons of dark organic material and lighter coloured sandy lenses (Fig. 8.3). The diatomite deposits rest on ochre coloured clay and clayey sand with subordinate goethite laminae (Fig 6.3). The base of the excavation was defined by a light to dark brown clayey sand (see Appendix 3 for core log).

### 8.1.2 Core P

Core P was collected in the Main Basin (27° 21.194' S, 32° 41.416' E) in a water depth of 26 m. The core recovery measured 3.70 m and consisted of light grey to dark charcoal grey muds overlying a light brown to light grey medium-grained sand. The muds vary from a slit at the top of the succession to a firm clay nearer the base. The clays are weakly laminated with alternating dark and light bands. A sharp contact defines the base of the clays where they rest on the underlying sandy sediments. The basal sediments are medium-grained, angular to sub-rounded, strongly bioturbated sands rich in microfossils and shell fragments (see Appendix 3 for core log).

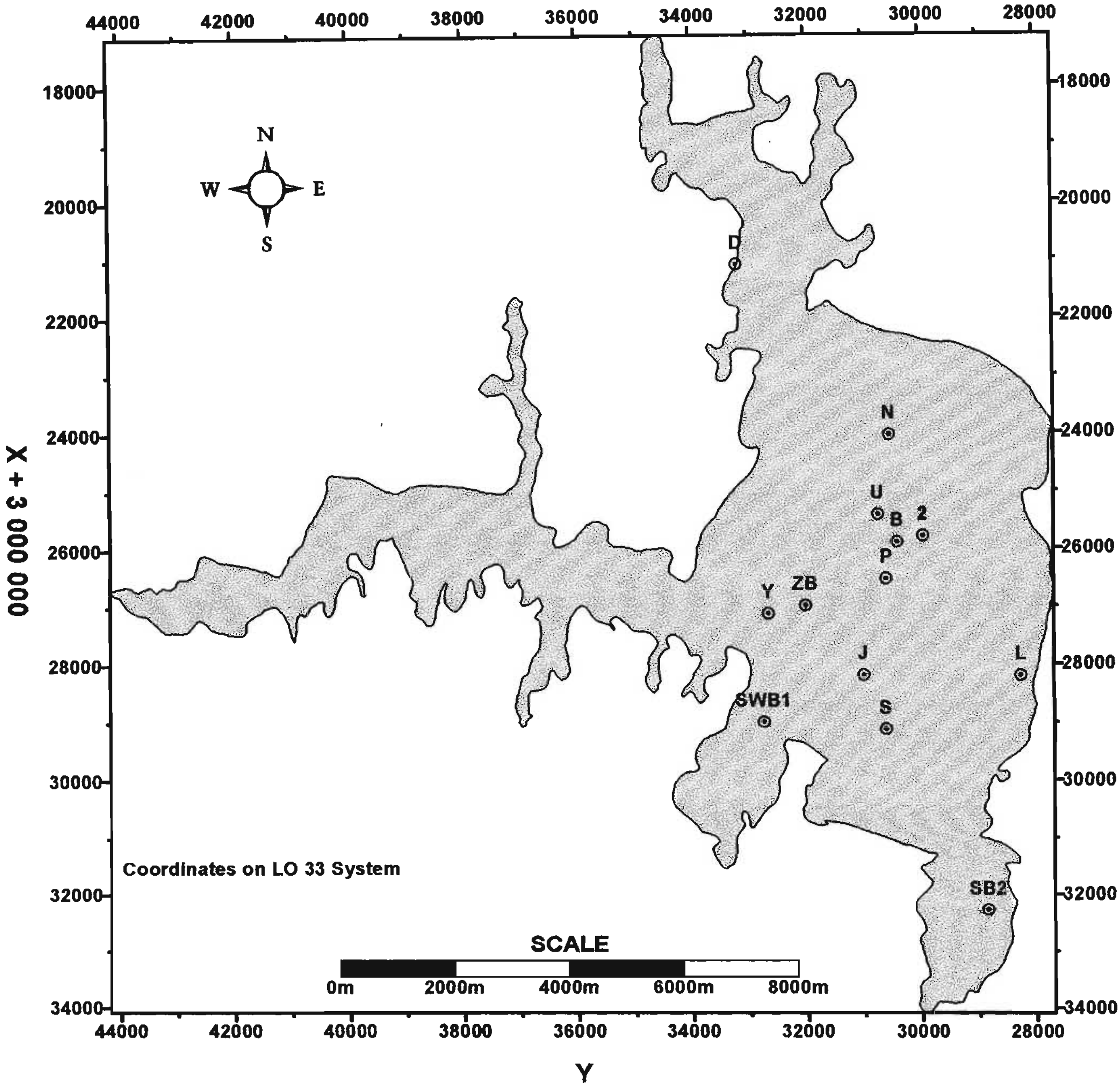


Fig 8.1 Locality map of Lake Sibaya sediment cores.

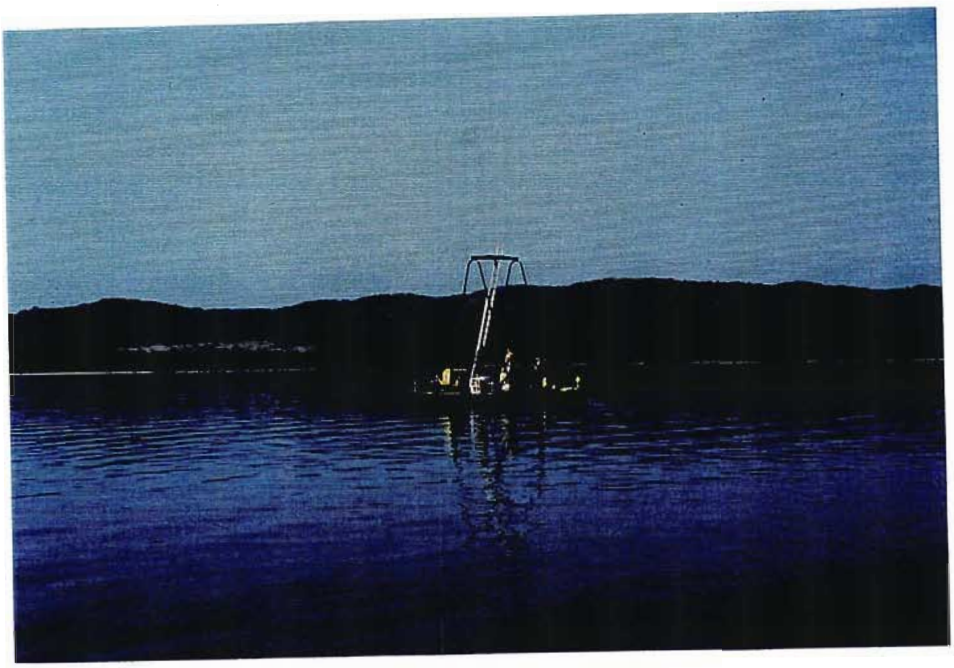

**Fig 8.2** A photograph of the coring barge used to collect the 6 m sediment cores from below Lake Sibaya. Note the four point anchoring system for stability during the coring operation.

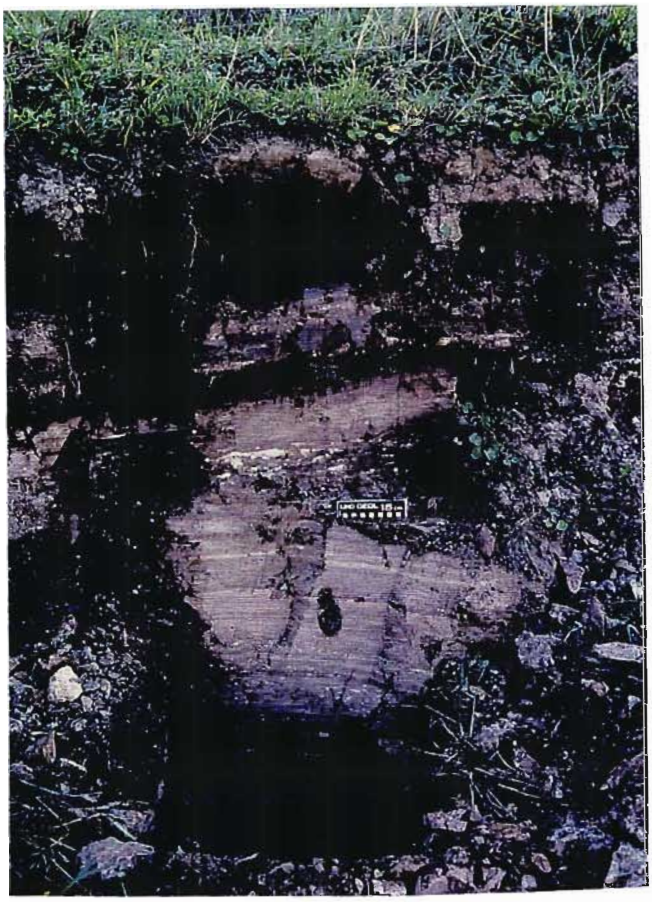

**Fig 8.3** The diatomite exposure which was excavated on the western shores of the Northern Arm (Fig 8.1: Core D). Note the highly laminated appearance of this sediment type and the presence of organic rich horizons. See Fig 8.6 for relevant core log and results of radiocarbon dating.

### 8.1.3 Core B

Core B was collected in the Main Basin (27° 20.853 S, 32° 41.536 E) in a water depth of 33.6 m. The core measured 4.40 m and consisted of light grey to dark grey muds overlying light grey fine to medium-grained sand rich in shell fragments and microfossils. These fossiliferous sediments overlie a succession of dark yellowish orange to dark reddish orange clay-rich sediments which exhibit soft sediment deformation structures (see Appendix 3 for core log).

### 8.1.4 Core SB2

Core SB2 was collected in the Southern Basin (27° 24.313' S, 32° 42.478' E) in a water depth of 24.2 m. The core measured 3.85 m and consisted of an upper unit of thinly bedded, bioturbated, fine to medium-grained sand and a basal unit of light grey to light brown, medium-grained sandy sediments with finely disseminated organic material (see Appendix 3 for core log).

### 8.1.5 Core J

Core J was collected in the Main Basin (27° 22.097' S, 32° 41.174 E) in a water depth of 33.6 m. The core measured 4.23 m and consists of a thin upper unit of pale olive, fine-grained sand overlying a thick (>3 m) succession of light grey sandy sediments with subordinate horizons of dark grey to black, strongly bioturbated sediments rich in organic material (see Appendix 3 for core log).

### 8.1.6 Core S

Core S was collected in the southern part of the Main Basin (27° 22.603 S, 32° 41.405 E) in a water depth of 7.5 m. The core consisted of an upper unit of calcareous diatomite sediments with subordinate horizons enriched in freshwater gastropods. This unit overlies pale grey medium-grained sands with freshwater shell fragments. The base of the core is defined by pale brown to light brown sandy sediments containing white kaolinized grains of microcline and exhibiting minor soft sediment deformation structures (see Appendix 3 for core log).

### 8.1.7 Core ZB

Core ZB was collected in the western area of the Main Basin (27° 21.442 S, 32° 40.561 E) in a water depth of 18.9 m. The core consisted of a thin ferruginous sandy lense underlain by a calcareous diatomite deposit with numerous freshwater shells and a basal dark grey clay horizon. The base of the core is defined by a black peat horizon which overlies a dark grey fine to medium-grained, strongly bioturbated sand with finely disseminated organic material (see Appendix 3 for core log).

### 8.1.8 Core 2

Core 2 was collected in the central part of the Main Basin (27° 20.796 S, 32°41.809 E) in a water depth of 40.1 m. The core consists of an upper unit of dark grey muds with subordinate thinner sand lenses overlying a medium-grained sand unit both rich in microfossils. A black organic mud defined the base of the fossiliferous sands and overlies a dark grey fine to medium-grained sand and a light grey clay. The base of the core is defined by a calcrete which consists of white, gravel sized calcareous nodules in a light grey, medium-grained sandy matrix (see Appendix 3 for core log).

### 8.1.9 Core Y

Core Y was collected in the western area of the Main Basin (27° 21.517 S, 32° 40.166 E) in a water depth of 10.3 m. The core comprises an upper unit of alternating fine-grained olive sands and diatomite layers containing freshwater molluscs. This unit overlies a succession of pale brown to light grey, fine-grained, free flowing sands with little interstitial clay material. The basal part of the core comprises light brown to dark brown, clay rich, fine-grained sand with kaolinised grains of microcline. These sediments display soft sediment deformation structures, are pliable when moist but alter to a very hard consistency upon desiccation (see Appendix 3 for core log).

### 8.1.10 Core U

Core U was collected in the northern part of the Main Basin (27° 20.594 S, 32° 41.333 E) in a water depth of 29.4 m. Core U consists of an upper unit of light olive to dark yellow fine-grained sands rich in freshwater molluscs and sponge spicules. This unit overlies a pale grey succession of fine-grained, bioturbated sands rich in microfossils. The basal unit comprises light reddish orange, fine grained sand rich in interstitial clay which displays soft sediment deformation structures (see Appendix 3 for core log). The basal sediments are pliable when moist but go hard upon dessication.

### 8.1.11 Core N

Core N was collected from the northern area of the Main Basin (27° 19.892 S, 32° 41.457 E) in a water depth of 10.2 m. This core consists of an upper unit of thinly bedded, pale brown to pale olive, fine-grained, mottled sands with freshwater shell fragments. These sediments overlie a succession of pale olive to dark yellow, hard, clay-rich sands which display soft sediment deformation structures (see Appendix 3 for core log).

### 8.1.12 Core SWB1

Core SWB1 was collected at the confluence of the Southwestern Bay and the Main Basin (27° 22.530 S, 32° 40.113 E) in a water depth of 18.5 m. Core SWB1 consists of an upper unit of light brown to dark grey, fine-grained sands rich in sponge spicules with subordinate dark yellow, strongly bioturbated horizons. These sediments overlie a unit of light grey, fine-grained, moderately bioturbated sand which in turn overlies a pale olive, fine-grained, non bioturbated sand unit. The base of this core comprises light brown, fine-grained, hard, clay rich sand (see Appendix 3 for core log).

### 8.1.13 Core L

Core L was collected in the eastern area of the Main Basin (27° 22.107 S, 32° 42.837 E) adjacent to the coastal dune complex. The core consists of a succession of light brown to light olive, fine to medium-grained sands with varying amounts of marine and freshwater microfossils. The succession is punctuated dark brown organic rich horizons, a dark yellow oxidised horizon and horizons of extreme bioturbation (see Appendix 3 for core log). The heavy mineral content of these sediments is above background values (visual estimation) for the Lake Sibaya area.

## 8.2 DESCRIPTION OF KEY STRATIGRAPHIC UNITS

The core logs have been subdivided into a number of recurring sedimentary facies on the basis of textural differences, fossil content, sedimentary structures, and organic carbon and calcium carbonate contents. Eight sedimentary facies have been identified and are discussed below.

### 8.2.1 Facies A

Facies A consists of thick accumulations (> 2.9 m) of light grey to dark grey gyttja in the deeper areas of the lake. The gyttja deposits vary from a soupy, sapropellic mud to a firmer organic clay with weakly defined lamination. The clay fraction of the gyttja deposits varies from 31 % to 95 % averaging 68 %. The organic carbon content varies from 3.2 % to 20.9 % and averages 15 %. The sand fraction of the gyttja deposits is fine-grained, moderately well sorted with near symmetrical grain size distributions. Fossil content of these sediments include pollen palynomorphs and sponge spicules. Carbonate contents vary considerably down core and higher values tend to be associated with the firmer organic clays. Values range from 0 % to 28.3 % and average 4.8 %. The sedimentary characteristics of Facies A are summarised in Table 8.1 below.

| $n = 32$ | **Mean** | **Sorting** | **Skewness** | **Mud %** | **C org. %** | **$CaCO_3$ %** |
|---|---|---|---|---|---|---|
| **Min.** | 3.10 | 0.49 | -0.25 | 31.0 | 3.2 | 0.0 |
| **Max.** | 1.98 | 0.88 | +0.08 | 95.1 | 20.9 | 28.3 |
| **Ave.** | 2.72 | 0.65 | -0.07 | 68.2 | 15.1 | 4.82 |
| **Color** | Light grey to dark grey | | | | | |
| **Sediment Type** | Soupy organic mud - "gyttja" to a firmer clay | | | | | |
| **Sedimentary Structures** | Weak 3 - 30 mm lamination | | | | | |
| **Fossils** | Pollen, sponge spicules, freshwater molluscs and diatoms | | | | | |

**Table 8.1 Sedimentary characteristics of Facies A.**

The clay mineralogy of the gyttja as determined from XRD analysis (Dr. D. Buhmann - Council for Geoscience) varies considerably downcore. (see Table 8.2 over leaf).

| | Smectite | Kaolinite | Quartz | Microcline | Aragonite | Calcite | Hematite |
|---|---|---|---|---|---|---|---|
| Top | 14% | 45% | 36% | 5% | - | - | - |
| Middle | 1% | 12% | 43% | - | 12% | 17% | 15% |
| Bottom | 2% | 9% | 59% | 6% | 9% | 15% | - |

**Table 8.2 Clay mineralogy variations from Core P**

### 8.2.2 Facies B

Facies B consists of fine-grained sand horizons in the shallow fringing areas of the lake. The sediments range in colour from pale olive to dark brown with occasional dark yellow oxidized horizons. These sediments are thinly bedded, fine-grained, well sorted sands with coarse skewed grain-size distributions. The thickness of the beds varies from 0.08 m to 1.9 m in the sediment cores and averages 0.47 m. The clay content of Facies B sediments ranges from 0 % to 20 % and averages 5.3 %. Organic carbon content averages 1.9 %. Facies B sediments are often strongly bioturbated and contain varying amounts of freshwater shells, sponge spicules and faecal pellets. The sedimentary characteristics of Facies B sediments are highlighted in Table 8.3 below.

| $n = 36$ | Mean | Sorting | Skewness | Mud % | C org. % | $CaCO_3$ % |
|---|---|---|---|---|---|---|
| **Min.** | 2.88 | 0.33 | -0.40 | 0.0 | 0.0 | 0.0 |
| **Max.** | 2.00 | 0.63 | 0.00 | 20.0 | 5.1 | 5.9 |
| **Ave.** | 2.44 | 0.46 | -0.19 | 5.3 | 1.9 | 0.0 |
| **Color** | Pale olive - dark brown; light grey; subordinate dark yellow horizons | | | | | |
| **Sediment Type** | Sand with subordinate silt layers and dark yellow oxidized horizons | | | | | |
| **Sedimentary Structures** | Bedding and bioturbation | | | | | |
| **Fossils** | Freshwater shells and shell fragments; sponge spicules | | | | | |

**Table 8.3 Sedimentary characteristics of Facies B.**

### 8.2.3 Facies C

Facies C consist predominantly of light grey to light brown, subangular to subrounded fine to medium-grained sandy sediments rich in microfossils. A firm fossiliferous silty clay sometimes forms the upper limit of Facies C. The clay content of fossiliferous silty clay averages ± 40 % and averages 5.7 % for the fine-grained sands. The sand fraction of Facies C is moderately well sorted to well sorted with a coarse skewed to near symmetrical grain-size distribution. Organic carbon content of the sediments varies between 0.8 % and 7.3 % averaging 2.2 %. The calcium carbonate content of these sediments varies from 0 % to 18.7 % averaging ± 1.4 % and is dependent on the presence of shell lags. The thickness of this unit varies from 0.8 m to greater than 3.7 m in core. The sand fraction varies in colour from light grey to light brown and the microfossil content indicates a probable marine origin for these sediments. The sedimentary characteristics of Facies C are summarised in Table 8.4 below.

| $n = 22$ | **Mean** | **Sorting** | **Skewness** | **Mud %** | **C org. %** | **$CaCO_3$ %** |
|---|---|---|---|---|---|---|
| **Min.** | 2.97 | 0.36 | -0.29 | 0.0 | 0.8 | 0.0 |
| **Max.** | 2.00 | 0.69 | -0.10 | 40.0 | 7.3 | 18.7 |
| **Ave.** | 2.35 | 0.48 | -0.16 | 5.6 | 2.2 | 1.4 |
| **Color** | Pale grey - dark grey; light brown; light olive | | | | | |
| **Sediment Type** | Predominantly sand although some firm clays are also present | | | | | |
| **Sedimentary Structures** | Bedding and bioturbation | | | | | |
| **Fossils** | Marine shells, Foraminifera, ostracods, bryozoans and sponge spicules | | | | | |

**Table 8.4 Sedimentary characteristics of Facies C.**

### 8.2.4 Facies D

Facies D consists of thick accumulations (1 - 3 m) of massive to crudely bedded, light olive to light brown, subangular to rounded, well sorted, medium-grained sands with varying amounts of heavy minerals and shell fragments. Facies D represents the coarsest unconsolidated sediments sampled during the coring programme and is characterised by coarse skewed to near symmetrical grain-size distributions. Organic carbon contents of these sediments varies from 0 to 25 %

averaging 3 % while calcium carbonate contents are seldom more than trace values (< 1 %). The interstitial clay content of Facies D varies from 0 to 4.5 % and averages 1.2 %. The sedimentary characteristics of Facies D are summarised in Table 8.5 below.

| $n = 23$ | **Mean** | **Sorting** | **Skewness** | **Mud %** | **C org. %** | **$CaCO_3$ %** |
|---|---|---|---|---|---|---|
| **Min.** | 2.21 | 0.21 | -0.15 | 0.0 | 0.0 | 0.0 |
| **Max.** | 1.71 | 0.57 | +0.13 | 4.5 | 25.0 | 0.8 |
| **Ave.** | 1.99 | 0.42 | -0.07 | 1.2 | 3.0 | 0.0 |
| **Color** | Light olive - light brown | | | | | |
| **Sediment Type** | Medium-grained sand with occasional thin beds enriched in organic material | | | | | |
| **Sedimentary Structures** | Massive with occasional crude bedding | | | | | |
| **Fossils** | Shell fragments and sponge spicules | | | | | |

**Table 8.5 Sedimentary characteristics of Facies D.**

### 8.2.5 Facies E

Facies E consists of a diatomite and subordinate fine-grained sandy sediments. Diatomite deposits are present in cores from the shallow areas (less than -20 m) of Lake Sibaya. Thickness of the diatomite deposits ranges from 0.45 m to 2.2 m and averages 1.4 m. The deposits consist of pale grey to dark grey, strongly laminated diatomite punctuated occasionally by light olive to dark yellow sandy horizons or shells lags. A fine-grained, well sorted sand with near symmetrical to coarse skewed grain-size distribution makes up the clastic content of the diatomite deposits. The mud fraction (<63 $\mu$) varies from 36 % to 100 % and averages 84 % while the organic carbon content ranges from 1 % to 22 % averaging 9 %. The carbonate content of the diatomite is highly variable, with high values being associated with shell lags. The carbonate content varies between 20 % and 72 % and averages 48 %. Fossil content includes diatoms and freshwater molluscs. The sedimentary characteristics of Facies E are summarised in Table 8.6 over leaf.

| $n = 17$ | Mean | Sorting | Skewness | Mud % | C org. % | $CaCO_3$ % |
|---|---|---|---|---|---|---|
| **Min.** | 2.67 | 0.37 | -0.23 | 36.0 | 1.0 | 19.6 |
| **Max.** | 2.10 | 0.85 | +0.02 | 100.0 | 21.8 | 72.2 |
| **Ave.** | 2.42 | 0.50 | -0.11 | 83.8 | 8.8 | 47.7 |
| **Color** | Light grey - dark grey | | | | | |
| **Sediment Type** | Diatomite and organic wetland deposits | | | | | |
| **Sedimentary Structures** | Lamination & shell lags | | | | | |
| **Fossils** | Freshwater diatoms and molluscs | | | | | |

**Table 8.6 Sedimentary characteristics of Facies E.**

### 8.2.6 Facies F

This sedimentary unit varies in thickness from 0.5 m to >3.4 m and is present in 54 % of the cores. Sediment colours include pale grey to dark grey, pale brown to light brown and pale olive. Thin dark brown horizons of organic rich sediments which dip at angles ranging from 0° to 45° are present in the sedimentary succession. Grain size ranges from fine to medium-grained and sediment sorting varies from moderately well sorted to very well sorted. Grain size distributions range from near symmetrical to strongly coarse skewed and mud fractions are typically low (average 1.8 %). Organic carbon values range from 0 % to 25 % and average 2.0 %, calcium carbonate contents are seldom more than trace values (<1 %). Fossil content of these sediments is sparse with only a few sponge spicules and freshwater molluscs being evident. Sedimentary structures include steeply inclined organic rich horizons and a few examples of soft sediment deformation. The sedimentary characteristics of Facies F are summarized in Table 8.7 over leaf.

| $n = 62$ | Mean | Sorting | Skewness | Mud % | C org. % | $CaCO_3$ % |
|---|---|---|---|---|---|---|
| **Min.** | 2.80 | 0.21 | -0.43 | 0.0 | 0.0 | 0.0 |
| **Max.** | 1.71 | 0.70 | +0.13 | 12.0 | 25.0 | 4.9 |
| **Ave.** | 2.27 | 0.47 | -0.16 | 1.8 | 2.0 | 0.1 |
| **Color** | Pale grey - dark grey; pale brown - light brown; pale olive; dark yellow | | | | | |
| **Sediment Type** | Free flowing sand | | | | | |
| **Sedimentary Structures** | Steeply dipping organic rich horizons; soft sediment deformation structures | | | | | |
| **Fossils** | Few sponge spicules and freshwater molluscs | | | | | |

**Table 8.7 Sedimentary characteristics of Facies F.**

### 8.2.7 Facies G

Facies G is only encountered in Core D (Appendix 3) and consists of a dark yellow firm clay with subordinate goethite laminae which grades downward into a dark yellow to light brown clay rich sand. The mud fraction (<63 $\mu$) ranges from 40 % to 87 % and averages 66 %. Organic carbon content varies from 2.4 % to 7.4 % averaging 4.7 % and calcium carbonate values are zero. The clastic fraction is well sorted, fine to very fine-grained sand with coarse skewed to near symmetrical grain-size distributions. Facies G characteristics are summarised in Table 8.8 below.

| $n = 4$ | Mean | Sorting | Skewness | Mud % | C org. % | $CaCO_3$ % |
|---|---|---|---|---|---|---|
| **Min.** | 3.30 | 0.36 | -0.27 | 40.0 | 2.4 | 0.0 |
| **Max.** | 2.98 | 0.47 | 0.12 | 87.0 | 7.4 | 0.0 |
| **Ave.** | 3.18 | 0.41 | -0.04 | 66.0 | 4.7 | 0.0 |
| **Color** | Dark yellow to light brown | | | | | |
| **Sediment Type** | Firm clays and clay rich sands | | | | | |
| **Sedimentary Structures** | Goethite laminae | | | | | |
| **Fossils** | None observed | | | | | |

**Table 8.8 Sedimentary characteristics of Facies G.**

### 8.2.8 Facies H

Facies H sediments consist of partly lithified, clay-rich, oxidised sandy sediments with well developed soft sediment deformation structures. Sediment colour ranges from dark yellowish orange to pale olive with dark yellow mottling. Mud fraction (<63 $\mu$) ranges from 8.2 % to 36.5 % and averages 18.4 % while organic carbon content varies from 1.6 % to 17.2 %, averaging 3.6 %. Calcium carbonate values are zero. The clastic fraction varies from moderately well sorted to very well sorted, fine to very fine-grained sand with coarse skewed to near symmetrical grain-size distributions. Sediment consistency varies considerably with moisture content, whereby the sediment is soft and pliable when moist but extremely hard when dry. The sedimentary characteristics of Facies H are summarised in Table 8.9 below.

| $n = 23$ | **Mean** | **Sorting** | **Skewness** | **Mud %** | **C org. %** | **$CaCO_3$ %** |
|---|---|---|---|---|---|---|
| **Min.** | 3.19 | 0.19 | -0.48 | 8.2 | 1.6 | 0.0 |
| **Max.** | 2.20 | 0.67 | 0.10 | 36.5 | 17.2 | 0.0 |
| **Ave.** | 2.93 | 0.34 | -0.13 | 18.4 | 3.6 | 0.0 |
| **Color** | Dark yellow to dark reddish orange; pale grey with dark yellow mottling | | | | | |
| **Sediment Type** | Ferruginous clays and clay rich sands | | | | | |
| **Sedimentary Structures** | Soft sediment deformation structures | | | | | |
| **Fossils** | None observed | | | | | |

**Table 8.9 Sedimentary characteristics of Facies H.**

## 8.3 INTERPRETATION OF KEY STRATIGRAPHIC UNITS

Sedimentological differences in conjunction with fossil material and radiocarbon dates obtained from core material has enabled each of the key stratigraphic units to be assigned to the lithostratigraphic framework proposed by Dr. G. Botha (1997). The facies interpretations are discussed, and the interpreted sedimentary core logs are illustrated below.

### 8.3.1 Facies A

Facies A represents the youngest sediments to be sampled in the coring programme. The unconsolidated nature of these "soupy" sediments along with the weak lamination, high organic carbon content and the presence of freshwater diatoms and molluscs indicate that this facies represents typical lake sediments similar to those accumulating in the deeper areas of Lake Sibaya at present. The change in clay mineralogy and increase in carbonate content "downcore" in this facies (Appendix 3, core P & core B) suggests that there has been a change in the water chemistry through time, from saline or brackish conditions to totally freshwater conditions. Diatom studies indicate the base of Facies A is dominated by marine and brackish water forms (*Hyalodiscus subtilis*) near the base of the succession while freshwater forms (*Aulacoseira italica*) appear higher up the succession and are only dominant in the upper metre of the sediments (*pers. Comm.* Prof. P.Alhonen, 1997: see Appendix 4). This is suggestive of a slow transition from marine/brackish conditions to freshwater conditions. It is interesting to note that the marine diatom forms dominated by *Hyalodiscus subtilis* are present throughout the sedimentary succession, suggesting that this species has adapted to freshwater conditions. Studies by Allanson *et al* (1966) revealed the existence of a typical estuarine component extant within Lake Sibaya, these include the crab *Hymenosoma orbiculare*, an isopod *Cyathura carinata*, and two species of amphipods. This gives further testament to a possible estuarine origin for Lake Sibaya.

The sponge spicule content of Facies A sediments is probably of wind blown origin as these are a recurring fossil assemblage throughout the sedimentary succession. A radiocarbon date of 5030 BP ± 70 from the base of Facies A (Fig. 8.4) indicates that the transition from marine conditions towards freshwater conditions began at about this time. Facies A represents distal (deep water) lake sediments with a lagoonal/estuarine component at the base of the succession. Thick accumulations of Facies A sediments are evident in cores P and B (Figs 8.4 & 8.5).

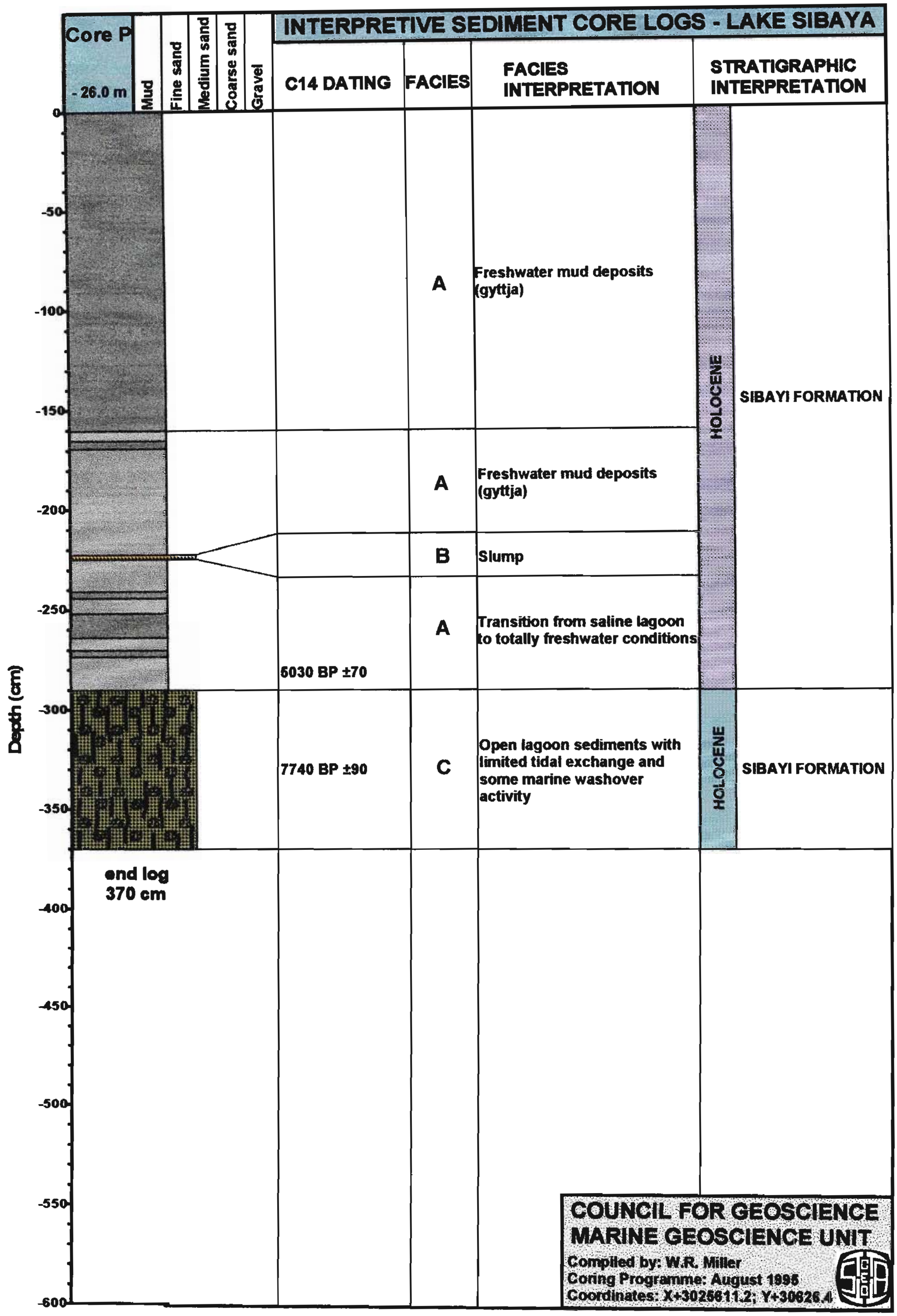


Fig 8.4 Interpretation of Core P (see Appendix 3 for descriptive core logs).

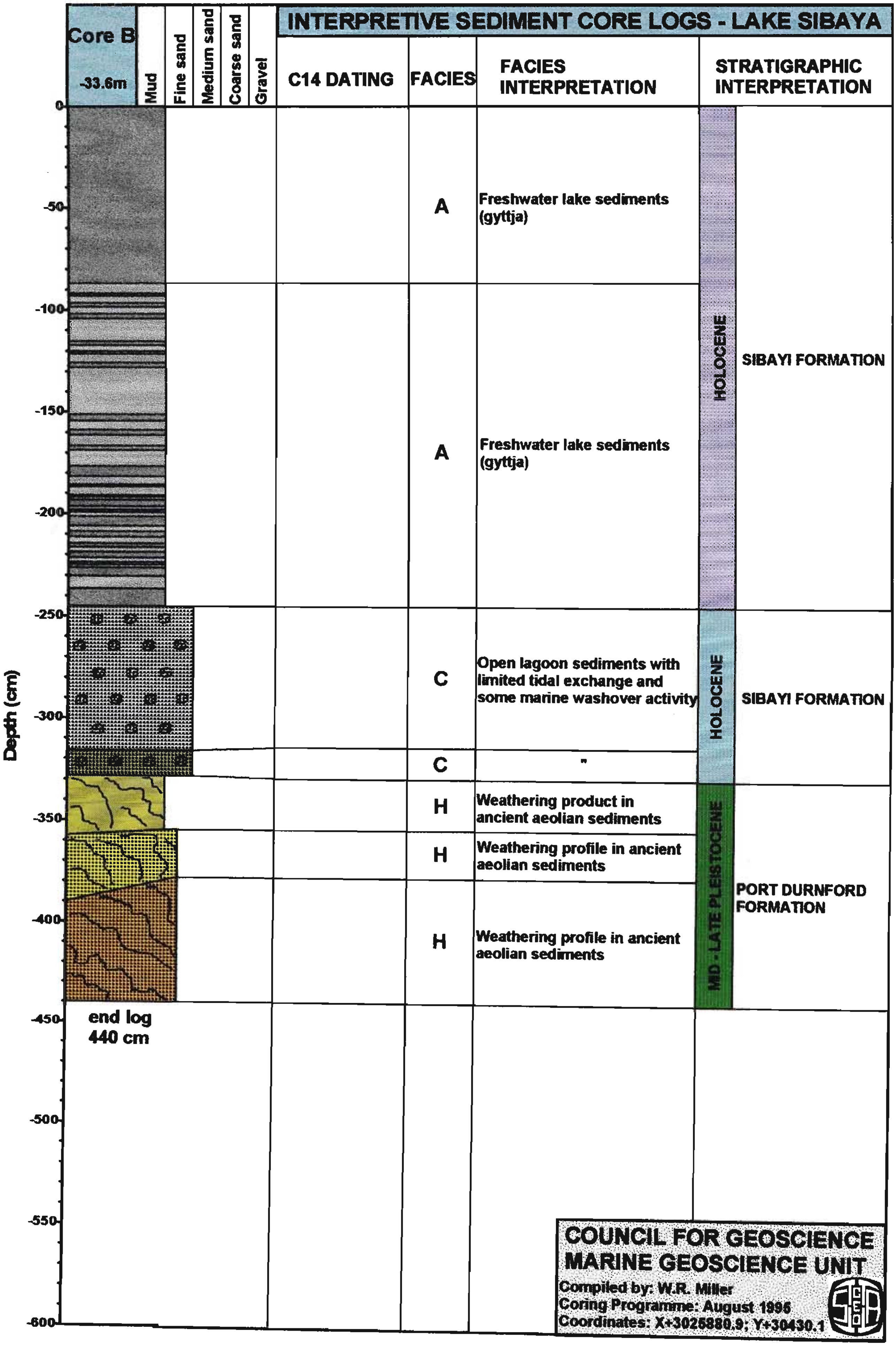


Fig 8.5 Interpretation of Core B (see Appendix 3 for descriptive core logs).

### 8.3.2 Facies B

Facies B sediments consist predominantly of fine-grained, well sorted, thinly bedded sands rich in extant species of freshwater molluscs and diatoms. The fact that these sediments have aeolian characteristics and contain a modern freshwater faunal assemblage suggests that this facies represents aeolian sediment which has slumped into the lake during periods of high water levels and subsequently been reworked by lacustrine processes. Facies B therefore represents shallow water, proximal lacustrine sediments of mid Holocene to recent age. No material from Facies B was sampled for radiocarbon dating. The molluscan assemblage for these sediments is summarised in Appendix 4.

### 8.3.3 Facies C

Facies C consists of fine to medium-grained sand rich in marine microfossils. The molluscan assemblage (identified by Dr. R.N Kilburn - Natal Museum) represents a tropical Indian Ocean marine lagoonal fauna similar to the modern Durban Bay type environment (see Appendix 5). The molluscan assemblage contains some juveniles and one mangrove/estuarine species (*Assiminea ovata*) which is suggestive of at least some tidal exchange with the open sea during the accumulation of this sediment. The Foraminifera (identified by I. McMillan - de Beers Marine) are typical of tropical Indian Ocean, shallow marine, well oxygenated, wave influenced environments with a coral reef or associated lagoonal setting (see Appendix 5). This suggests that the sediment accumulated in a lagoon with at least limited tidal exchange with the open sea. The more mature and coarser grained nature of this sediment type in comparison to the other predominantly aeolian sediments in the Lake Sibaya region suggests that this sediment was introduced from the marine environment, probably as a series of washover fans. A radiocarbon date from the molluscan shell fragments yields an age of 7740 BP ± 90 (Fig. 8.4) indicating that this sediment accumulated during early to mid Holocene times. A radiocarbon date from coastal wetland deposits below the lagoonal sediments in Core 2 (Fig 8.6) yields a maximum possible age of the 8810 ± 100 BP for the lagoonal sediments. Facies C represents a marine lagoonal depositional environment that was subject to frequent infilling by marine washover sediments. The sediment is Holocene in age and therefore falls under the Sibayi Formation in the lithostratigraphic framework proposed by Dr. G.A. Botha (1997).

**8.3.4 Facies D**

Facies D consists of thick successions of medium grained, well sorted sand with near symmetrical grain-size distributions and variable amounts of shell fragments and heavy minerals. This facies is found in core L (Fig. 8.7) and core SB2 (Fig. 8.8) which are located in the eastern areas of the Main Basin and Southern Basin proximal to the modern coastal dune barrier. Core L comprises a thick succession of medium-grained sand rich in shell fragments which is interbedded with medium-grained lagoonal sediments rich in marine microfossils. Core SB2 is comparable in texture to core L but lacks the heavy mineral and shell fragment content of these sediments. The sediments of Facies D represent the coarsest clastic material sampled during the coring programme (with the exception of the calcrete in core 2; Fig 8.6). The symmetrical grain-size distributions and well sorted nature of these sediments implies an aeolian origin for Facies D, while the heavy mineral and shell fragment content of these sediments combined with a medium grain-size implies a barrier washover environment. The fact that this sediment type is located proximal to the modern coastal dune barrier at elevations slightly lower than mean sea-level (-4 to -5 m below MSL) reinforces the argument for a barrier depositional environment.

The variation in heavy mineral and shell fragment content of Facies D sediments in cores L and SB2, can probably be explained by the proximity of the core sites, to breaches created in the coastal dune barrier during the LGM erosion event, and also to the relative sizes of these breaches. The Southern Basin is incised to elevations of more than 6 m below MSL indicating that the coastal dune barrier was probably breached in this area during the late Pleistocene. The Southern Basin is significantly smaller and shallower than the Main Basin suggesting that less incision took place in this area. Smaller volumes of sediment would therefore have been required to seal the Southern Basin breach and this may have been accomplished by normal aeolian processes prior to the recovery of sea-level to near present levels. This mechanism would explain the similarity in texture between Facies D sediments in cores L and SB2 and the lack of shell fragments in core SB2. The sediments of Facies D therefore probably represent coastal barrier sediments of Holocene age and thus form part of the Sibayi Formation.

**8.3.5 Facies E**

Facies E consists of a substantial thickness of well laminated, freshwater diatomite with subordinate lenses/horizons of fine-grained sand or shell lags. Two ages of diatomite are found in the Lake Sibaya area: a late Pleistocene diatomite which contains no calcium carbonate, and a Holocene diatomite which has an average calcium carbonate content of ± 48 % (Table 8.5). For simplicity sake the late Pleistocene diatomite will be referred to as Facies E' and the Holocene diatomite will be referred to as Facies E. The late Pleistocene diatomites are found adjacent to the lake and represent lacustrine deposits of the proto-Lake Sibaya. The calcareous diatomites form part of the modern lake floor and are believed to have accumulated in shallow interdune wetlands during the Holocene development of the lake.

The late Pleistocene diatom assemblages (Facies E') were studied by Prof. P. Alhonen of the University of Helsinki who concluded that the diatoms were largely freshwater forms with minor amounts of brackish water forms and some marine forms at the top of the succession in core D (see Appendix 6). Two organic rich horizons from core D yielded radiocarbon dates of 25500 BP ± 420 near the top of the diatomite succession and 43500 BP +2600 - 2000 near the base of the succession (Fig 8.9). The proximity of the late Pleistocene diatomite exposure to modern sea-level (+ 21m) precludes the possibility that the marine forms are *in situ* and are most likely wind transported. The majority of the late Pleistocene diatomite exposure is dominated by alkaliphilous planktonic forms which indicates open water deposition in a deep (>10 m) freshwater lake (Miller *et al*, 1997). The thin sandy horizons in the diatomite imply terrestrial input into the lake while the organic rich horizons probably represent episodes of desiccation which allowed for the development of shallow peatlands or marshes to develop (Miller *et al*, 1997). A radiocarbon date from coastal wetland deposits at the base of a calcareous diatomite (Facies E) in Lake Sibaya (core ZB) yields a maximum possible age of 7060 BP ± 80 ( Fig. 8.10) which sets the calcareous diatomites apart from the late Pleistocene diatomites.

Freshwater diatomite and interdune wetland deposits of latest Pleistocene age show regional development on the Maputaland Coastal Plain and are consequently given a formation status (KwaMbonambi Formation) in the proposed Maputaland Group (Botha, 1997). The radiocarbon dates measured from the Lake Sibaya diatomite bracket the latest Pleistocene period (43500 BP - 25500 BP) and are comparable to dates measured from other diatomite exposures at the Mseleni (32100 BP ± 580 & 36400 BP ± 460; Botha, 1997) and Mbazwane (24800 BP ± 350; Maud *et al*, 1993). The subaqueous exposures of calcareous diatomite of Facies E are Holocene in age and therefore form part of the Sibayi Formation.

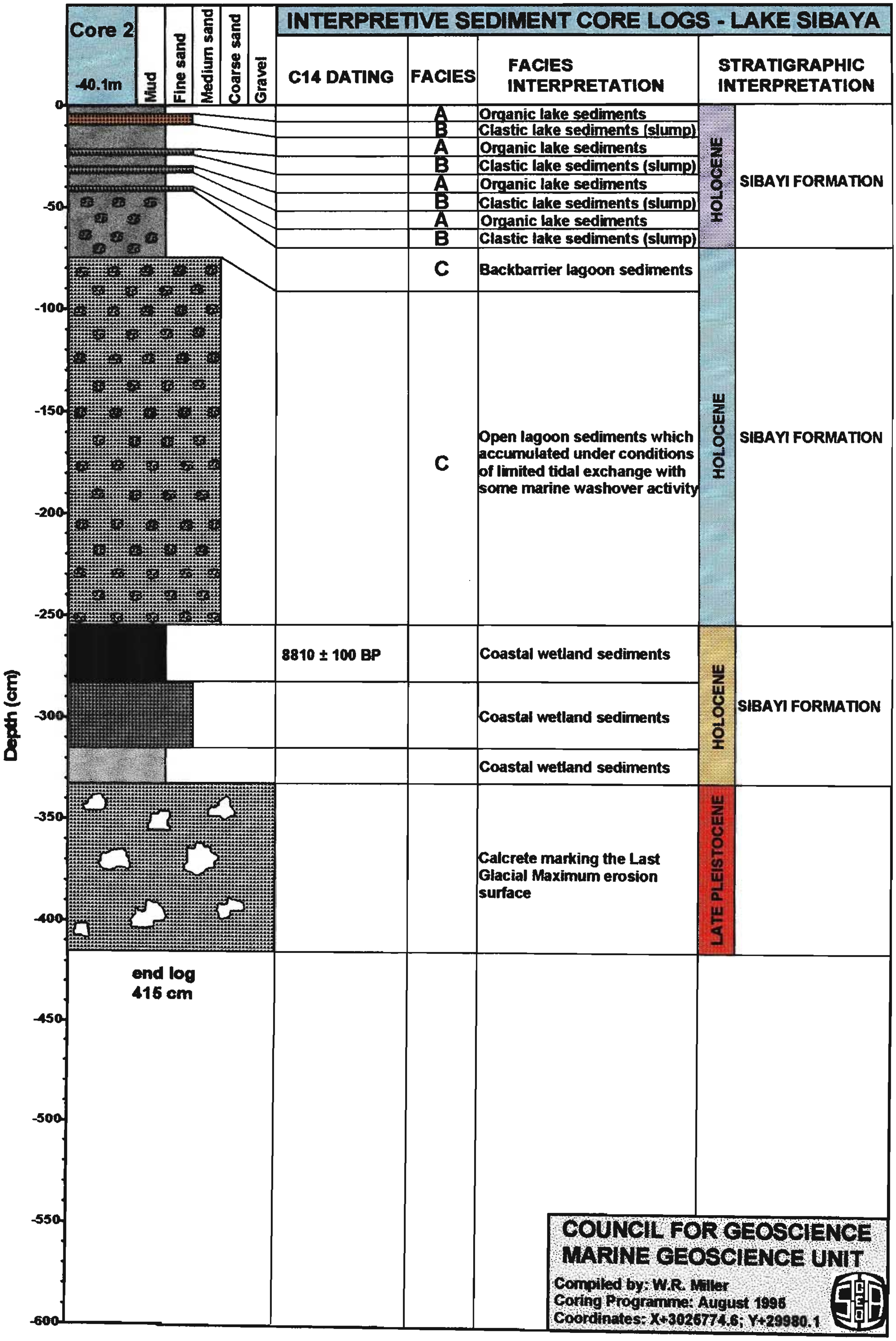


Fig 8.6 Interpretation of Core 2 (see Appendix 3 for descriptive core logs).

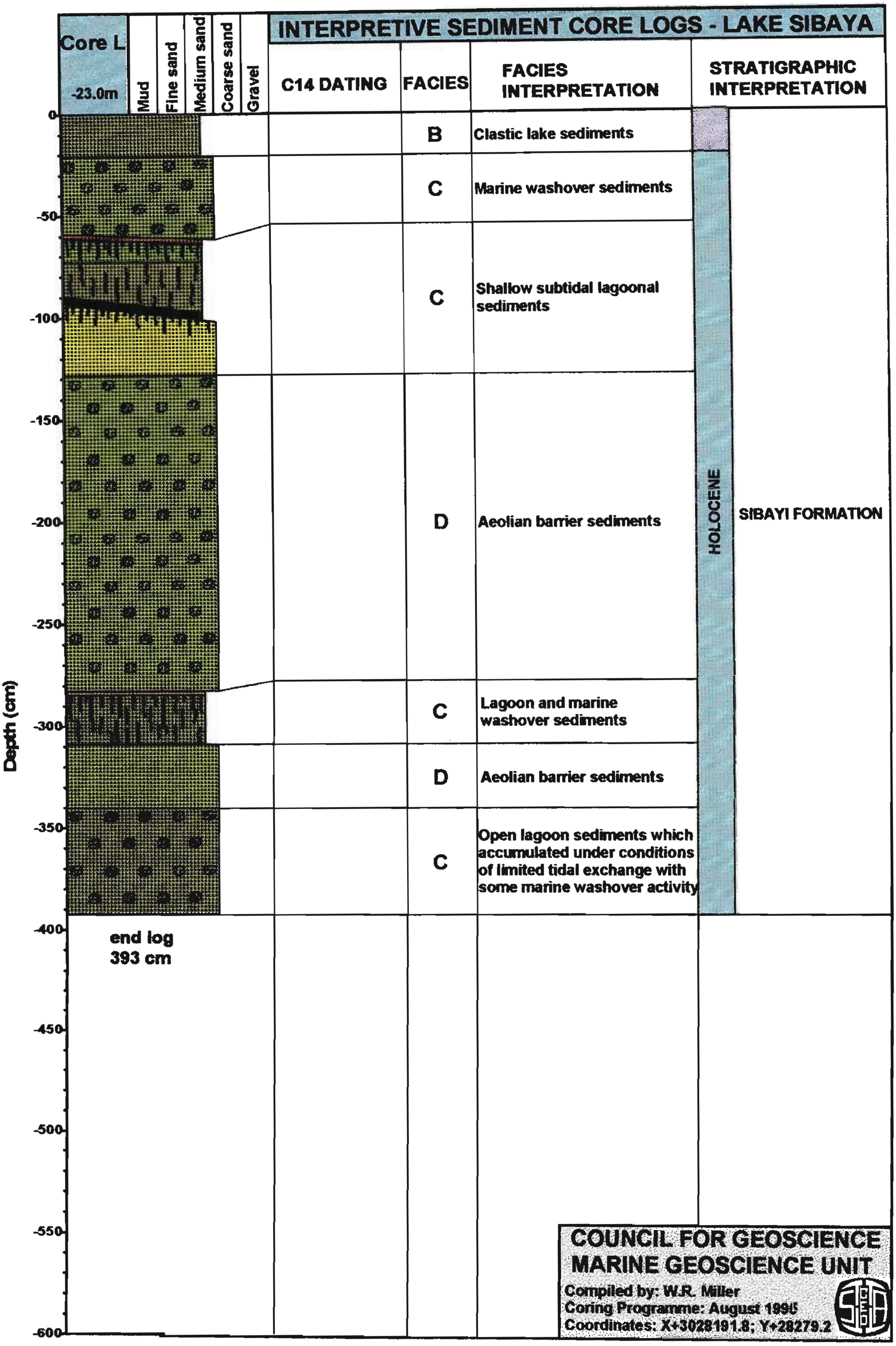


Fig 8.7 Interpretation of Core L (see Appendix 3 for descriptive core logs).

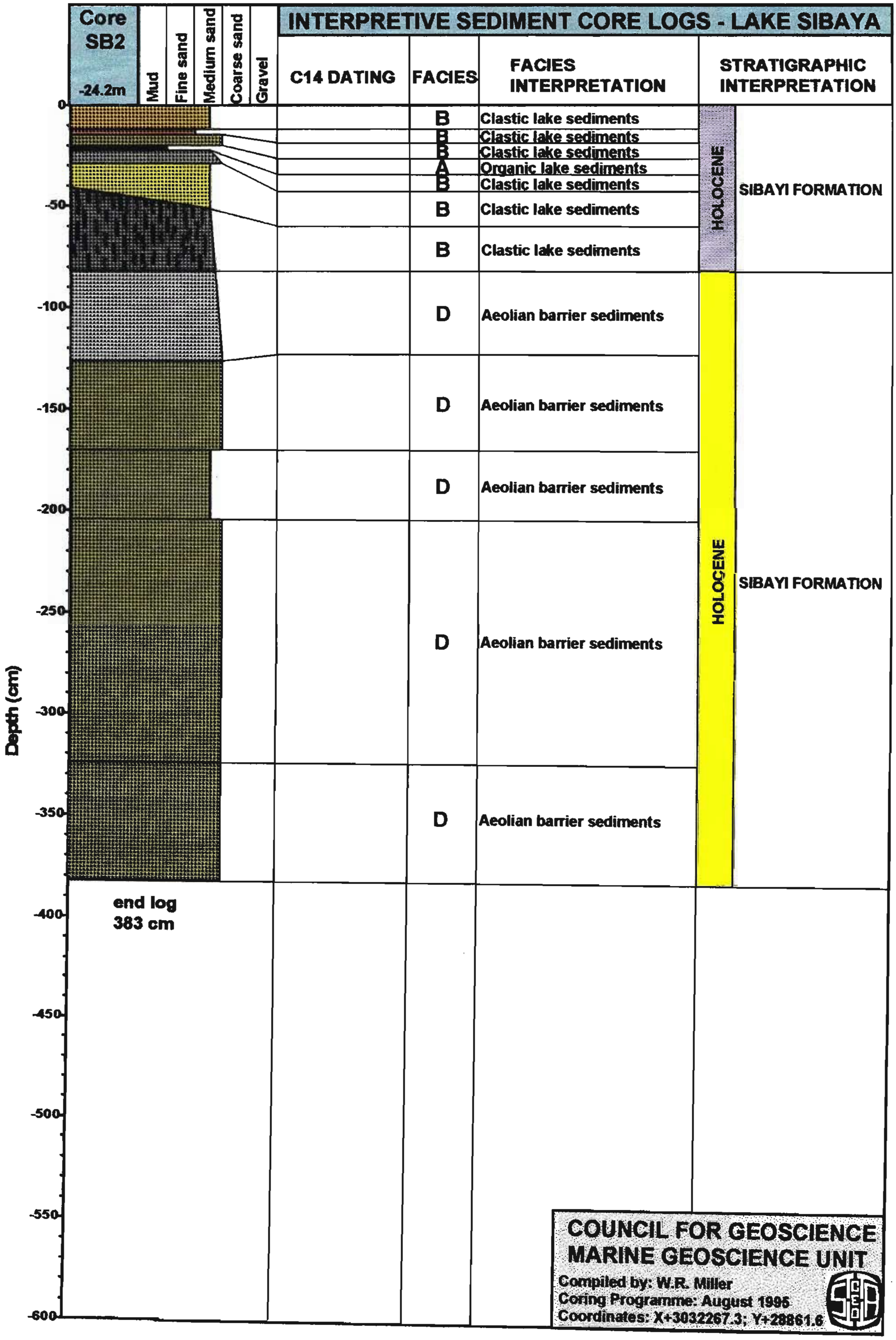


Fig 8.8 Interpretation of Core SB2 (see Appendix 3 for descriptive core logs).

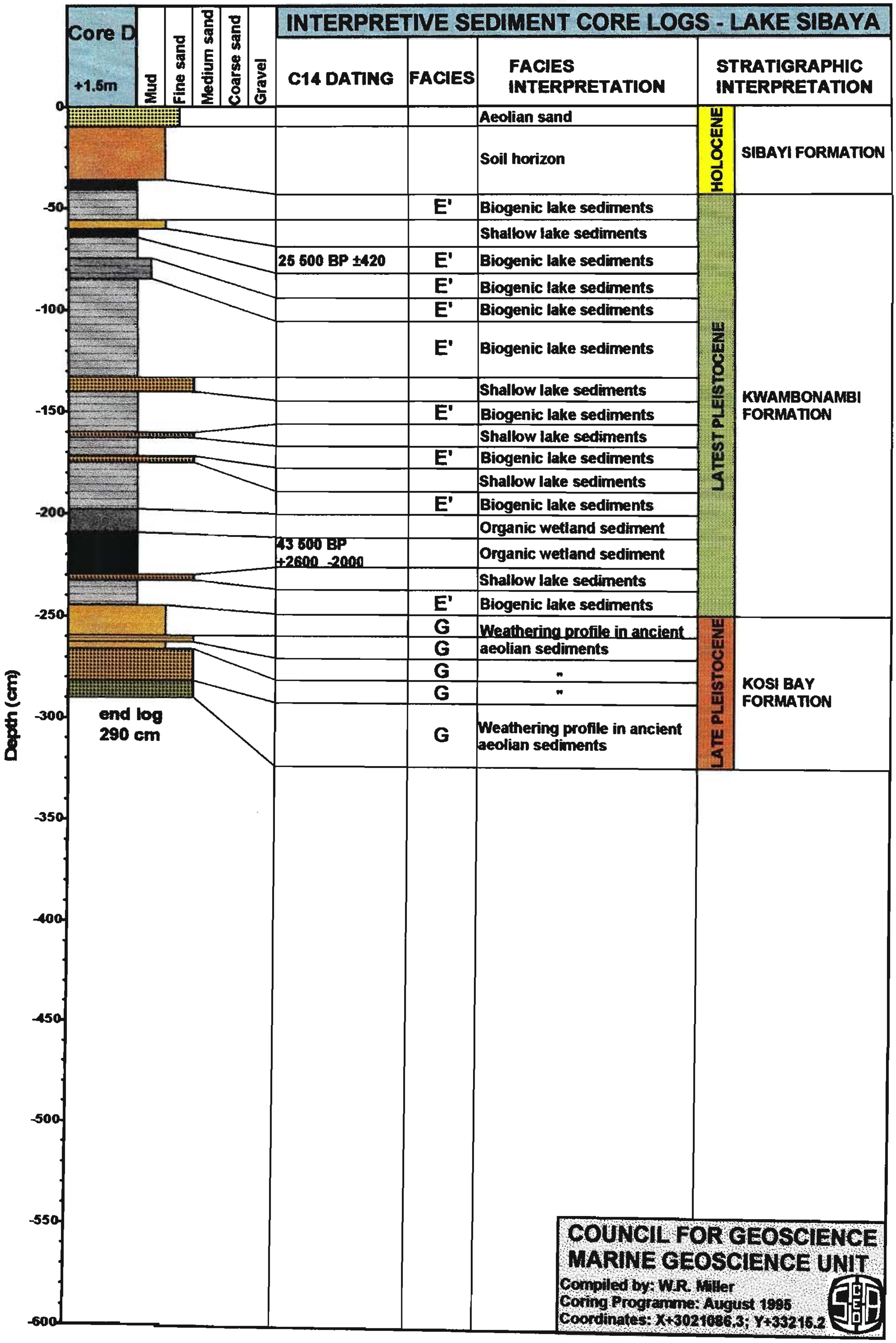


Fig 8.9 Interpretation of Core D (see Appendix 3 for descriptive core logs).

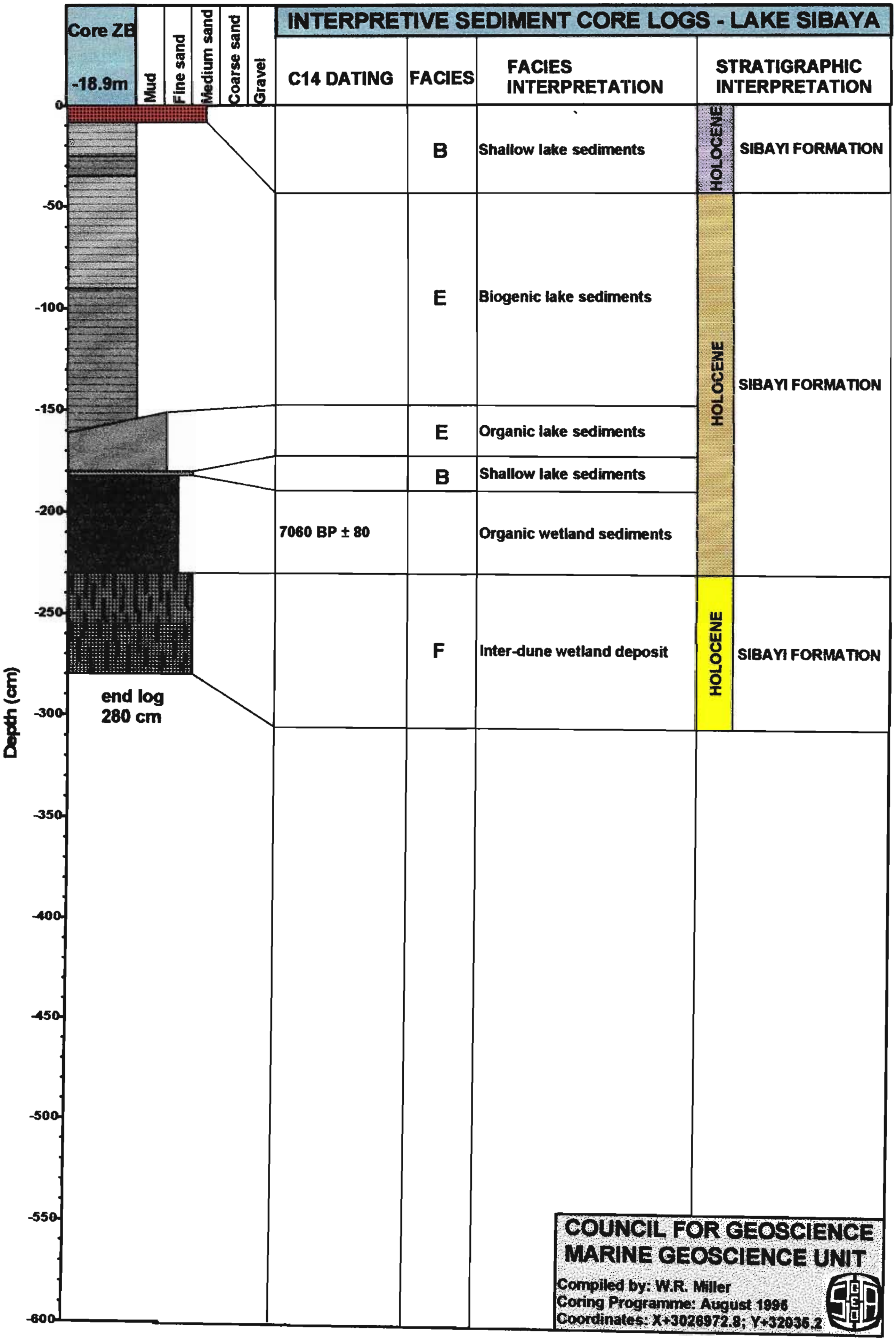


Fig 8.10 Interpretation of Core ZB (see Appendix 3 for descriptive core logs).

**8.3.6 Facies F**

Facies F consists of pale grey to dark yellow, fine-grained, free flowing, well sorted sand with coarse skewed grain size distributions. The sediment colour and grain size statistics are consistent with subaerially weathered aeolian sand. Facies F underlies the freshwater lake and Holocene diatomite deposits of Facies D making the minimum age of this sediment older than 7060 ± 80 BP (see Figs. 8.10, 8.11 & 8.12). The fossil content of these sediments is very sparse and is of no use in revealing a maximum age of deposition. A radiocarbon date from Core J (Fig 8.13) yielded an age of 5610 ± 80 BP for Facies F.

Facies F probably represents unconsolidated Holocene dune sands, which accumulated in the topographic low created by the draining of the proto-Lake Sibaya during late Pleistocene times. Facies F therefore represents part of the Sibayi Formation in the proposed Maputaland Group (Botha, 1997).

**8.3.7 Facies G**

Facies G consists of dark yellow to light brown clay rich sediments with subordinate goethite laminae. The fine-grained, well sorted grain-size distribution of the sand fraction implies an aeolian origin for these sediments, while the high clay content, the presence of goethite laminae and the high organic carbon content implies an ancient weathering profile or wetland deposit. The available evidence suggests that Facies G represents aeolian sediments that were flooded to form interdune wetlands. The fact that Facies G underlies the late Pleistocene diatomite deposits of the KwaMbonambi Formation (Facies D') adjacent to Lake Sibaya (Fig. 8.9) implies a minimum age of 43 500 BP for these sediments. Facies G probably represents the late Pleistocene aeolian sediments of the Kosi Bay Formation (Botha, 1997).

**8.3.8 Facies H**

Sediments of Facies H are characterised by dark yellow, partially lithified , clay rich sands with soft sediment deformation structures and grain size statistics reminiscent of weathered aeolian sediments. Facies H underlies Facies F (Fig. 8.14) and by virtue of the oxidised and lithified nature of the sediment is clearly the oldest sediment sampled during the coring programme at Lake Sibaya. A high clay and organic carbon content of Facies H sediments are suggestive of an ancient weathering profile. Outcrops of Facies H are evident around the margins of Lake Sibaya, where they are associated with an intermittently developed, fossiliferous ground water ferricrete. These characteristics typify the upper Port Durnford Formation in the Richards Bay area (personal observations at 5 mile beach north of Richards Bay and RBM mining ponds). Numerous stone implements have been recovered from the palaeosol horizon at the Lake Sibaya and Richards Bay sites, suggesting a similar age of deposition. The fact that Holocene sediments of the Sibayi Formation rest unconformably on sediments of Facies H in core N and core U suggests a period of erosion prior to the Holocene, which eroded the late Pleistocene sediments of the KwaMbonambi and Kosi Bay Formations (Figs. 8.15 & 8.16). This erosion episode is most likely to be the LGM event which eroded down to the more competent sediments of the Port Durnford and St. Lucia Formations (see Chapter 7).

The aeolian characteristics of the grain-size distributions of Facies H, combined with the depositional geometry (sequence 3 Chapter 7) and partly lithified nature of the sediments, suggests that these sediments represent weathered aeolian sediments of the Port Durnford Formation.

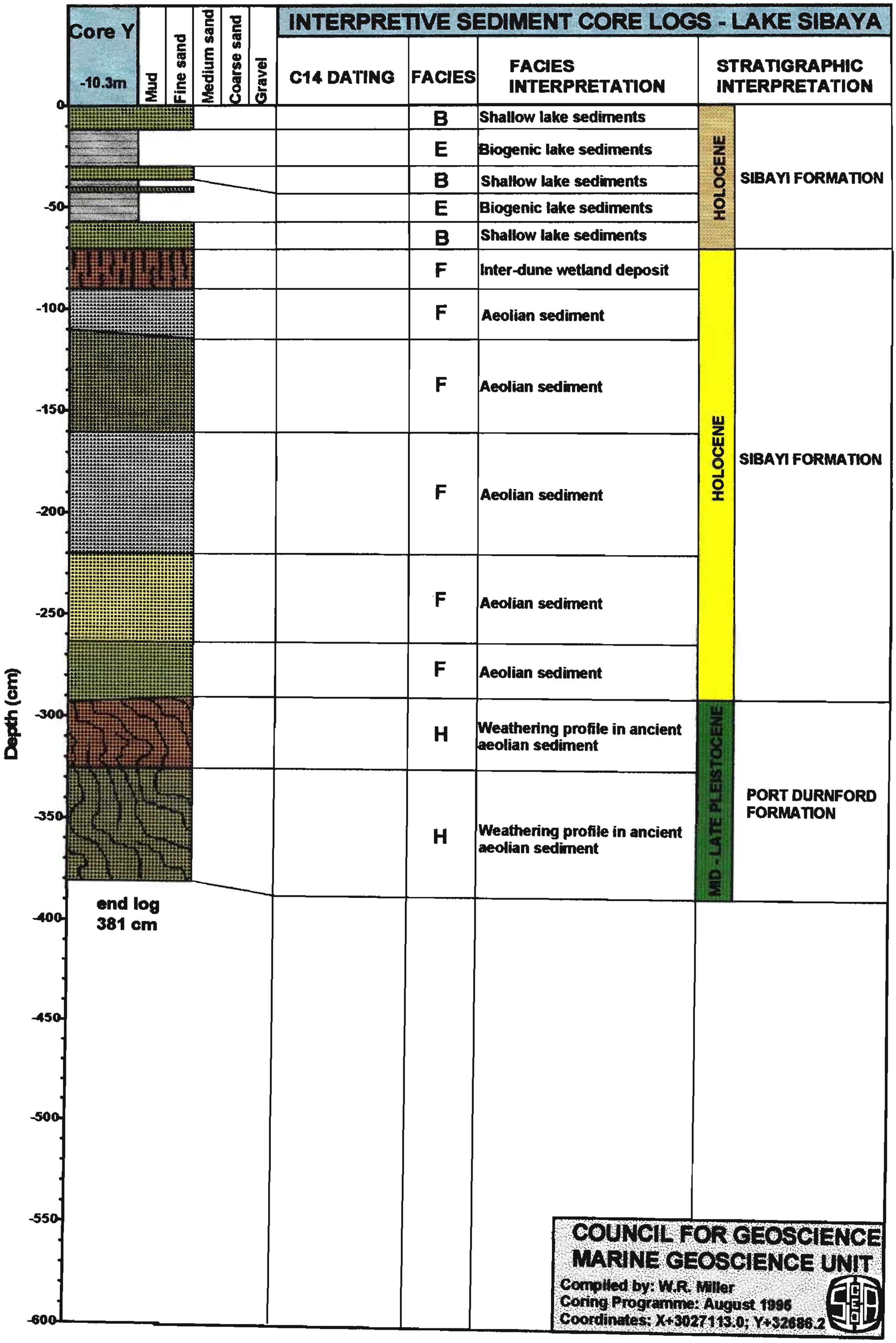


Fig 8.11 Interpretation of Core Y (see Appendix 3 for descriptive core logs).

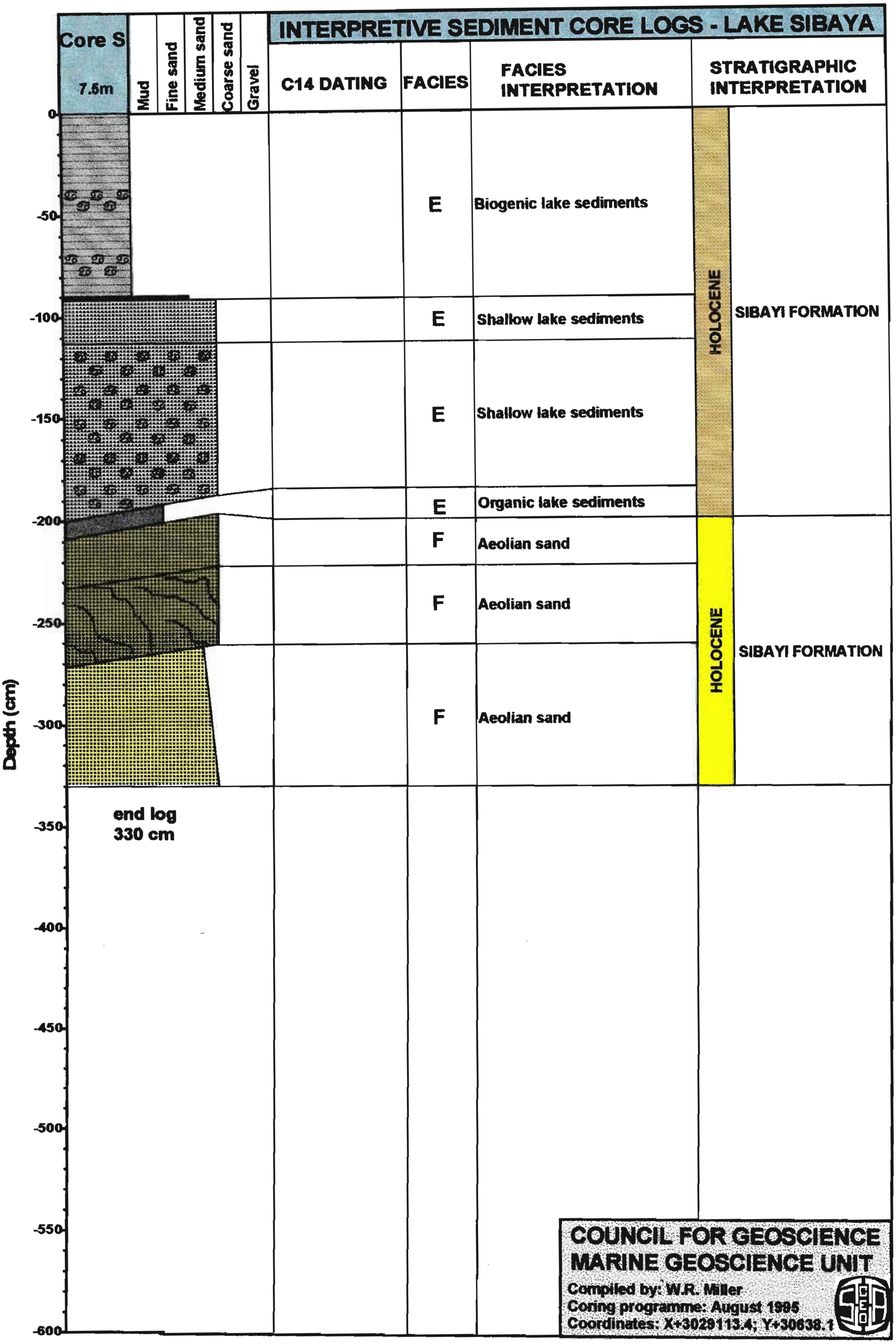


Fig 8.12 Interpretation of Core S (see Appendix 3 for descriptive core logs).

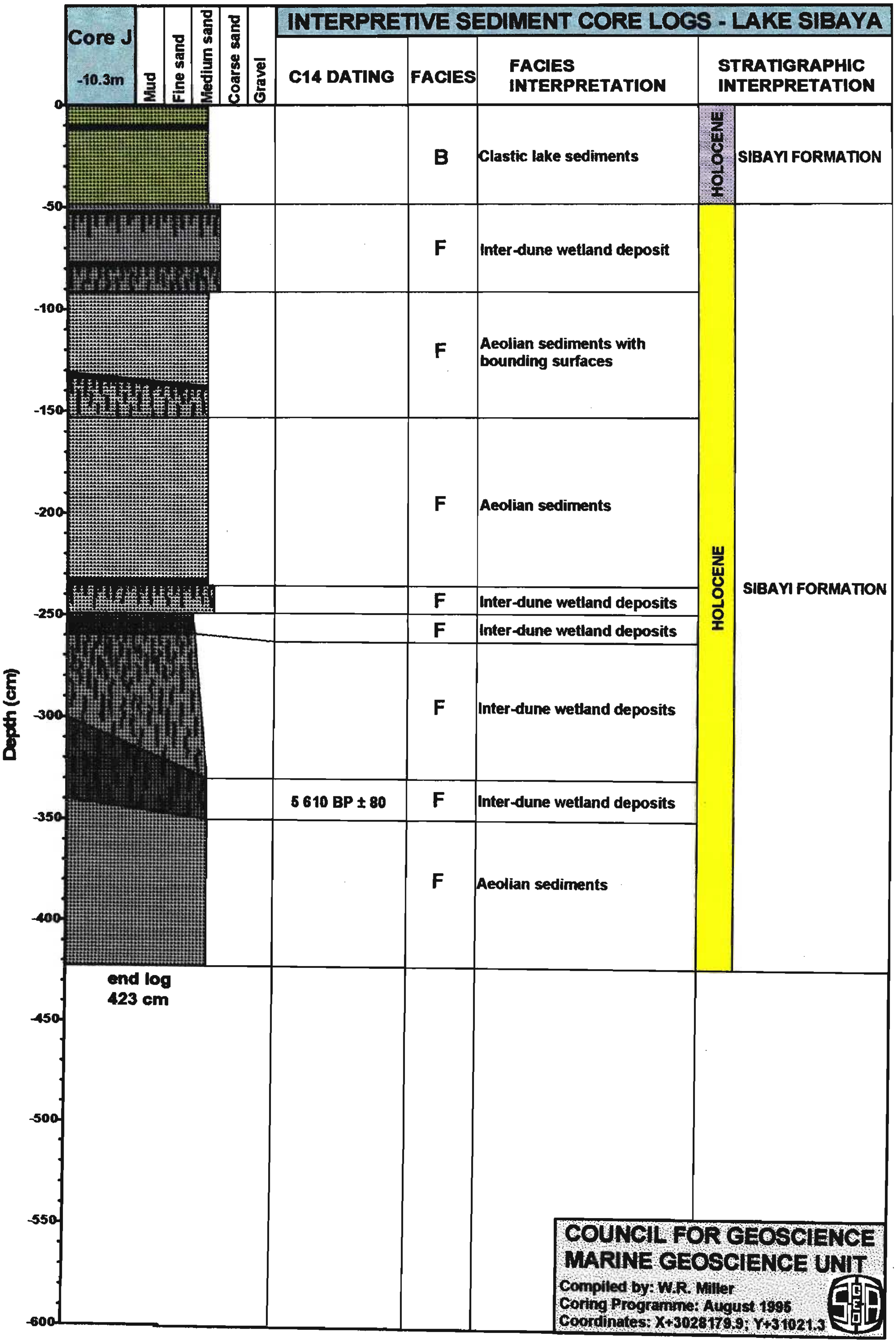


Fig 8.13 Interpretation of Core J (see Appendix 3 for descriptive core logs).

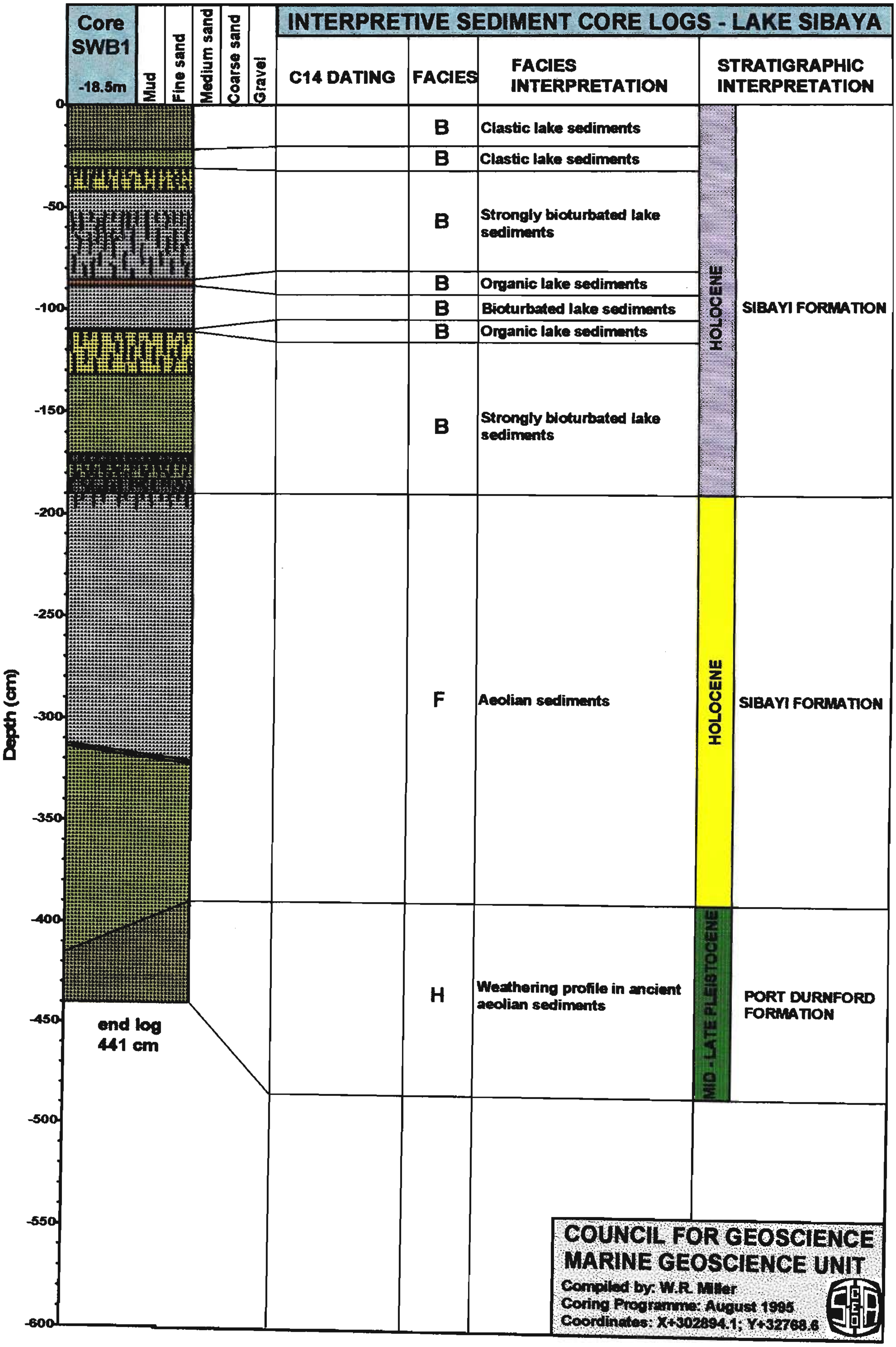


Fig 8.14 Interpretation of Core SWB1 (see Appendix 3 for descriptive core logs).

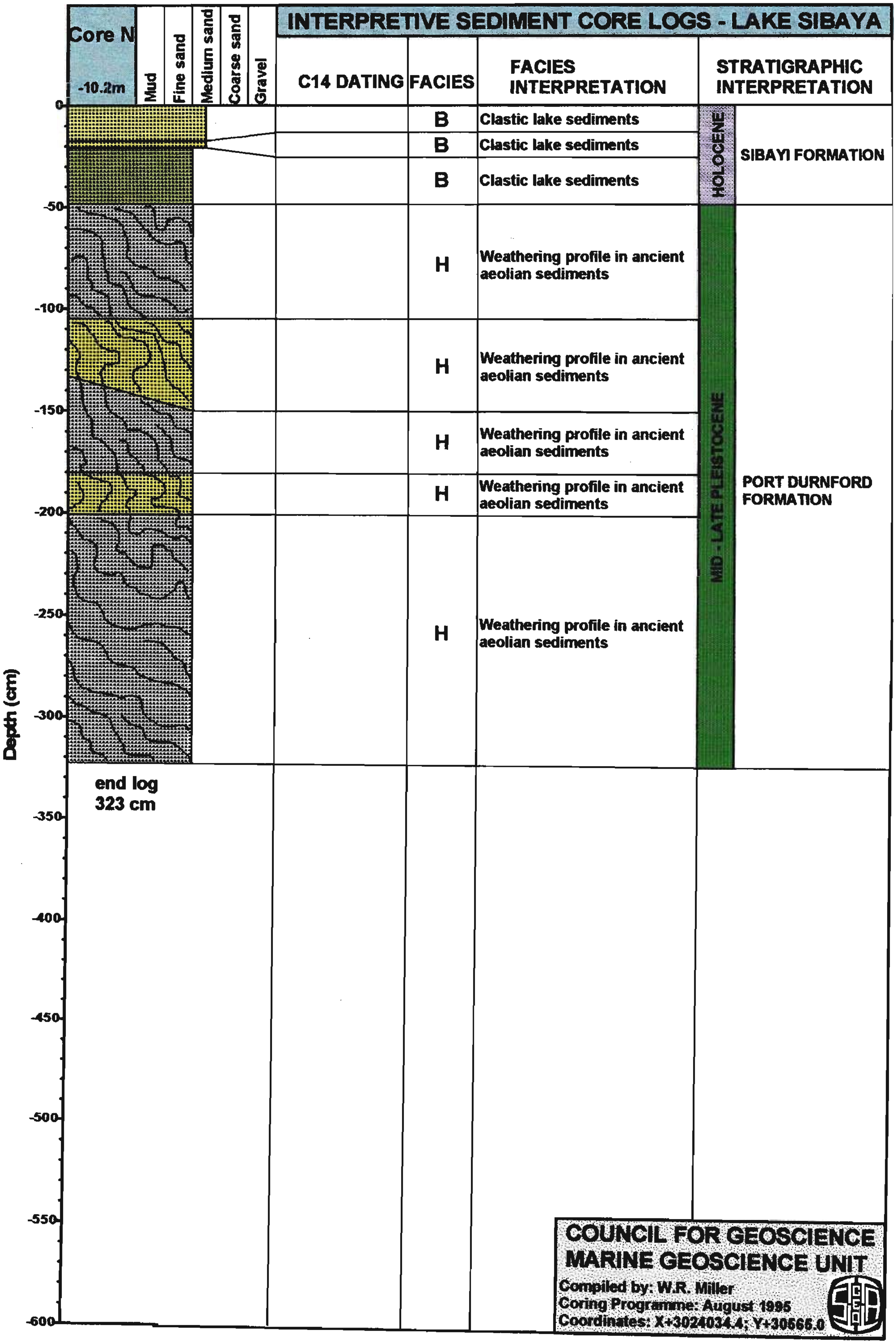


Fig 8.15 Interpretation of Core N (see Appendix 3 for descriptive core logs).

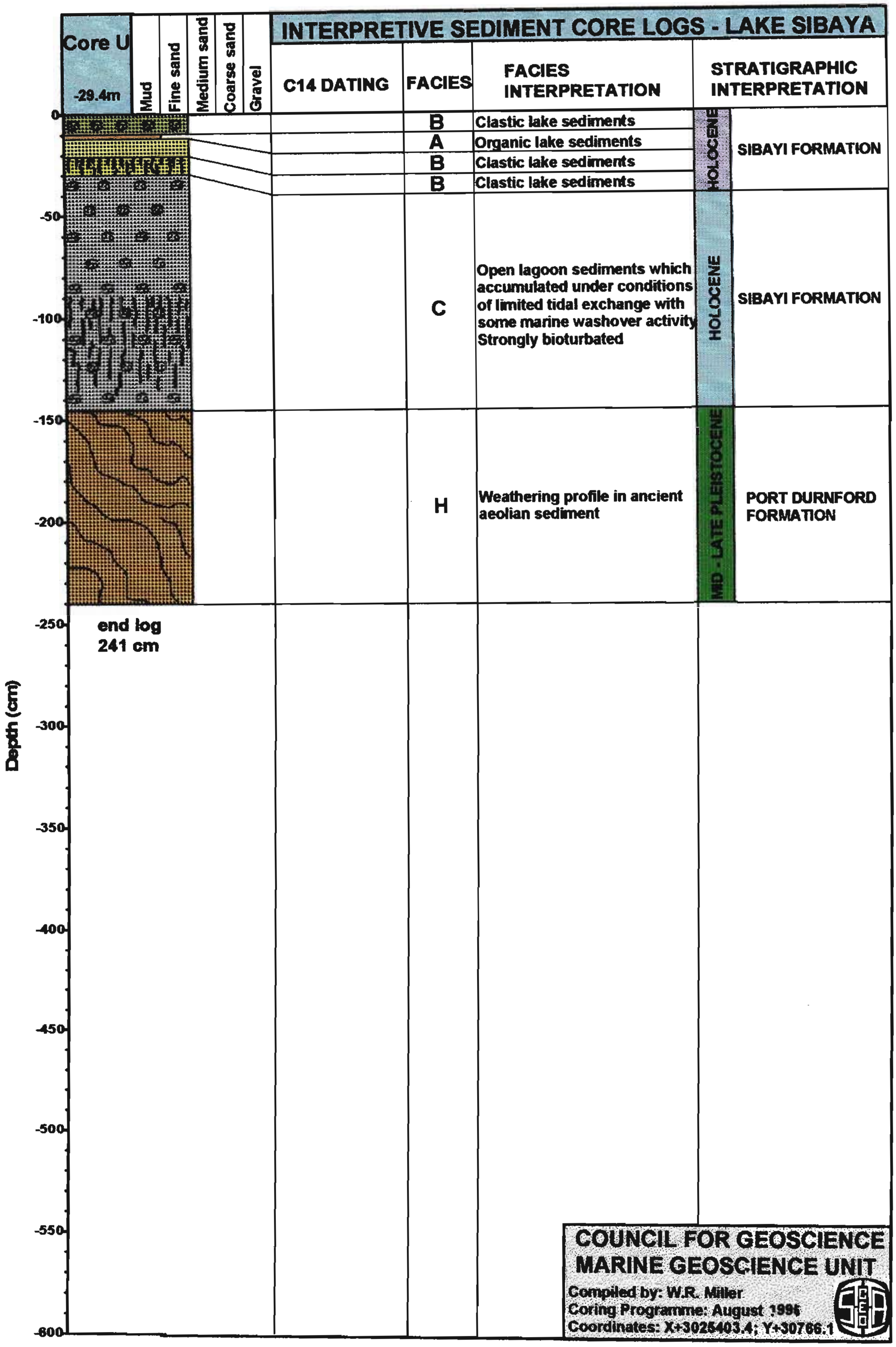


Fig 8.16 Interpretation of Core U (see Appendix 3 for descriptive core logs).

**8.4 DISCUSSION**

The Holocene sediments of the Sibayi Formation comprise six different facies in the core samples. Facies A represents lacustrine muddy sediments with a marine/lagoonal influence at the base of the succession. Facies B represents clastic lacustrine sediments while Facies C consists of clastic lagoonal sediments with a marine washover and barrier influence (Facies D). Facies E consists of freshwater diatom deposits which rest unconformably on Holocene aeolian sediments of Facies F. Radiocarbon dating has confined the lagoonal sediments to an age of 8810 ± 100 BP and younger (Fig. 8.6) and has placed the lagoon/lake transition at 5030 BP ± 70 BP (Fig. 8.4). The freshwater diatomites of Facies E have been confined to an age of younger than 7060 ± 80 BP (Fig. 8.10) while a date of 5610 ± 80 BP was obtained from organic material in Facies F (Fig. 8.13). This date is anomalous when considered in the context of chronostratigraphic principles, but could be explained by the fact that these dates come from different cores, collected in different water depths in different areas of the lake. The radiocarbon date of 7060 ± 80 BP was calculated on a peat sample collected from core ZB (Fig 8.10) at an elevation of ± 1 m below present sea-level while the radiocarbon date of 5610 ± 80 BP was calculated for an organic clay sample obtained from core J (Fig 8.13) at an elevation of ± 7 m above present sea-level. A difference in elevation of ± 8 m exists between the samples, which is critical when considering the position of the water table during the early to mid Holocene evolution of the coastal plain in the Lake Sibaya area. The lower lying topography would have been subject to higher water table conditions and such areas would have been more likely to support free-standing water bodies necessary for the accumulation of laminated diatomite sediments. Higher lying areas may not have supported free standing water and the aeolian sediments may have remained "dry" and hence mobile for a longer period of time, than the same sediment type at lower elevations. This implies that the Holocene aeolian sands are diachronous and continued to accumulate throughout the development of the modern Lake Sibaya. The more elevated exposures of this sediment type were probably subject to wetland conditions only once the water table had started to rise on a regional scale. It is therefore not surprising that there is a similarity in the radiocarbon dates between that of the reestablishment of the coastal dune barrier (5030 ± 70 BP; Fig. 8.4) which was the catalyst to start the filling of the modern Lake Sibaya, and the date of 5610 ± 80 BP from organic material within the Holocene dune sands. The organic material from core J (Fig 8.13) probably represents wetland deposits on more distal dune topography that was only drowned once the flooding of Lake Sibaya had begun in earnest.

The unconformity defining the LGM event (Sequence boundary SB4 - Chapter 7) was sampled and found to consist of a light grey to white, nodular calcrete. The calcrete probably represents a mixture of reworked sediments of Cenozoic to late Pleistocene age (see Fig.8.6) that became cemented as a result of exposure to subaerial weathering and surface runoff during the period following the LGM.

The sediments of the Kosi Bay Formation (Facies G) underlie the coastal wetland deposits of the KwaMbonambi Formation. These sediments have aeolian characteristics and a high interstitial clay content. The Kosi Bay Formation represents low undulating inland dune topography that was drowned during the late Pleistocene development of the proto-Lake Sibaya. The sediments of the KwaMbonambi Formation comprising Facies E' accumulated under coastal wetland conditions on the aeolian sediments of the Kosi Bay Formation for the time period ± 43500 BP to ± 25500 BP (Fig. 8.7). This was a wet climatic period that saw the accumulation of freshwater diatomites and peat deposits in a series of shallow coastal lakes and swamps (Maud *et al*, 1997 & Miller *et al*, 1997). The coastal dune barrier was intact at this time.

Like the sediments of the Kosi Bay Formation the sediments of the Port Durnford Formation (Facies G) have low carbonate content values and high values of interstitial clay material. The Port Durnford Formation sediments, however, have a hard, semi-lithified nature and a highly oxidised appearance. All of these criterion testify to an older age of deposition and a greater length of subaerial exposure of these sediments. No dateable material was found in the Port Durnford Formation samples from the cores.

The Cretaceous aged sediments of the St. Lucia Formation were not sampled during the coring programme due to a greater depth of burial in comparison to the other sediment types. The silstones of the St. Lucia Formation are evident as isolated exposures in the western areas of the coastal plain (Fig. 2.5).

The coring programme provided access to sediment samples from sedimentary sequences identified during the seismic profiling survey. The coring programme results show that there is a good correlation between the seismic stratigraphy and the lithostratigraphy of the Maputaland Group proposed by Botha (1997). The radiocarbon dating of core samples has enabled a refining of the depositional time scale for the accumulation of the lithostratigraphic units of the Maputaland Group.

The radiocarbon dating (Appendix 7) and sedimentological investigations of core samples (Appendix 3) enable a clearer understanding of the palaeo-environment under which the sediments of the Maputaland Group accumulated. This together with the depositional geometry inferred from the seismic profiling investigations, provides a comprehensive picture of the geological evolution of the Maputaland coastal plain in the Lake Sibaya area.

# CHAPTER 9 : GEOLOGICAL EVOLUTION OF LAKE SIBAYA

The data presented in previous chapters has been used in conjunction with published literature, to infer palaeo-environmental conditions during the evolution of Lake Sibaya. Stratigraphic units discussed in the text will be referred to under the titles, proposed by G. Botha as outlined in Table 2.1 and Fig 2.6. Relevant sea-level oscillations (transgressions and regressions) discussed in the text are based on the second order eustatic cycles proposed by Siesser and Dingle (1981). The major emphasis will be on the Cenozoic evolution of the lake and surrounding area.

## 9.1 CENOZOIC

Sediments of late Cretaceous age (St. Lucia Fm.) and early Palaeocene age were deposited under transgressive conditions (Worthington, 1978). These sediments along with early Cretaceous sediments underwent planation to a wide gently easterly dipping erosional surface during sea-level oscillations in early to middle Tertiary times (Siesser & Dingle, 1981; Kruger & Meyer, 1988). The seismic records suggest that the planation surface underwent small-scale faulting during mid Tertiary times. This faulting is most likely to be associated with uplift during the early Miocene (Partridge & Maud, 1987) which resulted in small horst structures with apparent throws of less than 10 m. These structures strike NW - SE and are superimposed on another set of faults which strike N - S and E - W (Fig.9.1).

The middle Miocene transgression reached a maximum of 90 m above sea-level, on the Maputaland coastline (Siesser & Dingle, 1981; Dingle *et al.*, 1983). The transgression was followed by a regressive phase which spanned the time period from late Miocene to early Pliocene (Siesser & Dingle, 1981). This regression saw the deposition of littoral sediments of the Uloa Formation (Lui, 1995) and the aeolian sediments of the Umkwelane Formation (Maud & Orr, 1975).

Renewed transgressive conditions in the early Pliocene to ± 50 m above sea-level (Wright, 1995) were followed by a late Pliocene/early Pleistocene regression to ± 80 m below present sea-level (Siesser & Dingle, 1981). A series of dune cordons accumulated during stillstands associated with this regression (Wright, 1995). Tertiary sediments of the Uloa and Umkwelane Formations underwent extensive erosion during the late Pliocene/early Pleistocene regression. The erosion

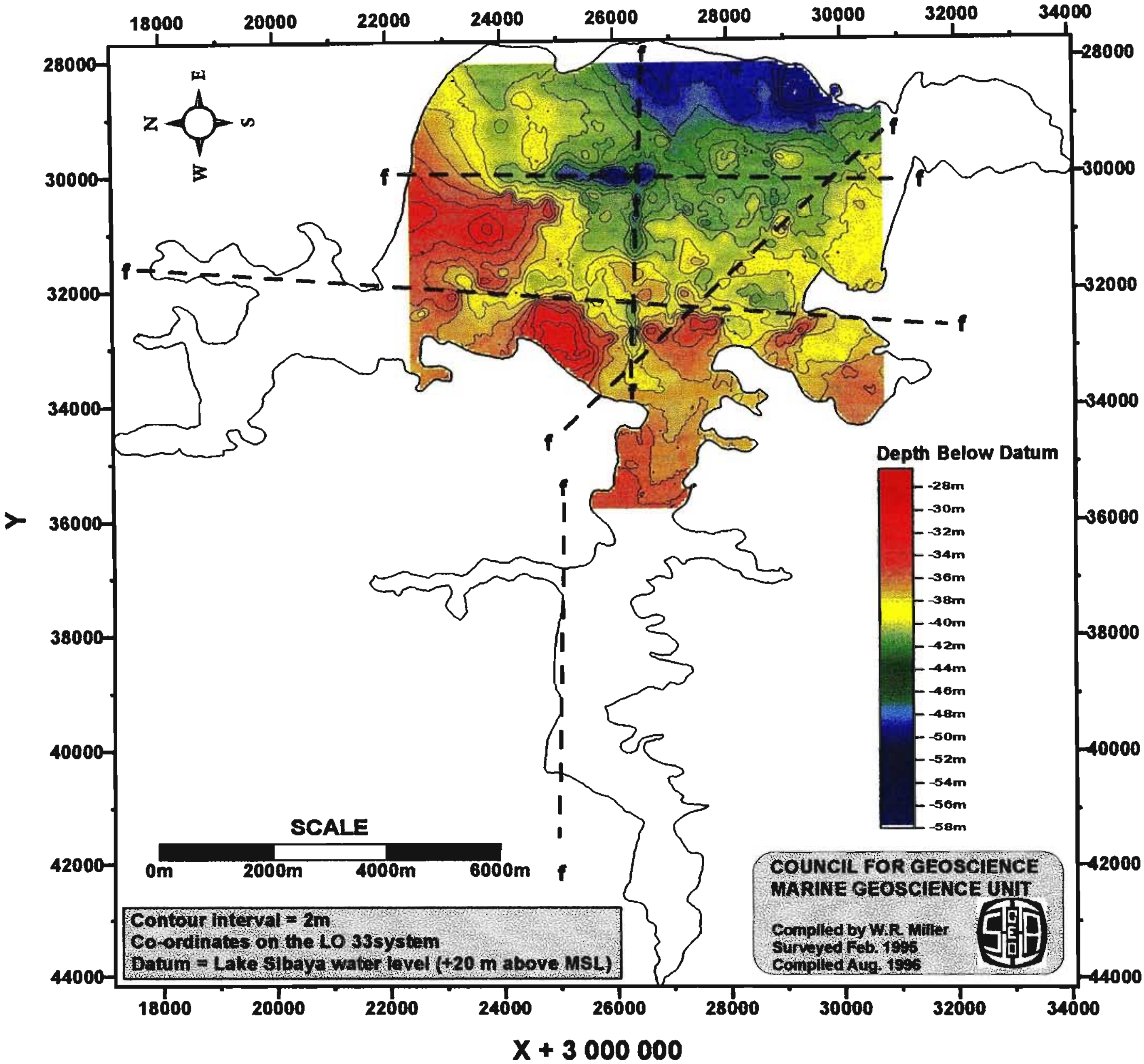


Fig. 9.1 Contour map of theelevation of the upper Cretaceous surface showing the infered faulting pattern.

manifested itself as a widespread unconformity which truncates Tertiary aged sediments to the west of the 30 000 Y co-ordinate (LO 33 system) and as channels incised into sediments of Tertiary and Cretaceous age in the Lake Sibaya area.

## 9.2 PLEISTOCENE

The time period during the early - mid Pleistocene saw the subaerial weathering of late Pliocene\early Pleistocene dune ridges to form the characteristic "Berea type" red sand (McCarthy, 1967; Wright, 1995). While there is no direct evidence to suggest that the regression which culminated in the Penultimate Glacial Maximum ± 150 000 BP affected the Lake Sibaya area, the possibility does exist that this period of erosion incised the coastal topography to create a topographic low on the lake site. The fact that younger Port Durnford sediments rest unconformably on Cretaceous aged sediments at elevations of up to -30 m below MSL in the Lake Sibaya area is evidence which could be cited in support of this theory. The transgression which followed the Penultimate Glacial Maximum saw the deposition of the Port Durnford Formation under conditions of oscillating sea-levels. This was a period of climatic extremes during which minor sea-level fluctuations were superimposed on an overall transgressive movement (Worthington, 1978). The transgressive event culminated in the last interglacial highstand and a planation surface elevated 4 - 5 m above sea-level 120 000 BP (Ramsay, 1996). The oscillating sea-levels allowed for periods of incision of fluvial channels (regression), accumulation of organic rich, lagoonal sediments behind a coastal barrier (stable sea-levels) and for periods of marine incursion (transgression).

Available evidence from the seismic records suggests that an initial transgressive event to ± 5 m above mean sea-level resulted in the deposition of a seaward thickening wedge of littoral sediments on top of the Uloa and Umkwelane Formations. A gradual regressive event which followed, led to the development of a widespread planation surface which dipped gently eastwards. Later, more rapidly dropping sea-levels led to incision of fluvial channels that were proximal to the coastline at that time. This erosive event incised the topography down to elevations of -10 m below sea-level to form a broad shallow depression in the vicinity of the Main Basin and Southern Basin of Lake Sibaya. Stabilisation of sea-levels resulted in the re-establishment of the coastal barrier and the development of lagoonal conditions behind it. The lagoon was subsequently infilled by marine washover sediments from the east and by aeolian processes predominantly from the south and west. During the period when the lagoon was filling, minor regressive events resulted in small-scale erosion of prograded material and the development of channel deposits containing reworked sediments of Port Durnford and Tertiary age. There is no evidence from the seismic records to suggest a second marine incursion (on top of the lagoonal sediments) that is evident in the Richards Bay exposures to the south (Hobday and Orme, 1974).

The regression which followed the last interglacial highstand spanned the period from ±120 000 BP to ±18 000 BP during which time sea-level dropped to -130 m about 18 000 BP (Ramsay, 1996). The regressive surface outcrops of the Maputaland continental shelf and are characterised by intermittent beachrock and aeolianite outcrops which range in age from 117 000 BP to 22 000 BP (Ramsay, 1996). These outcrops define a sequence of palaeocoastlines which range in elevations from -20 m to -90 m below present sea-level (Ramsay, 1996). The time period from ± 100 000 BP to ± 45 000BP saw the accumulation of the aeolian sediments of the Kosi Bay Formation on top of the Port Durnford sediments in an unconformable relationship. Subaerial weathering of stabilised (vegetated) exposures of these sediments led to the development of the ochre coloured weathering profile which is intermittently exposed around the margins of Lake Sibaya. Sediment supply to the coastal region was still quite high at this stage and was sufficient to re-establish the coastal dune barrier and lead to the formation of a series of large, coastal freshwater lakes ± 43 500 BP including a proto Lake Sibaya.

Radiocarbon dating and analysis of diatom assemblages indicate that the time period from ± 43 500 BP to ± 25 500 BP was dominated by wet climatic conditions and saw the formation of coastal freshwater lakes and the regional development of coastal wetlands behind a mid-late Pleistocene coastal dune barrier(Maud *et al* 1997; Miller *et al*, 1997; Mazus & Grundling, 1997). Freshwater diatomite deposits accumulated on the drowned dune topography of the Kosi Bay Formation that was submerged by the developing lakes. The freshwater diatomites together with coastal wetland deposits and redistributed aeolian sands which blanket the sediments of Kosi Bay Formation, constitute the KwaMbonambi Formation sediments which accumulated under coastal wetland conditions for the period ±43 500 BP to ± 25 500 BP.

As sea-levels dropped towards the LGM level of -130 m below MSL (Ramsay, 1996), an increase in hydraulic head between water levels in the coastal lakes and the dropping sea-levels caused a breaching of the coastal dune barrier and draining of the proto-Lake Sibaya. The breaching of the coastal dune barrier occurred between ± 24 000 BP and ± 18 000BP and the accompanying erosion scoured a NW - SE oriented channel which breached the coastal dune cordon between the X co-ordinates 3 027 000 and 3 030 000 (LO 33 system). This erosive event incised the coastal plain topography down to depths of greater than -40 m below MSL and created a channel lag deposit on the Lake Sibaya site. The incision was concentrated in areas proximal to the breached coastal dune barrier where all post Cretaceous sediments were eroded. In the more distal areas of the proto-Lake Sibaya, only the sediments of the KwaMbonambi and Kosi Bay Formations were eroded, exposing the underlying sediments of the Port Durnford Formation.

## 9.3 HOLOCENE

Following the draining of the proto-Lake Sibaya, large volumes of paralic and littoral sediments were exposed to aeolian processes. These sediments were reworked into the LGM erosion scar, where substantial thicknesses (15 - 20 m) of low undulating dune sand accumulated. As sea-level recovered to near its present elevation ± 8000 BP the transgressing sea began reworking the aeolian deposits and infilling the LGM erosion channel with marine washover deposits. The coastal barrier began to be reestablished at this time, forming a marine lagoon in the west. Lagoonal sediments accumulated on the now drowned Holocene dune topography for the time period ± 8810 BP to ± 5030 BP. The more distal (elevated) exposures of Holocene dune sand remained mobile until ±7060 BP, transporting sediment inland. The grain-size distributions of these sediments testify that the region was sediment starved at the time and that the aeolian sediments became deflated. Coastal wetland conditions developed inland of the lagoon ± 7060 BP and the Holocene dune topography was flooded to form small interdune lakes. These small water bodies had high levels of productivity and were the accumulation sites of thin lenses of calcareous freshwater diatomite. At ± 5610 BP to ±5030 BP the coastal barrier was established allowing beach/aeolian processes to begin infilling the breach in the coastal dunes and for the lagoon to begin evolving towards freshwater conditions. Open water conditions developed as Lake Sibaya slowly filled, diatom productivity levels dropped and gyttja became the dominant sediment type. The clay mineralogy and the now sparse diatom assemblages of the gyttja deposits indicate that the transition from saline to freshwater conditions was slow. This theory is further reinforced by the presence of a relict estuarine fauna which is still extant in Lake Sibaya (Allanson *et al.*, 1966).

During the last 5000 years a substantial thickness of aeolian sediment has accumulated to seal the breached coastal dune barrier. The dune topography rises up to elevations of 166 m in the area that was only 5000 years ago a shallow sand bar that separated a saline lagoon from the open sea. The only sediments which have accumulated in Lake Sibaya in the last 5000 years is a thin veneer of lacustrine muds (gyttja) in deeper areas of the lake and a small amount of aeolian sediment which is stripped from surrounding dune cordons during high lake levels.

## 9.4 RECENT

Modern sedimentary processes in the lake are driven by fluctuating water levels and wind driven currents. These processes are instrumental in redistributing and sorting the clastic sediments in the shallow areas of the lake to form mobile bedforms. These bedforms migrate in downwind directions and coalesce to form larger prograding sedimentary features such as sand spits and cuspate forelands which are the driving force behind the lake segmentation processes. The wind driven current and wave energy are also responsible for transporting finely disseminated organic material to the deeper more sheltered areas of the lake where it accumulates as gyttja.

The predominance of symmetrical grain-size distributions in the southern area of Lake Sibaya indicates that the "White Sands" parabolic dune system was a conduit through which aeolian sand was transported to the lake. The stabilisation of the "White Sands" dunefield in the 1960's interrupted this supply of sediment to the southern areas of Lake Sibaya.

# REFERENCES

Allanson, B.R. (ed.), 1979. Lake Sibaya. Monographiae Biologicae, 36, W. Junk, The Hague: 364 pp.

Allanson, B.R. 1979b. The physico-chemical limnology of Lake Sibaya. In: Allanson, B.R. (ed.), 1979. Lake Sibaya. Monographiae Biologicae, 36, W. Junk, The Hague: 364 pp.

Allanson, B.R., Hill, B.J., Boltt, R.E. & Schultz, V. 1966. An Estuarine Fauna in a Freshwater Lake in South Africa. Nature, 209, 532 -533.

Allsop, H.L., Manton, W.I., Bristow, J.W. & Erlank, A.J. 1984. Rb-Sr geochronology of Karoo felsic volcanics. Spec. Publ. geol. Soc. S. Afr., 13, 273 - 280.

Botha, G.A. 1997. The Maputaland Group: A Provisional Lithostratigraphy For Coastal KwaZulu-Natal. Maputaland focus on the Quaternary evolution of the south-east African coastal plain. International Union for Quaternary Research Workshop Abstracts, Council for Geoscience, Private Bag X112 Pretoria, South Africa: 21 - 26 pp.

Boucher, K. 1975. Global Climate. The English Universities Press Ltd., London, 323 pp.

Browne, I., 1994. Seismic stratigraphy and relict coastal sediments off the east coast of Australia. Marine Geology., 121: 81 - 107.

Browne, L.F. & Fisher, W.L. 1979. Principles of Seismic Stratigraphic Interpretation. Interpretation of Depositional Systems and Lithofacies from Seismic Data. Ass. Am. Pet. Geol. Bookstore. Austin Texas. 125 pp.

Cooper, J.A.G. & Mason, T.R. 1987. Sedimentation in the Mgeni Estuary. SEAL Report No.2. Department of Geology and Applied Geology, University of Natal, Durban. 97 pp.

Cooper, M.R. & McCarthy, M.J. 1988. The stratigraphy of the Uloa Formation. Ext. Abstr. 22nd Earth Sci. Congress, Geol. Soc. S. Afr., 121 - 124.

De Dekker, R.H. 1987. The geological setting of diamondiferous deposits on the inner shelf between the Orange River and Wreck Point, Namaqualand. Bull. Geol. Surv. S. Afr. 86: 99 pp.

Diab, R.D. & Sokolic, F. 1996. Report on wind and wind turbine monitoring at Mabibi - period: September 1994 to February 1996. Department of Mineral & Energy Affairs Report. 8pp.

Dingle, R.V. 1981. The Campanian and Maastrichtian ostracods of south east Africa. Ann. S. Afr. Mus. 85: 1 - 181.

Dingle, R.V., Siesser, W.G. & Newton, A.R. 1983. Mesozoic and Tertiary Geology of Southern Africa. A.A. Balkema, Rotterdam. 375 pp.

Dunlevey, J.N. 1997. The Berea Red Sands. Heavy Minerals 1997. Johannesburg, South African Institute of Mining and Metallurgy, 1997. Pp 237 - 240.

Du Preez, J.W. & Wolmarans, L.G. 1986. Die geologie van die gebied Kosibaai. Toeligting van blad 2632. Geol. Surv. S. Afr. 19 pp.

Dyer, K.R. 1986. Coastal and Estuarine Sediment Dynamics. John Wiley & Sons, 342 pp.

Folk, R.L. & Ward, W. 1957. Brazos River Bar: a study in the significance of grain-size parameters. J. Sed. Petrol., 27: 3 - 26.

Frankel, J.J. 1966 The basal rocks of the Tertiary at Uloa, Zululand, South Africa. Geol. Mag., 103, 214 - 230.

Hart, R.C. 1979. The invertebrate communities: zooplankton, zoobenthos and littoral fauna. In: Allanson, B.R. (ed.). Lake Sibaya, Monographiae Biologicae, 36, Dr. W Junk, The Hague, 108 - 161.

Hill, B.J. 1969. The Bathymetry and Possible Origin of Lakes Sibaya, Nhlange and Sifungwe in Zululand. Transactions of the Royal Society of South Africa, 38 (3) 205-216.

Hill, B.J. 1979. Bathymetry, morphometry and hydrology of Lake Sibaya. In: Allanson, B.R. (ed.). Lake Sibaya, Monographiae Biologicae, 36, Dr. W Junk, The Hague, 34-41.

Hobday, D.K. 1979. Geological evolution and geomorphology of the Zululand coastal plain. In: Allanson, B.R. (ed.). Lake Sibaya, Monographiae Biologicae, 36, Dr. W Junk, The Hague, 1-20.

Hobday, D.K. & Orme, A.R. 1974. The Port Durnford Formation: A major Pleistocene Barrier-Lagoon complex along the Zululand coast. Trans. geol. Soc. S. Afr., 77: 141 - 149.

Hunter, I.T. 1988. Climate and weather off Natal. In: Schumann, E.H. (ed.). Coastal Ocean Studies off Natal, South Africa. Lecture Notes on Coastal and Estuarine Studies, 26, 81-100.

Kennedy, W.J. & H.C. Klinger, 1975. Cretaceous faunas from Zululand and Natal, South Africa. Introduction, Stratigraphy. Bull. Brit. Mus. Nat. Hist. Geol., 25: 265 - 315

Kennett, P. & Ross, C.A. 1983. Geophysics. Longman Group Limited, York. 32 pp.

Kruger, G.P. & Meyer, R. 1988. A sedimentological model for the northern Zululand coastal plain. ext. abstr. 22nd earth sci. congress, Geol. Soc. S. Afr., 423 - 426.

Lewis, D.W. 1984. Practical Sedimentology. Hutchinson Ross, Stroudsburg, Pennsylvania, 299 pp.

Lui, K.W. 1995. Diagenesis of the Neogene Uloa Formation of Zululand, South Africa. S. Afr. J. Geol., 98: 25 - 34.

McLaren, P. & Bowles, D. 1985. The effects of sediment transport on grain-size distributions. J. Sed. Petrol., 55: 457 - 470.

Maud, R.R. & Orr, W.N. 1975. Aspects of post-Karoo geology in the Richards Bay area. Trans. geol. Soc. S. Afr., 78: 101 - 109.

Maud, R.R. 1993. Port Durnford Formation. In: Quaternary Geology of the Natal and Zululand coast South Africa. IUGS/CLIP/GSO Fieldguide. 32 pp.

Maud, R.R., Partridge, T.C, Alhonen, P., Donner, J & Vogel, J.C. 1997. A Preliminary Assessment of the Environmental Conditions Represented by the Mbazwana Diatomite (Zululand Coast). Maputaland focus on the Quaternary evolution of the south-east African coastal plain. International Union for Quaternary Research Workshop Abstracts, Council for Geoscience, Private Bag X112 Pretoria, South Africa: 73 - 74 pp.

Mazus, H. & Grundling, P. 1997. Pollen and Ash Analyses of the Mfabeni Peat Deposit: Implications for the Origin of the St. Lucia Estuary. Maputaland focus on the Quaternary evolution of the south-east African coastal plain. International Union for Quaternary Research Workshop Abstracts, Council for Geoscience, Private Bag X112 Pretoria, South Africa: 41 - 42 pp.

Miller, W.R. 1994. Morphology and bathymetry of Lake Sibaya. S. Afr. Geol. Surv. Rep. 1994-0162 30 pp.

Miller, W.R. 1996. Sequence stratigraphy of the latest Mesozoic and Cenozoic sediments below Lake Sibaya, Northern KwaZulu-Natal. S. Afr. Geol. Surv. Rep. 1996-0318, 38 pp.

Miller, W.R., Alhonen, P. & Vogel, J.C. 1997. A late Pleistocene diatomite exposure on the western shores of Lake Sibaya. Maputaland focus on the Quaternary evolution of the south-east African coastal plain. Botha, G.A. (ed.). International Union for Quaternary Research Workshop Abstracts, Council for Geoscience, Private Bag X112, Pretoria, South Africa: 64-69 pp.

Miller, W.R. 1998. The Sedimentology of Lake Sibaya Northern KwaZulu Natal. S. Afr. Geol. Surv. Rep. 1998-0139, 26 pp.

Mitchum, R.M., Vail, P.R. & Sangree, J.B. 1977. Seismic stratigraphy and global changes of sea-level, part 6: Stratigraphic interpretation of seismic reflection patterns in depositional sequences, In: Seismic stratigraphy--Applications to hydrocarbon exploration, C.E. Payton. ed. AAPG Mem. 26, Tulsa, Oklahoma, 516 pp.

Mountain, A. 1990. Paradise under Pressure. Southern Book Publishers (Pty) Ltd, Bergvlei, Johannesburg. 149 pp.

Orme, A.R. 1973. Barrier and Lagoonal Systems Along the Zululand Coast, South Africa. Office of Naval Research, Technical Report 1.

Partridge, T.C. & Maud, R.R. 1987. Geomorphic evolution of southern Africa since the Mesozoic. S. Afr. J. Geol. 90: 179 - 208.

Pitman, W.V. & Hutchinson, I.P.G. 1975. A preliminary hydrological study of Lake Sibaya. Hydrological Research Unit Report., 4/75: 35 pp.

Ramsay, P.J. 1990. Use of computer graphics software to produce a three-dimensional morphological and bathymetric model for a Zululand coral reef. S. Afr. J. Sci., 86 (3), 130 -131.

Ramsay, P.J. 1991. Sedimentology, coral reef zonation, and late Pleistocene coastline models of the Sodwana Bay continental shelf, northern Zululand. Unpublished PhD thesis, University of Natal, 202 pp.

Ramsay, P.J. 1996. Quaternary marine geology of the Sodwana Bay continental shelf, northern KwaZulu-Natal. Bull. Geol. Surv. S. Afr., 117: 85pp.

Ramsay, P.J. 1997. Quaternary Marine Geology and Sea-level Changes: Sodwana Bay Shelf. Maputaland focus on the Quaternary evolution of the south-east African coastal plain. Botha, G.A. (ed.). International Union for Quaternary Research Workshop Abstracts, Council for Geoscience, Private Bag X112, Pretoria, South Africa: 53-56 pp.

Sheriff, R.E. 1985. Aspects of seismic resolution. In: Seismic stratigraphy 2. An integrated approach. AAPG Mem. 39: 1 - 10.

Siesser, W.G. & Dingle, R.V. 1981. Tertiary Sea-level Movements Around South Africa. J. Geol. , 89, 523 - 536 pp.

Stapleton, R.P., 1977. Planktonic Foraminifera and the age of the Uloa *Pecten* bed. Papers on Biostratigraphic Research. Bull. Geol. Soc. S. Afr., 60: 11 - 17.

Stratten, T. 1970. Late Karoo igneous rocks of the southern Lebombo mountain range. In: Second Gondwana Symposium: Proceedings and Papers, Pretoria, CSIR, 441 - 444.

Tucker, M.E. 1991. Sedimentary Petrology. Second Edition, Blackwell Scientific Publications, 259 pp.

Vail, P.R., Mitchum, R.M. & Thompson, S. 1977. Seismic stratigraphy and global changes of sea-level, part 3: Relative changes of sea-level from coastal onlap: In: Payton, C.E. (ed.) Seismic Stratigraphy - Applications to hydrocarbon exploration. Am. Ass. Pet. Geol., Studies in Geology, 26: 63 - 81.

Watkeys, M.K., Mason, T.R. & Goodman, P.S. 1993. The role of geology in the development of Maputaland, South Africa. J. Afr. Earth Sci., 16: 205 - 221.

Wentworth, C.K. 1922. A scale grade and class terms for clastic sediments. J. Geol. 30: 377 - 392.

Wolmarans, L.G. & Du Preez, J.W. 1986. The geology of the St. Lucia area. Explanation of Sheet $27^{1/2}32$. Geol. Surv. S. Afr. 42 pp.

Worthington, P.F. 1978. Groundwater conditions in the Zululand coastal plain around Richards Bay. CSIR Geophysics Division Research Report 182. 209 pp.

Wright, C.I. & Mason T.R. 1988. Lake Sibaya: Pleistocene Drainage. Extended Abstract. 22nd. Earth Science Congress of the Geological Society of South Africa, University of Natal, Durban.

Wright, C.I & Mason, T.R. 1990. The sedimentation of Lake Sibaya, North Kwa-Zulu. S. Afr. Geol. Surv. Rep. 1990-0147, 12 pp.

Wright, C.I. 1995. A reconnaissance study of the Zululand coastal plain dune cordon chronology. Geol. Surv. S. Afr. Rep.195-0132. 7 pp.

Wright, C.I. 1997. A broad overview of the Cenozoic evolution of the northern KwaZulu-Natal coastal plain. Maputaland focus on the Quaternary evolution of the south-east African coastal plain. Botha, G.A. (ed.). International Union for Quaternary Research Workshop Abstracts, Council for Geoscience, Private Bag X112, Pretoria, South Africa: 27-33 pp.

# APPENDIX 1

## THE BATHYMETRY OF LAKE SIBAYA AFTER HILL (1969)

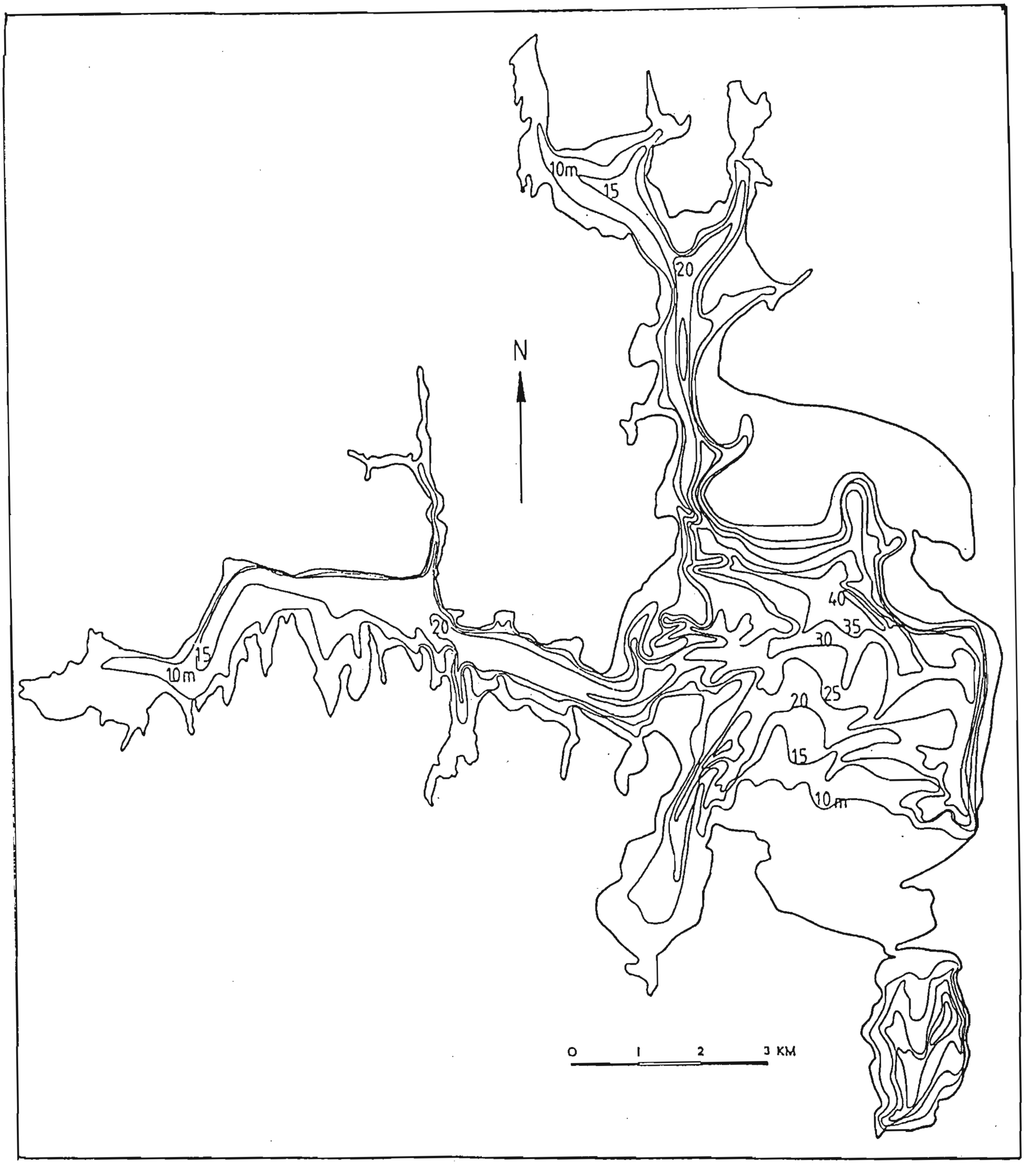

# APPENDIX 2

## LAKE SIBAYA SEDIMENT DISTRIBUTION MAPS (WRIGHT & MASON, 1990)

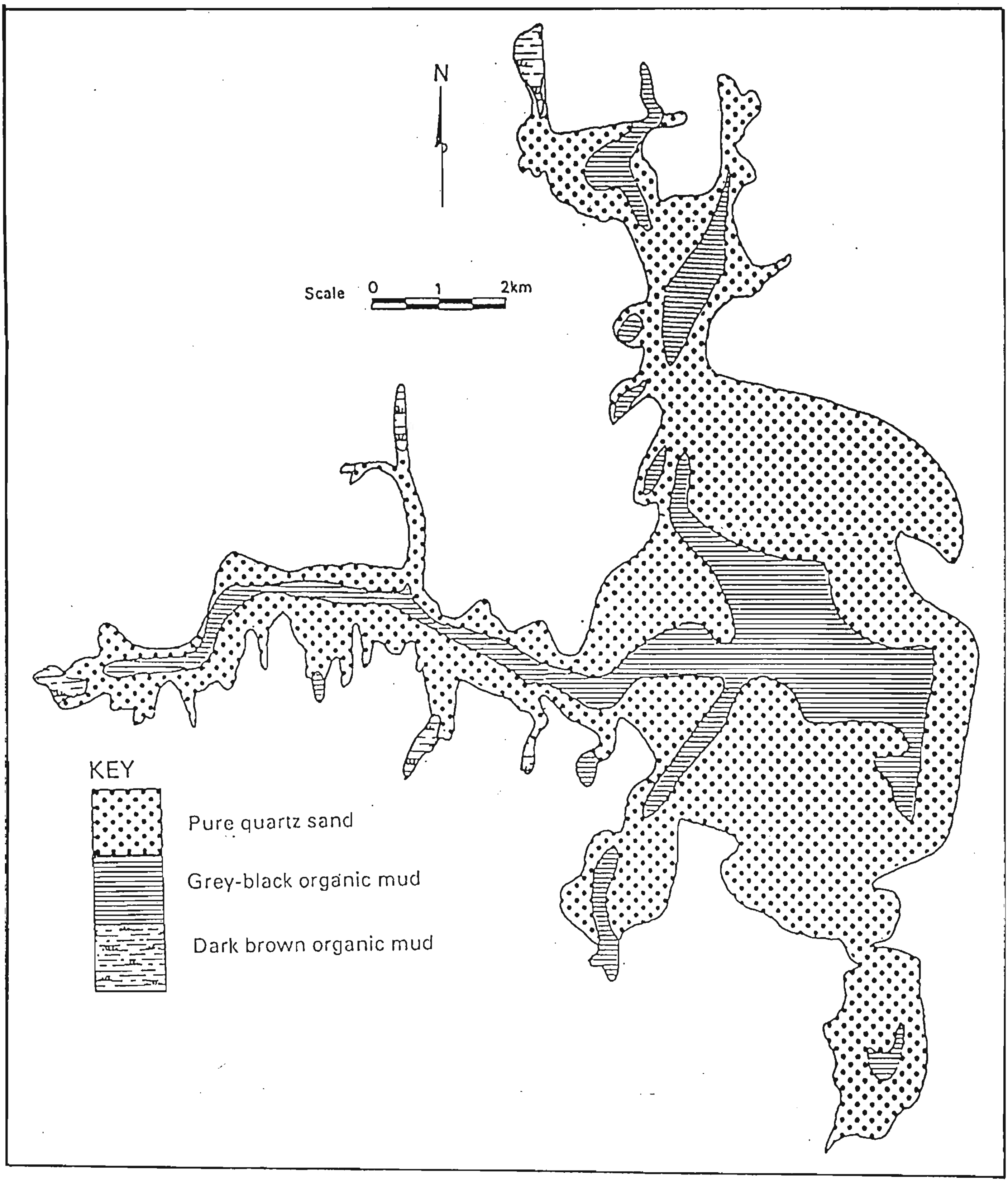

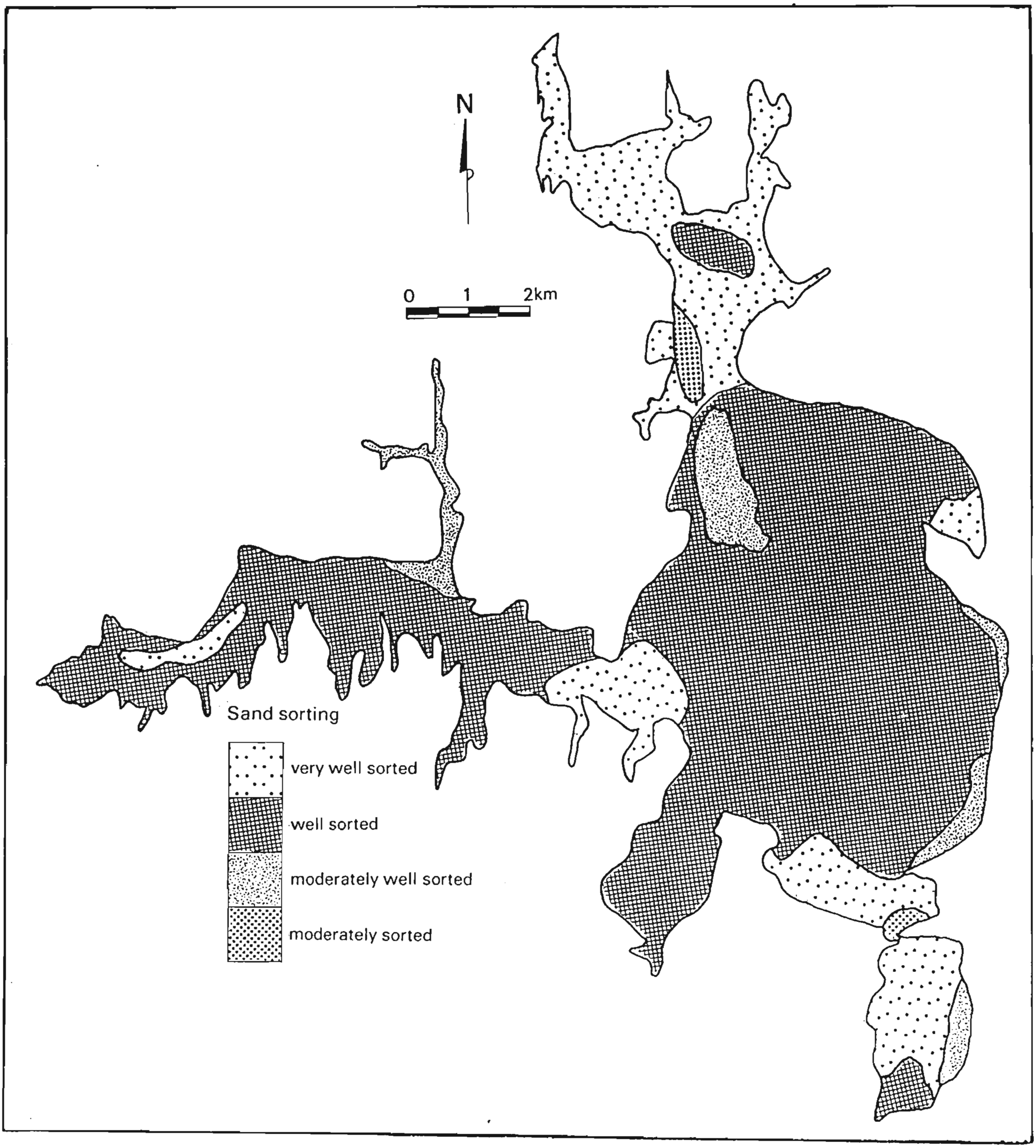
N
0 1 2km
Sand sorting
very well sorted
well sorted
moderately well sorted
moderately sorted

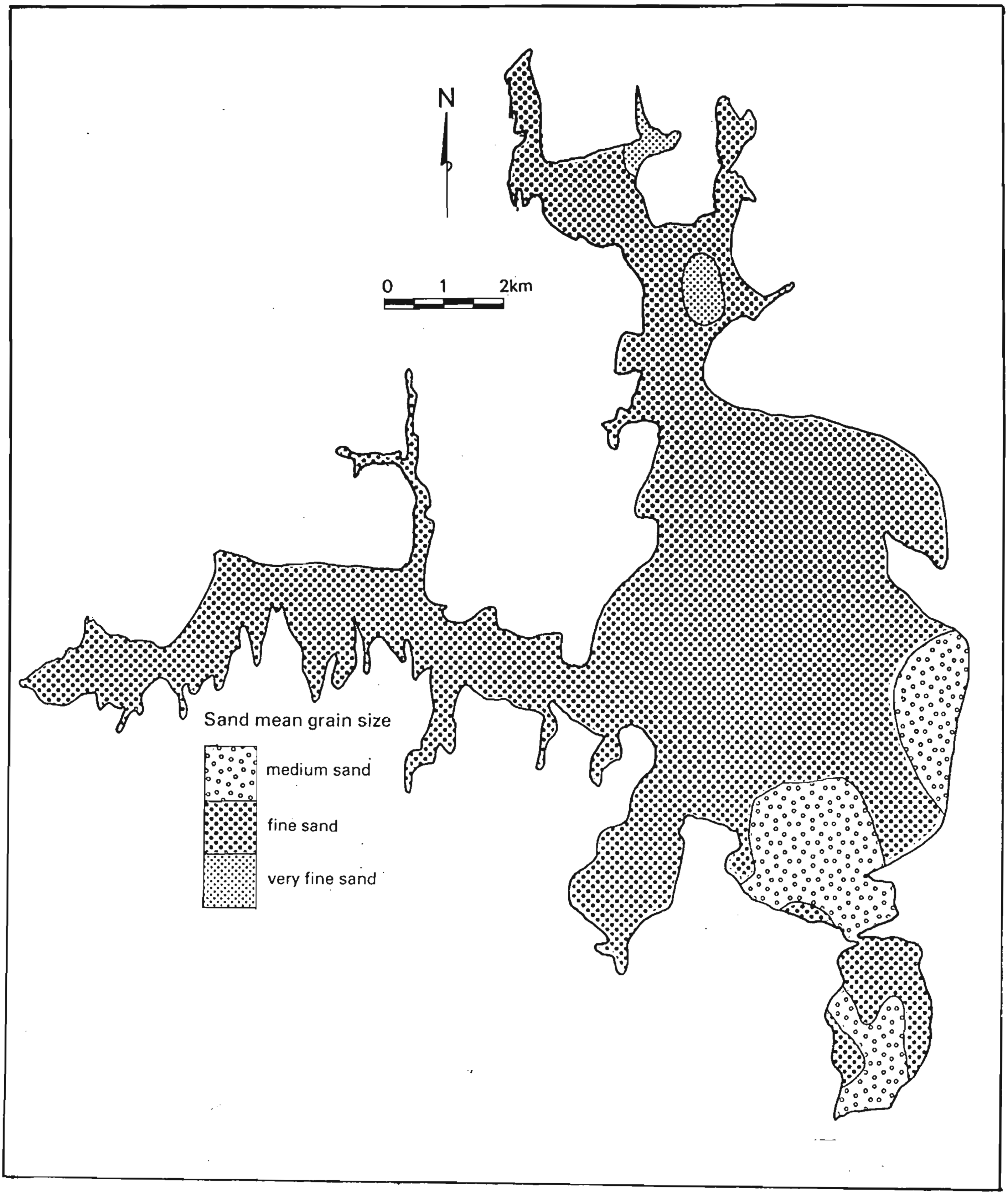

N
0
1
2km
Sand mean grain size
medium sand
fine sand
very fine sand

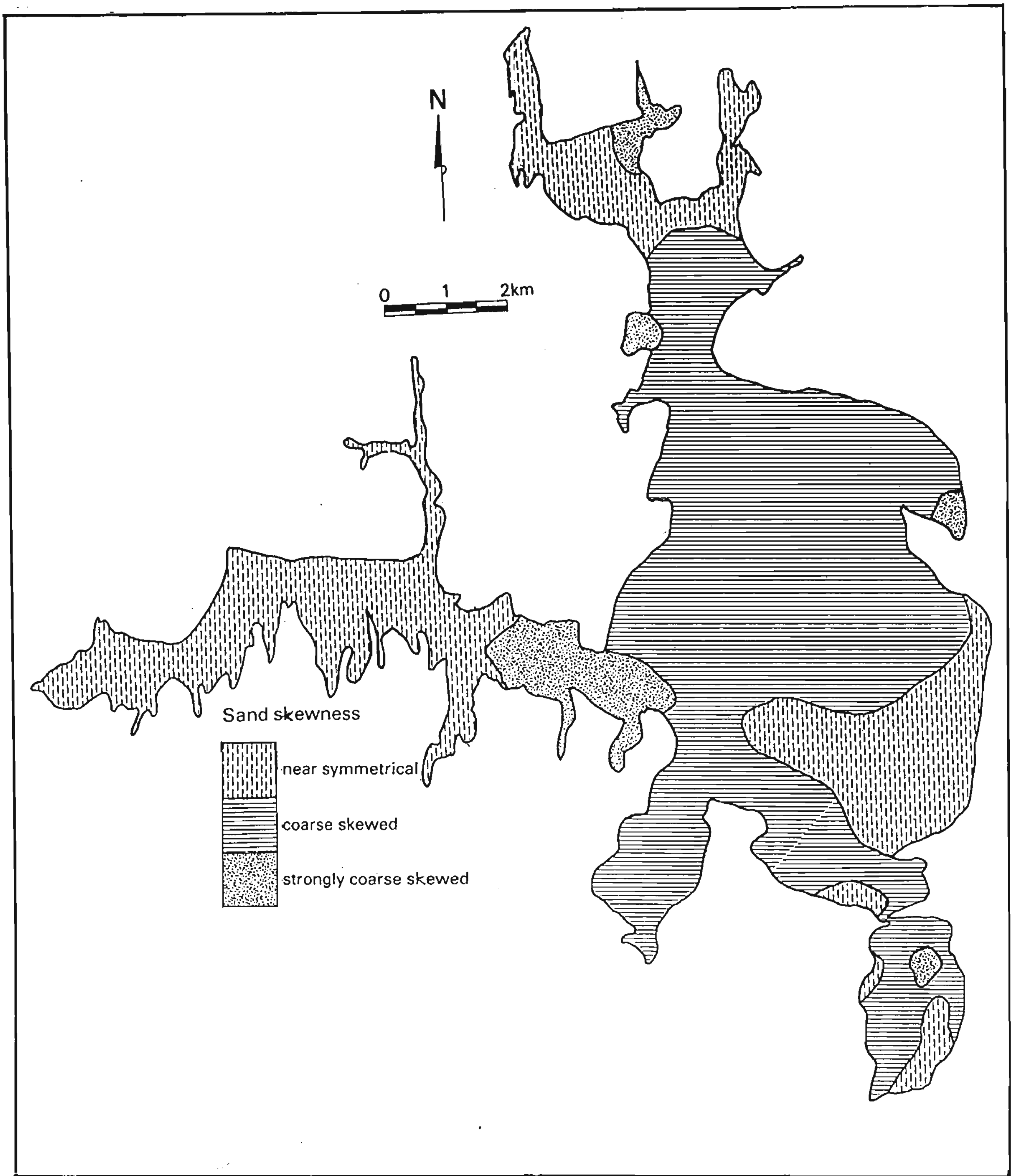
N
0
1
2km
Sand skewness
near symmetrical
coarse skewed
strongly coarse skewed

# APPENDIX 3

## DESCRIPTIVE SEDIMENT CORE LOGS - LAKE SIBAYA

# DESCRIPTIVE SEDIMENT CORE LOGS - LAKE SIBAYA

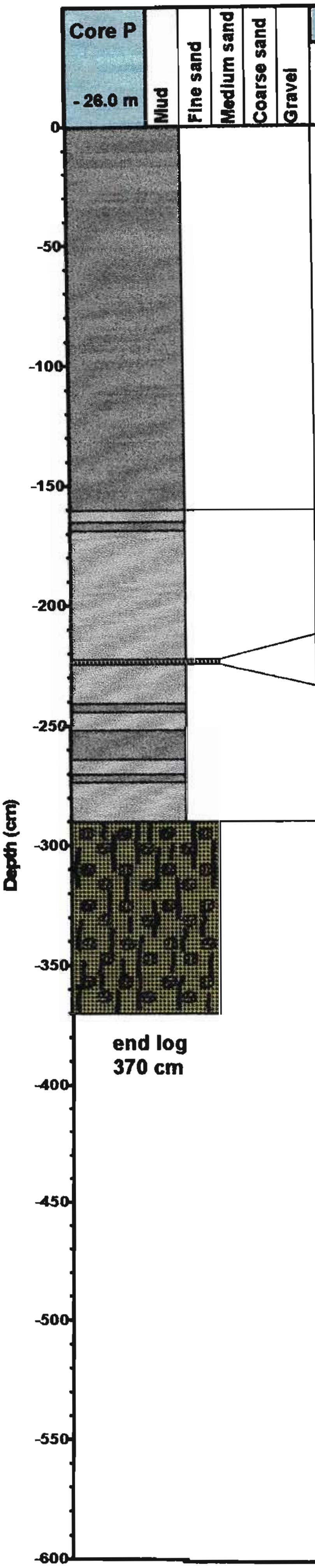


| Colour | Sand (phi) Stats: Mean | Sorting | Skew | % <63µ | % C (org) | % CaCO3 | Fossils | Comments |
|---|---|---|---|---|---|---|---|---|
| Dark Charcoal Grey | | | | 99.0 | 16.1 | 0.0 | Pollen | Dark, soupy, sapropelic mud |
| | | | | 99.0 | 15.1 | 0.0 | | |
| | | | | 99.0 | 20.2 | 0.0 | | |
| | | | | 98.0 | 13.8 | 0.0 | | |
| | | | | 98.0 | 17.1 | 0.0 | | |
| | | | | 98.0 | 16.7 | 0.0 | | |
| | | | | 99.0 | 18.6 | 0.0 | | |
| | | | | 99.0 | 16.1 | 0.0 | | |
| Light grey with dark grey lamminae | 2.72 | 0.65 | +0.14 | 88.0 | 18.1 | 0.0 | Pollen | Firm weakly laminated clay |
| | | | | 99.0 | 19.0 | 0.0 | | |
| | 2.34 | 0.51 | -0.15 | 82.0 | 18.4 | 0.0 | | |
| Dark Yellowish Orange | 2.40 | 0.47 | - 0.20 | 18.0 | 7.4 | 0.0 | | Sandy horizon |
| Light grey with dark grey lamminae | | | | 99.0 | 18.0 | 0.0 | Pollen | Firm strongly laminated clay. Carbonate content increases towards base while organic carbon content decreases |
| | | | | 98.0 | 18.6 | 8.9 | | |
| | | | | 99.0 | 15.9 | 9.2 | | |
| | 2.17 | 0.56 | -0.23 | 90.0 | 14.0 | 27.4 | | |
| | 2.19 | 0.59 | -0.23 | 94.0 | 10.3 | 28.3 | | |
| Light brown to light grey | 2.33 | 0.43 | -0.14 | 1.0 | 0.8 | 1.0 | Sponge spicules, shells, forams & ostracods | Strongly bioturbated subangular to subrounded sand rich in microfossils |
| | 2.33 | 0.39 | -0.14 | 4.0 | 2.0 | 1.0 | | Trace fossils include Ophiomorpha and Planolites |
| | 2.38 | 0.39 | -0.17 | 1.0 | 2.5 | 1.0 | | |

**COUNCIL FOR GEOSCIENCE**
**MARINE GEOSCIENCE UNIT**

Compiled by: W.R. Miller
Coring Programme: August 1995
Coordinates: X+3025611.2; Y+30626.4

# DESCRIPTIVE SEDIMENT CORE LOGS - LAKE SIBAYA

Core B -33.6m

Mud | Fine sand | Medium sand | Coarse sand | Gravel

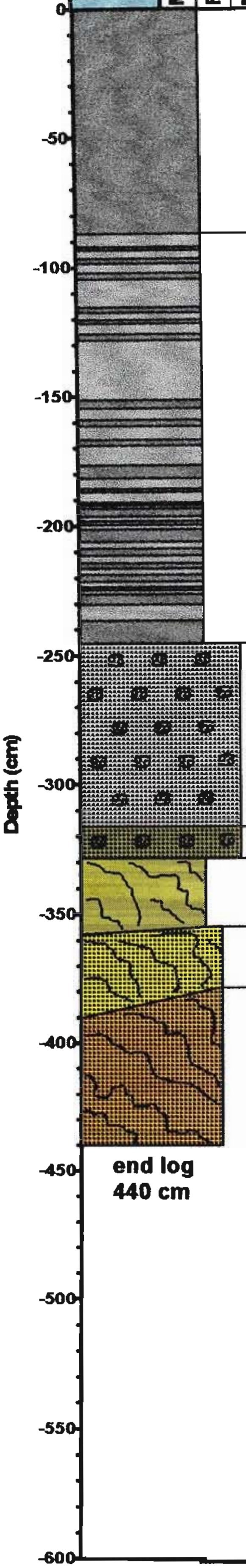


| Colour | Sand (phi) Stats: Mean | Sorting | Skew | % <63µ | % C (org) | % CaCO3 | Fossils | Comments |
|---|---|---|---|---|---|---|---|---|
| Dark grey | 3.1 | 0.71 | -0.25 | 64.6 | 15.6 | 0.0 | Pollen | Dark, soupy, sapropelic mud |
| | 3.0 | 0.77 | +0.04 | 62.7 | 17.0 | 0.0 | | |
| | 3.06 | 0.78 | -0.28 | 90.0 | 20.2 | 0.0 | | |
| | 3.04 | 0.85 | -0.15 | 88.5 | 20.9 | 0.0 | | |
| Light grey with fewer darker grey horizons | 2.72 | 0.65 | +0.08 | 43.1 | 13.4 | 0.0 | Pollen | Firmer, laminated clay |
| | 2.47 | 0.49 | -0.14 | 82.2 | 15.8 | 3.3 | | |
| | 2.57 | 0.51 | -0.07 | 95.1 | 16.8 | 20.5 | | |
| | | | | | 17.7 | 23.8 | | |
| | 1.98 | 1.18 | -0.21 | 90.5 | 15.7 | 20.1 | | |
| | 2.72 | 0.81 | +0.16 | 91.1 | 15.8 | 14.0 | | |
| | 2.74 | 0.88 | +0.14 | 89.8 | 14.0 | 0.0 | | |
| | 2.81 | 0.82 | -0.01 | 87.8 | 18.4 | 0.0 | | |
| | 2.73 | 0.69 | -0.13 | 80.7 | 17.8 | 0.0 | | |
| Light grey | 2.56 | 0.60 | -0.22 | 19.4 | 2.1 | 0.0 | Sponge spicules, shells, forams & ostracods | Angular to subrounded fossiliferous sand |
| | 2.62 | 0.57 | -0.23 | 13.4 | 2.6 | 1.6 | | |
| | 2.54 | 0.68 | -0.20 | 12.5 | 1.5 | 3.4 | | |
| | 2.40 | 0.69 | -0.23 | 10.2 | 2.7 | 12.7 | | |
| Light brown | 2.60 | 0.61 | -0.29 | 11.9 | 2.1 | 5.9 | " | " |
| Dark yellowish orange | 2.75 | 0.58 | -0.48 | 36.5 | 3.9 | 0.0 | Sponge spicules | Soft sediment deformation |
| | 2.91 | 0.44 | -0.43 | 35.8 | 4.3 | 0.0 | | |
| Dark yellow | 3.08 | 0.34 | -0.27 | 32.3 | 5.0 | 0.0 | | Soft sediment deformation |
| | 3.16 | 0.24 | -0.04 | 9.3 | 3.0 | 0.0 | | |
| Dark reddish orange | 3.16 | 0.23 | +0.02 | 24.7 | 4.1 | 0.0 | | Soft sediment deformation |
| | 3.19 | 0.23 | -0.03 | 24.0 | 4.1 | 0.0 | | |
| | 3.08 | 0.28 | -0.17 | 29.5 | 4.0 | 0.0 | | |


**COUNCIL FOR GEOSCIENCE**
**MARINE GEOSCIENCE UNIT**
Compiled by: W.R. Miller
Coring Programme: August 1995
Coordinates: X+3025880.9; Y+30430.1

# DESCRIPTIVE SEDIMENT CORE LOGS - LAKE SIBAYA

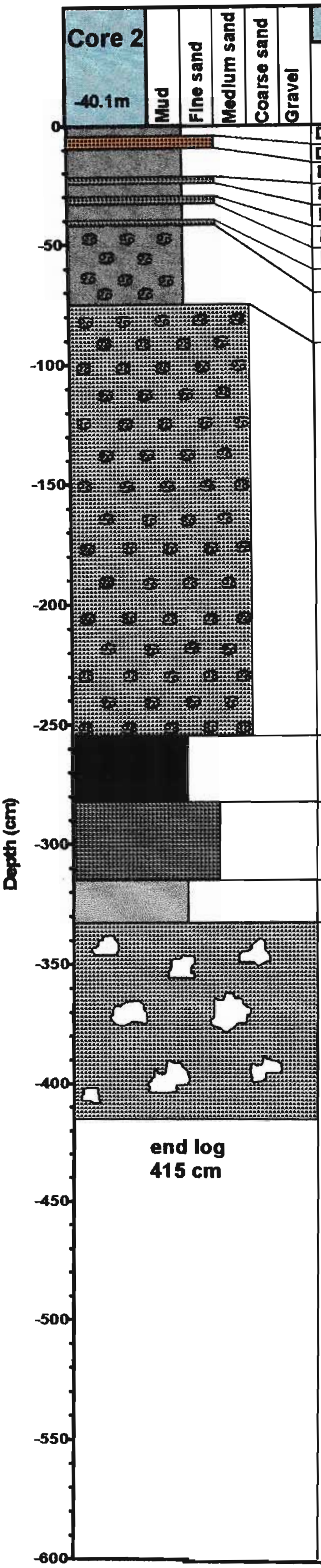


| Colour | Sand (phi) Stats Mean | Sorting | Skew | % <63µ | % C (org) | % CaCO3 | Fossils | Comments |
|---|---|---|---|---|---|---|---|---|
| Dark grey | 2.37 | 0.52 | -0.23 | 58.0 | 7.9 | 0.0 | | Soupy organic mud |
| Dark brown | 2.84 | 0.57 | 0.00 | 22.0 | 4.3 | 0.0 | Sponge | Sand horizon |
| Dark grey | 2.54 | 0.51 | -0.05 | 31.0 | 7.5 | 0.0 | spicules | Soupy organic mud |
| Light grey | 2.50 | 0.48 | -0.08 | 8.0 | 2.2 | 0.0 | " | Sand horizon |
| Dark grey | 2.50 | 0.53 | -0.09 | 55.0 | 14.6 | 0.0 | " | Soupy organic mud |
| Light grey | 2.52 | 0.52 | -0.04 | 7.0 | 5.1 | 5.9 | " | Sand horizon |
| Dark grey | 2.73 | 0.63 | -0.04 | 38.0 | 5.1 | 0.0 | " | Soupy organic mud |
| Light grey | 2.74 | 0.63 | -0.01 | 40.0 | 3.8 | 0.0 | " | Sand horizon |
| Dark grey | 2.53 | 0.59 | -0.13 | 39.0 | 3.2 | 3.6 | Shells, forams & ostracods | Firm organic clay |
| | 2.54 | 0.53 | -0.14 | 40.0 | 4.6 | 0.0 | | |
| Light grey | 2.54 | 0.56 | -0.12 | 24.0 | 4.9 | 0.0 | Shells, forams, ostracods & sponge spicules | Subangular to subrounded fossiliferous sand |
| | 2.44 | 0.54 | -0.24 | 22.0 | 3.5 | 0.0 | | |
| | 2.39 | 0.59 | -0.19 | 19.0 | 3.9 | 0.0 | | |
| | 2.28 | 0.64 | -0.27 | 10.0 | 3.0 | 0.0 | | |
| | 2.21 | 0.65 | -0.25 | 9.0 | 1.4 | 0.0 | | |
| | 2.34 | 0.61 | -0.22 | 9.0 | 3.3 | 0.0 | | |
| | 2.31 | 0.60 | -0.17 | 12.0 | 3.7 | 0.0 | | Bioturbation near base |
| | 2.42 | 0.60 | -0.24 | 13.0 | 4.9 | 0.0 | | |
| Black | 2.37 | 0.58 | -0.25 | 32.0 | 7.3 | 0.0 | Sponge spicules | Horizon rich in organic material |
| Dark grey | 2.66 | 0.52 | -0.23 | 18.0 | 6.7 | 0.0 | | Subangular to subrounded sand with organic material |
| | 2.56 | 0.52 | -0.12 | 14.0 | 3.0 | 0.0 | | |
| Light grey | 2.58 | 0.47 | -0.16 | 22.0 | 3.7 | 0.0 | | Hard when dry |
| | 2.63 | 0.49 | -0.11 | 37.0 | 4.0 | 0.0 | | |
| Light grey with white carbonate nodules | 1.65 | 1.04 | -0.30 | 25.0 | 3.9 | 58.2 | | Subangular to rounded sandy matrix with white microcline grains & angular calcareous nodules. After leaching sand turns white |
| | 1.81 | 1.25 | -0.38 | 26.0 | 3.3 | 78.3 | | |
| | 1.51 | 1.38 | -0.21 | 16.0 | 2.4 | 68.8 | | |
| | 1.59 | 1.50 | -0.29 | 13.0 | 0.7 | 61.0 | | |


COUNCIL FOR GEOSCIENCE
MARINE GEOSCIENCE UNIT
Compiled by: W.R. Miller

Coring Programme: August 1995
Coordinates: X+3025774.6; Y+29980.1

# DESCRIPTIVE SEDIMENT CORE LOGS - LAKE SIBAYA

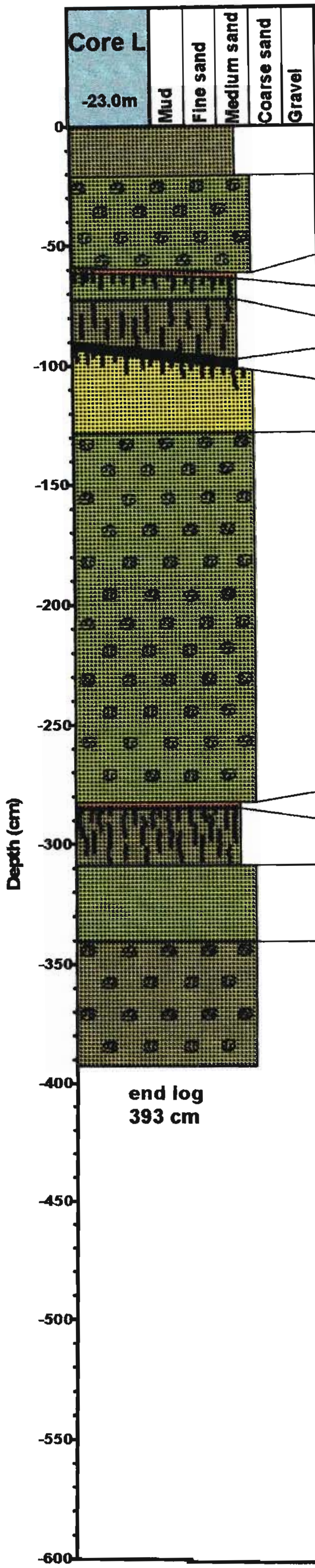


| Colour | Sand (phi) Stats Mean | Sorting | Skew | % <63µ | % C (org) | % CaCO3 | Fossils | Comments |
|---|---|---|---|---|---|---|---|---|
| Light brown | 2.27 | 0.41 | -0.16 | 0.0 | 2.7 | 0.0 | FW shell fragments | Mottled angular to rounded sand |
| Light olive | 2.07 | 0.38 | -0.13 | 0.0 | 1.4 | 0.76 | Shell frags & forams | Angular to rounded sand with heavy minerals |
| Dark brown | | | | | | | Organics | Strong bioturbation |
| Light olive | 2.53 | 0.39 | -0.10 | 1.0 | 2.7 | 0.0 | | Moderate bioturbation |
| Light brown | 2.51 | 0.39 | -0.05 | 1.0 | 1.9 | 0.0 | | Extreme bioturbation |
| Black | 2.53 | 0.39 | -0.08 | 1.0 | 3.4 | 0.0 | Organics | Extreme bioturbation |
| Dark yellow | 2.00 | 0.39 | -0.11 | 0.0 | 1.8 | 0.0 | | Subangular to rounded sand with "heavies" |
| Light olive | 2.06 | 0.37 | -0.12 | 0.0 | 0.9 | 0.0 | Shell fragments | Subangular to rounded sand with heavy minerals. No bioturbation |
| | 2.03 | 0.36 | -0.10 | 0.0 | 1.9 | 0.8 | | |
| | 1.91 | 0.41 | -0.14 | 0.0 | 1.7 | 0.0 | | |
| | 1.97 | 0.43 | -0.14 | 0.0 | 2.9 | 0.8 | | |
| | 2.08 | 0.42 | -0.15 | 0.0 | 0.9 | 0.0 | Fewer shell fragments | |
| Dark brown | | | | | | | Organics | |
| Light brown | 2.21 | 0.41 | -0.08 | 1.0 | 2.9 | 0.0 | Sponge spicules | Moderate to strong bioturbation |
| Light olive | 2.05 | 0.39 | -0.07 | 0.0 | 0.9 | 0.0 | | Subangular to subrounded sand with heavy minerals |
| Light brown | 2.00 | 0.41 | -0.14 | 0.0 | 1.2 | 0.0 | Shell fragments & forams | Subangular to subrounded sand with heavy minerals |
| | 2.05 | 0.40 | -0.10 | 0.0 | 3.8 | 0.0 | | |
| | 2.07 | 0.50 | -0.12 | 0.0 | 0.8 | 0.0 | | |

**COUNCIL FOR GEOSCIENCE**
**MARINE GEOSCIENCE UNIT**
Compiled by: W.R. Miller
Coring Programme: August 1995
Coordinates: X+3028191.8; Y+28279.2

# DESCRIPTIVE SEDIMENT CORE LOGS - LAKE SIBAYA

Core SB2

-24.2m

Mud | Fine sand | Medium sand | Coarse sand | Gravel

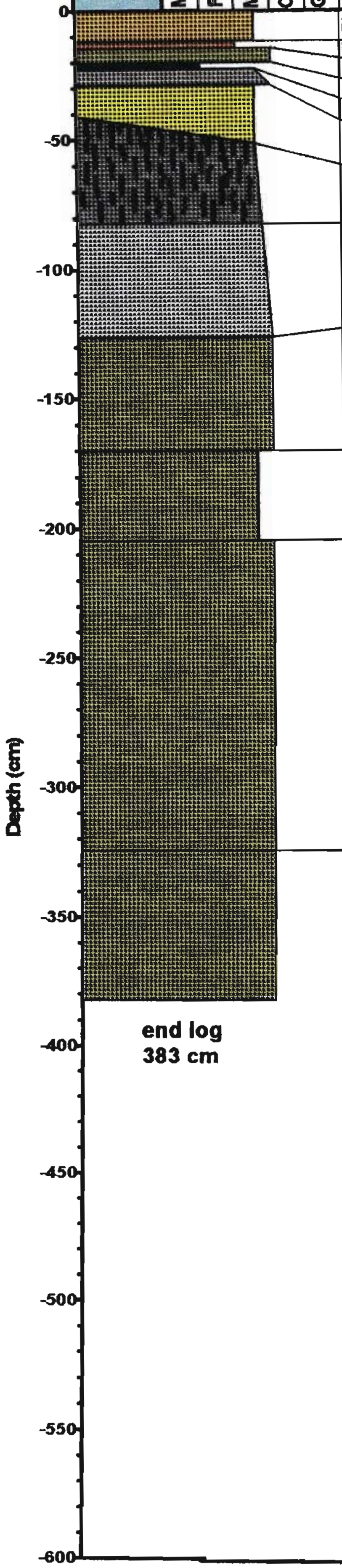


| Colour | Sand (phi) Stats: Mean | Sorting | Skew | % <63µ | % C (org) | % CaCO3 | Fossils | Comments |
|---|---|---|---|---|---|---|---|---|
| Pale brown | 2.09 | 0.58 | -0.10 | 8.4 | 2.1 | 0.0 | Sponge spicules | Bioturbation |
| Dark brown | 2.26 | 0.55 | -0.21 | 10.3 | 4.6 | 0.0 | " | Strong bioturbation |
| Light brown | 2.00 | 0.58 | -0.12 | 4.4 | 2.6 | 0.0 | " | Bioturbation |
| Black | 2.20 | 0.57 | -0.15 | 42.1 | 15.7 | 0.0 | " | |
| Light grey | 2.01 | 0.60 | -0.08 | 4.0 | 2.9 | 0.0 | " | Bioturbation |
| Dark yellow | 2.20 | 0.57 | -0.18 | 9.4 | 3.3 | 0.0 | | Bioturbation |
| | 2.12 | 0.61 | -0.10 | 8.2 | 3.6 | 0.0 | | |
| Dark grey | 2.22 | 0.63 | -0.12 | 11.1 | 2.4 | 0.0 | | Strongly bioturbated |
| | 2.21 | 0.62 | -0.12 | 6.0 | 1.5 | 0.0 | | |
| Light grey with dark grey mottling | 2.18 | 0.57 | -0.13 | 3.3 | 1.4 | 0.0 | | Mottled sediment with finely disseminated organic material |
| | 1.98 | 0.51 | -0.09 | 4.5 | 0.0 | 0.0 | | |
| Light brown | 2.04 | 0.51 | -0.08 | 3.2 | 2.9 | 0.0 | | Subangular to subrounded sand with finely disseminated organic material |
| | 2.01 | 0.50 | -0.06 | 2.7 | 0.0 | 0.0 | | |
| | 2.01 | 0.49 | -0.12 | 2.7 | 0.6 | 0.0 | | |
| Light brown | 2.12 | 0.48 | -0.16 | 2.5 | 1.8 | 0.0 | | " |
| Light brown | 1.82 | 0.48 | -0.07 | 1.4 | 0.9 | 0.0 | | Subangular to subrounded sand with finely disseminated organic material |
| | 1.80 | 0.41 | -0.11 | 1.4 | 16.7 | 0.0 | | |
| | 1.74 | 0.41 | +0.07 | 1.3 | 0.8 | 0.0 | | |
| | 1.76 | 0.38 | +0.12 | 1.0 | 25.0 | 0.0 | | |
| Light brown with dark yellow mottling | 1.71 | 0.37 | +0.13 | 1.0 | 0.0 | 0.0 | | Subangular to subrounded sand with finely disseminated organic material |
| | 2.02 | 0.29 | +0.06 | 1.1 | 0.0 | 0.0 | | |
| | 2.03 | 0.21 | 0.00 | 1.0 | 1.28 | 0.0 | | |

**COUNCIL FOR GEOSCIENCE**
**MARINE GEOSCIENCE UNIT**

Compiled by: W.R. Miller
Coring Programme: August 1995
Coordinates: X+3032267.3; Y+28861.6

# DESCRIPTIVE SEDIMENT CORE LOGS - LAKE SIBAYA

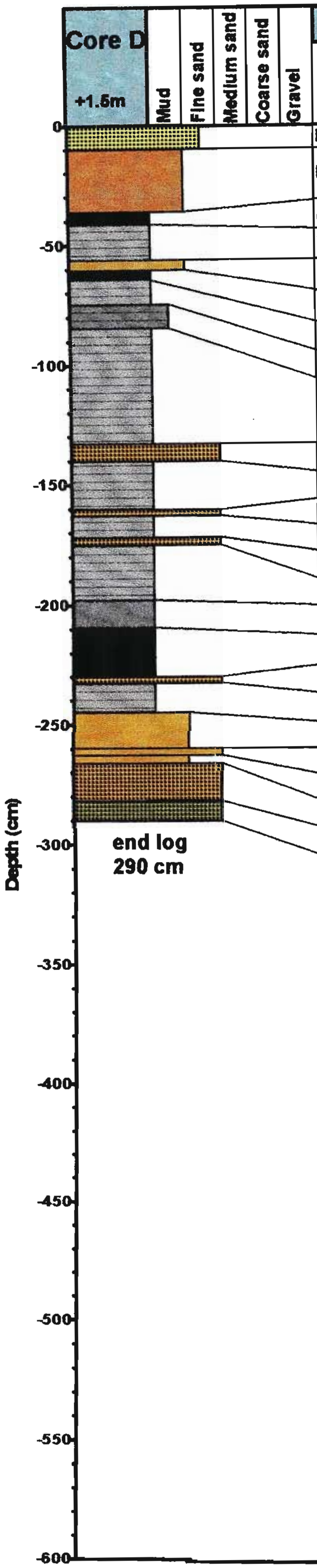


| Colour | Sand (phi) Stats Mean | Sorting | Skew | % <63µ | % C (org) | % $CaCO_3$ | Fossils | Comments |
|---|---|---|---|---|---|---|---|---|
| Pale brown | 2.84 | 0.59 | -0.14 | 27.0 | 4.9 | 0.0 | | Aeolian sand |
| Brown | 3.18 | 0.48 | +0.04 | 77.0 | 4.9 | 0.0 | | Soil horizon |
| Black | 2.90 | 0.63 | -0.19 | 77.0 | 8.1 | 0.0 | Organics | Friable organic clay |
| Light grey | 3.30 | 0.60 | -0.66 | 86.0 | 5.7 | 0.0 | Diatoms | Laminated diatomite |
| Dark yellow | | | | | | | | Ferruginous sand layer |
| Black | | | | 98.0 | 10.6 | 0.0 | Organics | Firm organic clay |
| Light grey | | | | 95.0 | 16.5 | 0.0 | Diatoms | Laminated diatomite |
| Dark grey | 2.92 | 0.34 | +0.02 | 40.0 | 6.0 | 0.0 | Diatoms | Laminated diatomite |
| Light grey | 2.82 | 0.37 | -0.26 | 81.0<br>96.0 | 7.0<br>6.0 | 0.0<br>0.0 | Diatoms | Laminated diatomite |
| Dark yellow | 2.64 | 0.41 | -0.05 | 49.0 | 9.9 | 0.0 | | Ferruginous sand layer |
| Light grey | 2.85 | 0.31 | -0.04 | 27.0 | 3.9 | 0.0 | Diatoms | Laminated diatomite |
| Dark yellow | | | | | | | | Ferruginous sand layer |
| Light grey | 3.19 | 0.45 | +0.13 | 83.0 | 6.1 | 0.0 | Diatoms | Laminated diatomite |
| Dark yellow | 2.76 | 0.35 | -0.06 | 46.0 | 4.8 | 0.0 | | Ferruginous sand layer |
| Light grey | | | | 94.0 | 9.9 | 0.0 | Diatoms | Laminated diatomite |
| Dark grey | 3.14 | 0.35 | +0.02 | 36.0 | 7.1 | 0.0 | Diatoms | Massive diatomite |
| Black | 3.11 | 0.45 | -0.03 | 72.0 | 8.5 | 0.0 | Organics | Firm organic clay |
| Dark yellow | 3.16 | 0.36 | +0.18 | 72.0 | 7.4 | 0.0 | | Ferruginous sand layer |
| Light grey | 2.97 | 0.30 | +0.01 | 70.0 | 8.6 | 0.0 | Diatoms | Massive diatomite |
| Dark yellow | 3.30 | 0.45 | -0.27 | 83.0 | 2.4 | 0.0 | | Firm clay |
| Dark yellow | 3.27 | 0.37 | +0.07 | 87.0 | 7.4 | 0.0 | | Goethite laminae |
| Dark yellow | | | | | | | | Firm clay |
| Dark yellow | 2.98 | 0.47 | -0.09 | 54.0 | 5.4 | 0.0 | | Clay rich sand |
| Light brown | 3.15 | 0.36 | +0.12 | 40.0 | 3.5 | 0.0 | | Clay rich sand |

**COUNCIL FOR GEOSCIENCE**
**MARINE GEOSCIENCE UNIT**
Compiled by: W.R. Miller
Coring Programme: August 1995
Coordinates: X+3021086.3; Y+33215.2

# DESCRIPTIVE SEDIMENT CORE LOGS - LAKE SIBAYA

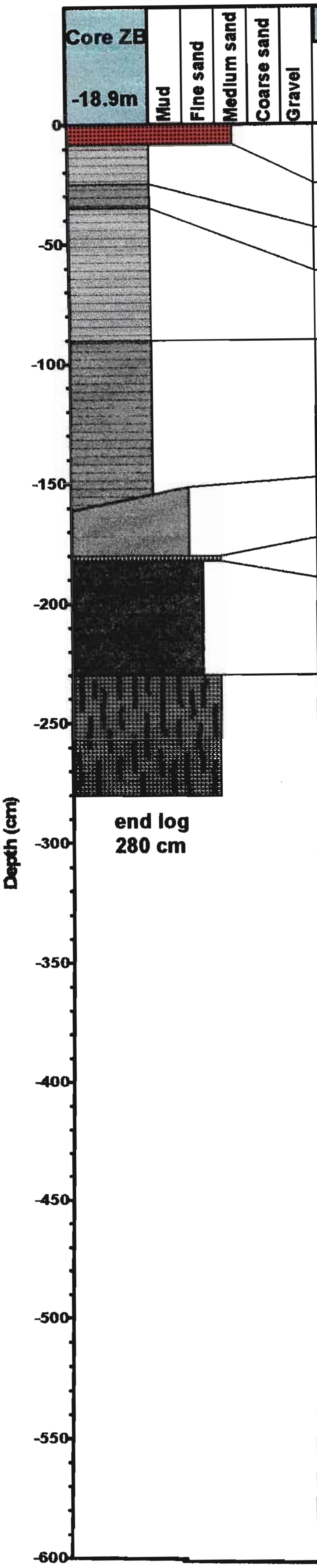


| Colour | Sand (phi) Stats: Mean | Sorting | Skew | % <63µ | % C (org) | % CaCO3 | Fossils | Comments |
|---|---|---|---|---|---|---|---|---|
| Light reddish brown | 2.39 | 0.48 | -0.34 | 3.0 | 3.7 | 0.0 | Faecal pellets | Angular to subrounded sand |
| Light grey | | | | 92.0 | 1.0 | 42.1 | Freshwater shells | Massive diatomite |
| Dark grey | | | | 79.0 | 13.4 | 39.3 | Freshwater shells | Massive diatomite |
| Light grey | | | | 96.0<br>89.0<br>99.0 | 9.1<br>8.8<br>11.2 | 32.2<br>56.8<br>53.5 | Freshwater shells | Laminated diatomite |
| Dark grey | | | | 96.0<br>100.0<br>94.0<br>97.0 | 1.0<br>10.7<br>21.8<br>8.8 | 41.5<br>56.3<br>47.0<br>46.0 | Freshwater shells | Massive diatomite |
| Dark grey | | | | 98.0 | 22.3 | 25.4 | Freshwater shells | Firm organic clay |
| Pale grey | 2.46 | 0.64 | -0.24 | 21.0 | 8.0 | 8.8 | Freshwater shells | Angular to subrounded sand layer |
| Black | 2.61<br>2.41<br>2.34 | 0.54<br>0.66<br>0.68 | -0.23<br>-0.34<br>-0.30 | 67.0<br>42.0<br>27.0 | 30.0<br>28.1<br>19.0 | 0.0<br>0.0<br>0.0 | Peat | Organic peat with shell fragments |
| Dark grey | 2.46<br>2.44<br>2.60 | 0.63<br>0.60<br>0.58 | -0.35<br>-0.34<br>-0.31 | 10.0<br>9.0<br>12.0 | 3.1<br>1.6<br>3.9 | 0.0<br>0.0<br>4.9 | | Strongly bioturbated angular to subrounded sand with finely disseminated organic material & white crystal rosettes of calcite |

**COUNCIL FOR GEOSCIENCE**
**MARINE GEOSCIENCE UNIT**

Compiled by: W.R. Miller
Coring Programme: August 1995
Coordinates: X+3026972.8; Y+32035.2

# DESCRIPTIVE SEDIMENT CORE LOGS - LAKE SIBAYA

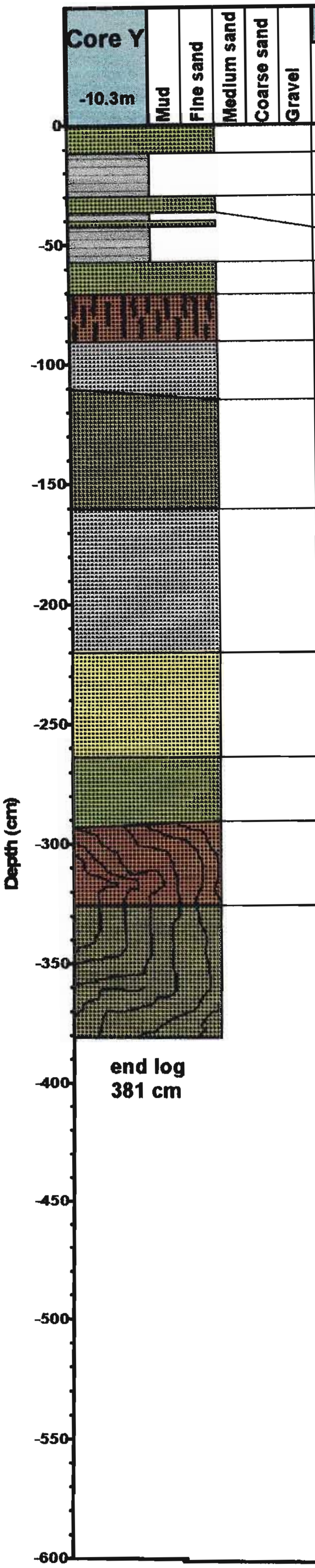


| Colour | Sand (phi) Stats: Mean | Sorting | Skew | % <63µ | % C (org) | % CaCO3 | Fossils | Comments |
|---|---|---|---|---|---|---|---|---|
| Light olive | 2.58 | 0.37 | -0.18 | 2.0 | 1.7 | 0.0 | Fw shells | |
| Light grey | 2.53<br>2.67 | 0.44<br>0.37 | -0.23<br>-0.11 | 68.0<br>53.0 | 10.7<br>7.4 | 26.3<br>19.6 | Fw shells & diatoms | Freshwater diatomite with shells |
| Light olive | 2.64 | 0.36 | -0.19 | 9.0 | 1.9 | 0.0 | | |
| Light grey | 2.67 | 0.31 | -0.20 | 36.0 | 5.5 | 29.0 | Fw shells & diatoms | Freshwater diatomite with shells |
| Light olive | 2.62 | 0.35 | -0.19 | 1.0 | 2.3 | 0.0 | | Bioturbated sand |
| Dark brown | 2.58 | 0.37 | -0.21 | 1.0 | 0.9 | 0.0 | | Extreme bioturbation |
| Light grey | 2.66 | 0.34 | -0.20 | 0.0 | 1.0 | 0.0 | | Moderately bioturbated subangular to rounded clean, running sand |
| Light brown | 2.41 | 0.37 | -0.20 | 2.0 | 0.8 | 0.0 | | Moderately bioturbated subangular to rounded clean, running sand |
| Pale grey | 2.55<br>2.54 | 0.44<br>0.42 | -0.23<br>-0.26 | 2.0<br>1.0 | 2.3<br>3.9 | 0.0<br>0.0 | | Angular to subrounded clean, running sand with white kaolinised grains of microcline & flat tabular transparent crystals |
| Pale brown | 2.10<br>2.45 | 0.70<br>0.49 | -0.26<br>-0.31 | 3.0<br>3.0 | 4.5<br>0.9 | 0.0<br>0.0 | | Angular to subrounded clean, running sand with white kaolinised grains of microcline |
| Pale olive | 2.53 | 0.44 | -0.23 | 3.0 | 3.9 | 0.0 | | " |
| Dark brown | 2.39<br>2.47 | 0.46<br>0.49 | -0.33<br>-0.31 | 14.0<br>14.0 | 2.7<br>2.7 | 0.0<br>0.0 | Sponge spicules | Angular to subrounded sand with white grains of kaolinised microcline & soft sed. deformation |
| Light brown | 2.38<br>2.20 | 0.49<br>0.67 | -0.33<br>-0.31 | 19.0<br>21.0 | 3.9<br>1.9 | 0.0<br>0.0 | | Angular to subrounded sand with soft sediment deformation and white kaolinised grains of microcline. Sediments are pliable when moist but hard when dry |

**COUNCIL FOR GEOSCIENCE**
**MARINE GEOSCIENCE UNIT**

Compiled by: W.R. Miller
Coring Programme: August 1995
Coordinates: X+3027113.0; Y+32886.2

# DESCRIPTIVE SEDIMENT CORE LOGS - LAKE SIBAYA


| Colour | Sand (phi) Stats: Mean | Sorting | Skew | % <63µ | % C (org) | % CaCO3 | Fossils | Comments |
|---|---|---|---|---|---|---|---|---|
| Light grey | 2.21 | 0.48 | -0.09 | 83.6 | 5.7 | 65.3 | Freshwater diatomite & shells | Firm, strongly laminated freshwater diatomite with shell lags |
| | 2.55 | 0.37 | -0.08 | 70.7 | 7.3 | 68.5 | | |
| | 2.10 | 0.65 | -0.05 | 92.0 | 7.8 | 72.2 | | |
| | 2.24 | 0.85 | +0.02 | 81.0 | 10.6 | 67.1 | | |
| Pale grey | 1.94 | 0.57 | -0.20 | 1.8 | 0.0 | 0.0 | | Subangular to subrounded sand |
| Pale grey | 1.98 | 0.58 | -0.15 | 1.8 | 0.0 | 0.0 | Freshwater shells | Subangular, moderately bioturbated sand with freshwater shell fragments |
| | 2.35 | 0.38 | -0.15 | 1.4 | 0.0 | 0.0 | | |
| | 2.18 | 0.57 | -0.16 | 1.3 | 0.5 | 0.0 | | |
| Dark grey | 1.88 | 0.53 | -0.14 | 28.2 | 4.7 | 1.6 | Shell fragments | Sandy clay |
| Light brown | 1.89 | 0.57 | -0.14 | 2.3 | 0.0 | 0.0 | Sponge spicules | Ferruginous nodules |
| | 2.22 | 0.47 | -0.26 | 1.2 | 0.0 | 0.0 | | |
| Light brown | 2.01 | 0.60 | -0.30 | 1.5 | 1.4 | 0.0 | | Soft sediment deformation |
| | 1.79 | 0.63 | -0.05 | 1.0 | 0.5 | 0.0 | | |
| Pale brown | 2.46 | 0.38 | -0.07 | 1.3 | 0.0 | 0.0 | | Subangular to subrounded sand with white kaolinised microcline grains |
| | 2.11 | 0.48 | -0.17 | 1.0 | 1.1 | 0.0 | | |
| | 2.08 | 0.47 | -0.11 | 0.5 | 0.6 | 0.0 | | |

**COUNCIL FOR GEOSCIENCE**
**MARINE GEOSCIENCE UNIT**

Compiled by: W.R. Miller
Coring programme: August 1995
Coordinates: X+3029113.4; Y+30638.1

# DESCRIPTIVE SEDIMENT CORE LOGS - LAKE SIBAYA

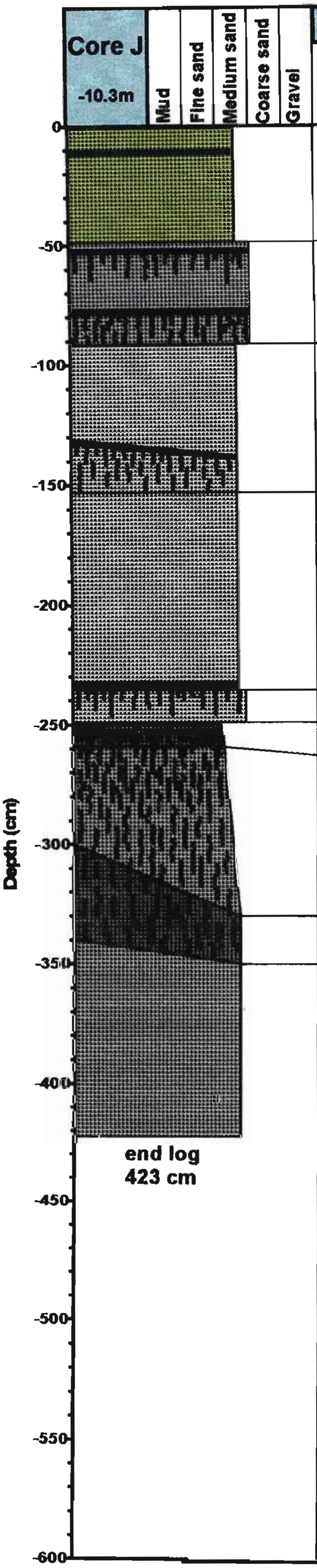


| Colour | Sand (phi) Stats: Mean | Sorting | Skew | % <63µ | % C (org) | % CaCO3 | Fossils | Comments |
|---|---|---|---|---|---|---|---|---|
| Pale olive | 2.3 | 0.42 | -0.13 | 0.0 | 0.9 | 0.0 | | Subangular to subrounded clean, free flowing sand |
| | 2.28 | 0.43 | -0.12 | 0.0 | 1.9 | 0.0 | | |
| | 2.23 | 0.34 | -0.01 | 0.0 | 0.8 | 0.0 | | |
| Light grey | 2.01 | 0.53 | -0.03 | 0.0 | 0.6 | 0.0 | | Strongly bioturbated |
| | 1.86 | 0.35 | -0.05 | 0.0 | 0.8 | 0.0 | | |
| | 2.12 | 0.42 | +0.03 | 0.0 | 3.8 | 0.0 | | |
| Pale grey | 2.40 | 0.36 | -0.15 | 0.0 | 0.0 | 0.0 | Sponge spicules | Strongly bioturbated |
| | 2.35 | 0.34 | -0.07 | 0.0 | 1.8 | 0.0 | | |
| | 2.37 | 0.42 | -0.03 | 1.0 | 1.8 | 0.0 | | |
| Pale grey | 2.53 | 0.38 | -0.21 | 0.0 | 1.0 | 0.0 | | Moderately bioturbated free flowing sand |
| | 2.49 | 0.36 | -0.10 | 0.0 | 0.6 | 0.0 | | |
| | 2.28 | 0.36 | -0.04 | 0.0 | 2.0 | 0.0 | | |
| Pale grey | 2.15 | 0.39 | +0.09 | 0.0 | 1.9 | 0.0 | | Strong bioturbation |
| Dark grey | 2.76 | 0.43 | -0.16 | 11.0 | 5.7 | 0.0 | FW Shells | Extreme bioturbation |
| Light grey | 2.80 | 0.40 | -0.16 | 1.0 | 4.6 | 0.0 | Sponge spicules | Strong bioturbation |
| | 2.50 | 0.44 | -0.07 | 1.0 | 1.6 | 0.0 | | |
| | 2.44 | 0.43 | -0.15 | 0.0 | 0.0 | 0.0 | | |
| Dark grey to black | 2.25 | 0.53 | -0.15 | 1.0 | 3.2 | 0.0 | Sponge spicules | Extreme bioturbation |
| Light grey | 2.26 | 0.47 | -0.15 | 0.0 | 3.0 | 0.0 | | Moderate bioturbation |
| | 2.31 | 0.56 | -0.13 | 1.0 | 0.9 | 0.0 | | |
| | 2.25 | 0.53 | -0.16 | 1.0 | 0.9 | 0.0 | | |
| | 2.09 | 0.50 | -0.08 | 0.0 | 0.9 | 0.0 | | |

COUNCIL FOR GEOSCIENCE
MARINE GEOSCIENCE UNIT
Compiled by: W.R. Miller
Coring Programme: August 1995
Coordinates : X+3028179.9; Y+31021.3

# DESCRIPTIVE SEDIMENT CORE LOGS - LAKE SIBAYA

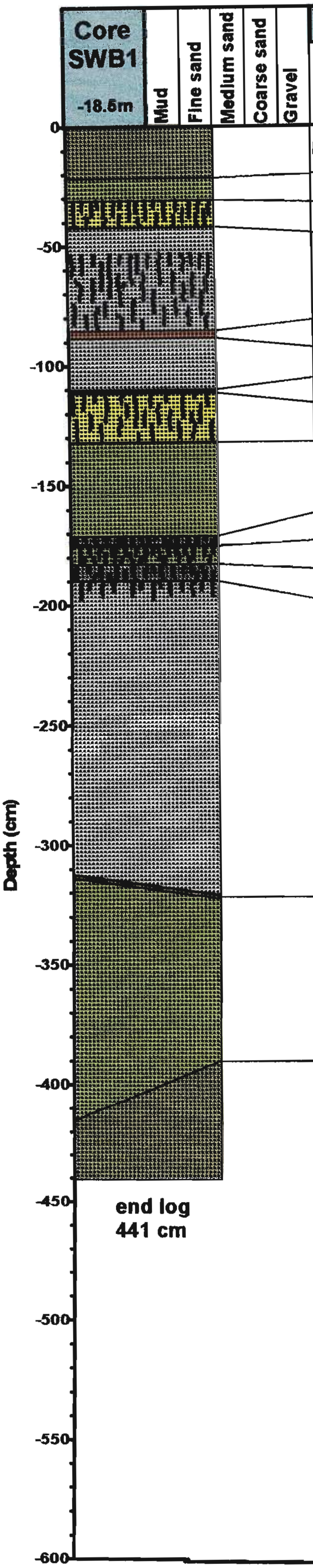


| Colour | Sand (phi) Stats: Mean | Sorting | Skew | % <63µ | % C (org) | % CaCO3 | Fossils | Comments |
|---|---|---|---|---|---|---|---|---|
| Light brown | 2.52 | 0.43 | -0.27 | 2.1 | 1.5 | 0.0 | Sponge spicules | Angular, light brown non-bioturbated sand |
| | 2.54 | 0.42 | -0.23 | 1.1 | 0.0 | 0.0 | | |
| Pale olive | 2.52 | 0.39 | -0.27 | 0.9 | 1.5 | 0.0 | " | Moderately bioturbated |
| Dark yellow | 2.51 | 0.43 | -0.24 | 1.7 | 0.9 | 0.0 | " | Strongly bioturbated |
| Pale grey | 2.52 | 0.41 | -0.22 | 1.7 | 0.0 | 0.0 | " | Moderately to strongly bioturbated |
| | 2.39 | 0.46 | -0.31 | 1.1 | 2.0 | 0.0 | | |
| Dark brown | 2.78 | 0.34 | -0.17 | 3.0 | 1.3 | 0.0 | " | Non-bioturbated |
| Pale grey | 2.30 | 0.51 | -0.28 | 1.3 | 1.3 | 0.0 | " | Moderately bioturbated |
| Black | 2.45 | 0.45 | -0.26 | 2.6 | 1.5 | 0.0 | " | Non-bioturbated |
| Dark yellow | 2.20 | 0.48 | -0.40 | 2.0 | 0.0 | 0.0 | " | Strongly bioturbated |
| Light olive | 2.43 | 0.44 | -0.27 | 1.0 | 0.0 | 0.0 | " | Moderately bioturbated |
| | 2.15 | 0.54 | -0.33 | 0.6 | 0.8 | 0.0 | | |
| Dark grey | 2.78 | 0.36 | -0.22 | 4.5 | 0.0 | 0.0 | " | Strongly bioturbated |
| Light olive | | | | | | | " | Strongly bioturbated |
| Dark grey | 2.34 | 0.56 | -0.31 | 3.7 | 1.8 | 0.0 | " | Moderately bioturbated |
| Light grey | 2.47 | 0.48 | -0.32 | 2.6 | 0.5 | 0.0 | | Strongly bioturbated 190cm to 201cm depth |
| | 2.55 | 0.45 | -0.25 | 2.8 | 0.0 | 0.0 | | |
| | 2.55 | 0.42 | -0.25 | 2.0 | 1.1 | 0.0 | | Moderately bioturbated |
| | 2.52 | 0.49 | -0.29 | 2.3 | 1.5 | 0.0 | | |
| | 2.47 | 0.51 | -0.36 | 1.6 | 0.0 | 0.0 | | Transparent crystal rosettes near base |
| Pale olive | 2.48 | 0.51 | -0.33 | 2.2 | 0.0 | 0.0 | | |
| | 2.39 | 0.50 | -0.40 | 1.2 | 0.0 | 0.0 | | Non-bioturbated subangular to subrounded sand |
| | 2.33 | 0.56 | -0.43 | 0.8 | 0.0 | 0.0 | | |
| | 2.42 | 0.56 | -0.36 | 2.1 | 0.0 | 0.0 | | |
| Light brown | 2.46 | 0.54 | -0.35 | 12.1 | 1.57 | 0.0 | | Subangular to subrounded mottled sand with a clay matrix. Sediment is pliable when moist but hard when dry. |
| | 2.41 | 0.54 | -0.34 | 12.1 | 3.0 | 0.0 | | |

**COUNCIL FOR GEOSCIENCE**
**MARINE GEOSCIENCE UNIT**

Compiled by: W.R. Miller
Coring Programme: August 1995
Coordinates: X+302894.1; Y+32768.6

# DESCRIPTIVE SEDIMENT CORE LOGS - LAKE SIBAYA

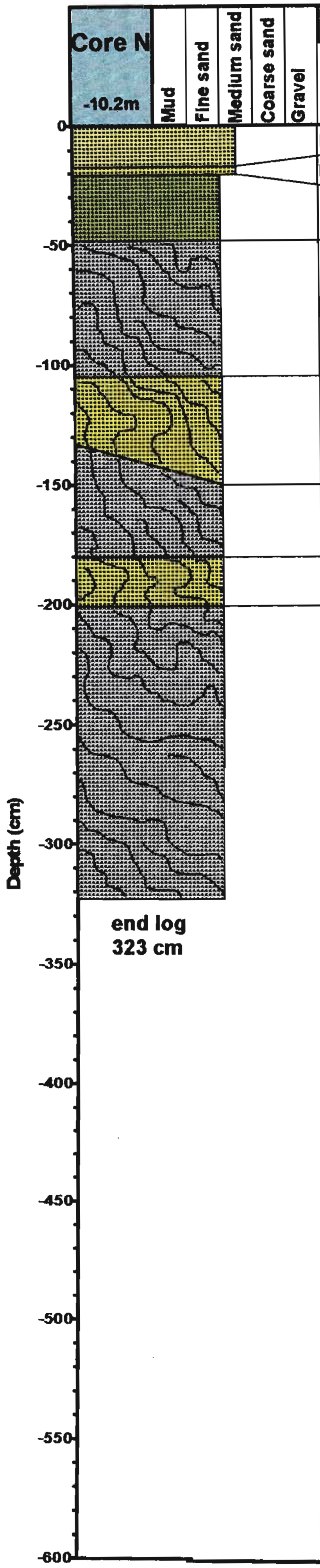


| Colour | Sand (phi) Stats Mean | Sorting | Skew | % <63µ | % C (org) | % CaCO3 | Fossils | Comments |
|---|---|---|---|---|---|---|---|---|
| Pale brown | 2.75 | 0.35 | -0.23 | 10.2 | 2.4 | 0.0 | Shell frags | Mottled sand |
| Dark yellow | 2.88 | 0.27 | -0.19 | 17.6 | 2.1 | 0.0 | | " |
| Pale olive | 2.89 | 0.24 | -0.06 | 15.5 | 1.5 | 0.0 | Freshwater shell frags | Fairly hard mottled sand |
| | 2.84 | 0.26 | -0.13 | 14.0 | 2.8 | 0.0 | | |
| Pale grey with dark yellow mottling | 3.07 | 0.22 | -0.01 | 19.9 | 2.6 | 0.0 | | Hard, subangular to subrounded clay rich sand exhibiting soft sediment deformation structures |
| | 3.06 | 0.22 | -0.04 | 13.7 | 2.3 | 0.0 | | |
| Dark yellowish orange | 3.17 | 0.19 | +0.10 | 17.9 | 3.5 | 0.0 | | " |
| Pale grey with dark yellow mottling | 2.94 | 0.29 | -0.19 | 8.2 | 2.9 | 0.0 | | " |
| Dark yellow | 3.12 | 0.21 | 0.00 | 15.3 | 2.8 | 0.0 | | " |
| Pale grey with dark yellow mottling | 3.11 | 0.25 | -0.06 | 15.9 | 2.5 | 0.0 | | " |
| | 3.09 | 0.21 | +0.08 | 11.5 | 1.7 | 0.0 | | |
| Pale grey with dark yellowish orange mottling | 3.09 | 0.25 | -0.08 | 12.5 | 1.8 | 0.0 | | |
| | 3.12 | 0.26 | +0.08 | 15.7 | 2.8 | 0.0 | | |

**COUNCIL FOR GEOSCIENCE**
**MARINE GEOSCIENCE UNIT**
Compiled by: W.R. Miller
Coring Programme: August 1996
Coordinates: X+3024034.4; Y+30565.0

# DESCRIPTIVE SEDIMENT CORE LOGS - LAKE SIBAYA

**Core U**

-29.4m

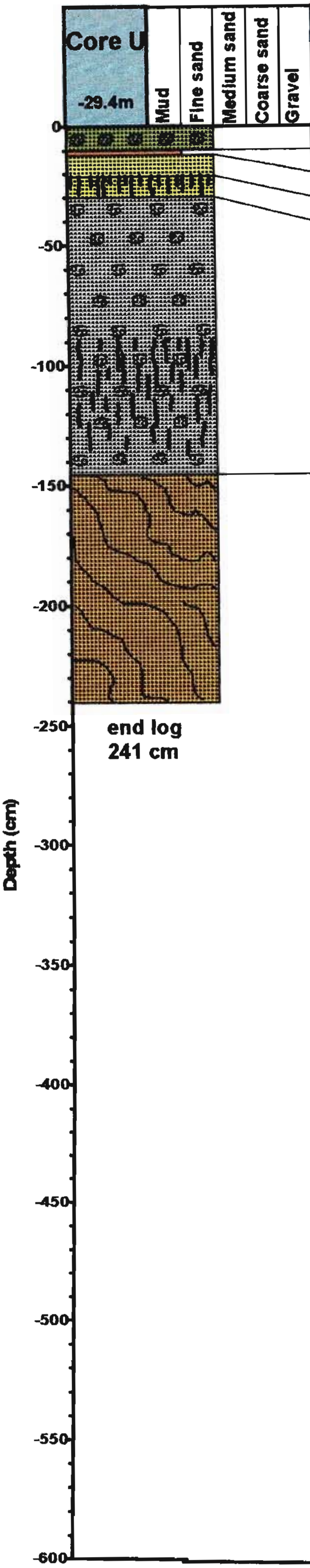


| Colour | Sand (phi) Stats: Mean | Sorting | Skew | % <63µ | % C (org) | % CaCO3 | Fossils | Comments |
|---|---|---|---|---|---|---|---|---|
| Light olive | 2.81 | 0.33 | -0.17 | 0.7 | 0.5 | 0.0 | FW shells | Fossiliferous sand |
| Dark brown | | | | | | | | Clay drape |
| Pale brown | 2.80 | 0.29 | -0.11 | 0.8 | 1.3 | 0.0 | Sponge | Massive sand |
| Dark yellow | 2.71 | 0.33 | -0.19 | 1.6 | 1.0 | 0.0 | Spicules | Mottled sand |
| Pale grey | 2.73 | 0.34 | -0.14 | 0.7 | 1.2 | 0.0 | Shells, forams, ostracods, bryzoans & crab claws | Moderately to intensely bioturbated, angular to subrounded sand rich in microfossils |
| | 2.73 | 0.34 | -0.15 | 1.4 | 0.8 | 18.7 | | |
| | 2.63 | 0.40 | -0.27 | 1.9 | 1.0 | 4.23 | | |
| | 2.69 | 0.40 | -0.23 | 3.0 | 0.8 | 0.0 | | |
| | 2.97 | 0.36 | -0.11 | 7.0 | 1.3 | 0.0 | | |
| Light reddish orange | 2.96 | 0.35 | -0.07 | 8.5 | 17.2 | 0.0 | | Hard, clay rich sand displaying soft sediment deformation structures |
| | 2.86 | 0.36 | -0.09 | 13.2 | 2.0 | 0.0 | | |
| | 2.93 | 0.33 | -0.04 | 14.8 | 2.2 | 0.0 | | |

**COUNCIL FOR GEOSCIENCE**
**MARINE GEOSCIENCE UNIT**

Compiled by: W.R. Miller
Coring Programme: August 1995
Coordinates: X+3025403.4; Y+30766.1

# APPENDIX 4

## HOLOCENE LACUSTRINE MICROFOSSILS

**MOLLUSCA:** From Hart (1979)

**Prosobranchia**

*Melanoides tuberculatus* (Müller, 1774)

*Bellamya capillata* (Frauenfeld, 1865)

**Pulmonata**

*Biomphalaria pfeifferi* (Krauss, 1848)

*Bulinus (Bulinus) natalensis* (Küster, 1841)

*Bulinus (Physopsis) globosus* (Morelet, 1866)

*Burnupina sp.*

*Ceratophallus sp.* (Brown & Mandahl-Barth, 1973)

*Gyraulus costulatus* (Krauss, 1848)

*Succinea patentissima* (Pfeiffer, 1853)

*Succinea striata* (Krauss, 1848)

**Lamellibranchia**

*Corbicula africana* (Krauss, 1848)

*Eupera ferruginea* (Krauss, 1848)

*Sphaerium capense* (Krauss, 1848)

**Diatoms**

Identified by Professor P. Alhonen - University of Helsinki

*Amphora libyca*

*Amphora mexicana*

*Amphora ovalis*

*Aulacoseira islandica*

*Aulacoseira italica*

# Appendix 5

## HOLOCENE LAGOONAL MICROFOSSILS

**GASTROPODA:**

Identified by Dr. R.N Kilburn (Natal Museum)

*Actaeopyramis sp.*

*Acteocina sp.*

*Anachis atrata* (Gould)

*Chemnitzia sp.*

*Chrysallida sp.*

*Cingulina sp.*

*Cylichna sp.*

*Epitonium sp.*

*Ethminolia durbanensis* (Kilburn)

*Leiocithara musae* (Thiele)

*Micratys sp.*

*Murex brevispina* juv.(Lamarck)

*Obitortio fragrans* (Barnard)

*Obitortio natalensis* (Smith)

*Odostomia sp.*

*Retusa concentrica* (A. Adams)

*Ringicula prismatica* (de Folin)

*Scaliola sp.*

*Turbonilla sp.*

Identified by Marcus Lussi (private collector)

*Acteocina smithi* (Bartsch, 1915)

*Atys cylindrica* (Helbling, 1779)

*Finella natalensis* (E.A. Smith 1899)

*Haminoea sp.*

*Melanella sp.*

**SCAPHAPODA:**

Identified by Dr. R.N. Kilburn (Natal Museum)

*Cadulus booceras* (Tomlin, 1926)

Identified by Marcus Lussi (private collector)

*Antalis longtrorsum* (Reeve, 1843)

*Vermetidae sp.*

**BIVALVIA:**

Identified by Dr. R.N. Kilburn (Natal Museum)

*Callista florida* (Lamarck)

*Cardiomya pulchella* (H. Adams)

*Diplodonta sp.*

*Galeomma sp.*

*Loripes pisidium* (Dunker)

*Lucina semperiana* (Issel)

*Melliteryx sp.*

*Musculus strigatus* (Hanley)

*Nucinella pretiosa* (Gould)

**FORAMINIFERA:**

Identified by Ian McMillan (de Beers Marine)

*Challengerella bradyi* (Billman, Hottinger & Oesterle)

*Massilina sp.*

*Operculina granulosa* (Leymerie)

*Rotalia schreiteri* (D'Orbigny)

*Spiroloculina communis* (Cushman & Todd)

*Triloculina rupertiana* (Brady)

*Triloculina tricarinata* (D'Orbigny)

# APPENDIX 6

## LATEST PLEISTOCENE DIATOM ASSEMBLAGE
## KWAMBONAMBI FORMATION

Identified by Professor P. Alhonen - University of Helsinki

*Aulacoseira italica*

*Aulacoseira distons*

*Epithemia zebra*

*Surirella linearis v. constricta*

*Cyclotella meneghiniana*

*Epithemia turgida*

*Diploneis puella*

*Surirella striatula*

*Amphora ovalis*

*Anomoeneis sphaerophora v. sculpta*

*Stauroneis anceps*

*Rhopalodia gibberula*

*Pinnularia major*

*Pinnularia gibba*

*Pinnulari gentilis*

*Pinnularia viridis*

*Thalassiosira baltica*

*Actinoptychus undulatus*

*Terpsinoe americana*

# APPENDIX 7

## LIST OF RADIOCARBON DATES

| SAMPLE NO. | CORE NO. | DESCRIPTION | AGE (Years BP) |
|---|---|---|---|
| Pta - 6408 | Core P | Organic clay | 5030 ± 70 |
| Pta - 6401 | Core P | Marine shell fragments | 7740 ± 90 |
| Pta - 6926 | Core D | Organic peat layer | 25 500 ± 420 |
| Pta - 6914 | Core D | Organic material | 43500 + 2600 -2000 |
| Pta - 7761 | Core 2 | Organic rich sand | 8810 ± 100 |
| Pta - 7793 | Core ZB | Organic peat | 7060 ± 80 |
| Pta - 7794 | Core J | Organic clay | 5610 ± 80 |